

DOI: 10.1002/mas.21844

TUTORIAL

WILEY

Mass spectrometry of polymers: A tutorial review

Chrys Wesdemiotis | Kayla N. Williams-Pavlantos | Addie R. Keating | Andrew S. McGee | Calum Bochenek

Department of Chemistry, The University of Akron, Akron, Ohio, USA

Correspondence

Chrys Wesdemiotis, Department of Chemistry, The University of Akron, Knight Chemical Laboratory 112, Akron, OH 44325-3601, USA.

Email: wesdemiotis@uakron.edu

Abstract

Ever since the inception of synthetic polymeric materials in the late 19th century, the number of studies on polymers as well as the complexity of their structures have only increased. The development and commercialization of new polymers with properties fine-tuned for specific technological, environmental, consumer, or biomedical applications requires powerful analytical techniques that permit the in-depth characterization of these materials. One such method with the ability to provide chemical composition and structure information with high sensitivity, selectivity, specificity, and speed is mass spectrometry (MS). This tutorial review presents and exemplifies the various MS techniques available for the elucidation of specific structural features in a synthetic polymer, including compositional complexity, primary structure, architecture, topology, and surface properties. Key to every MS analysis is sample conversion to gas-phase ions. This review describes the fundamentals of the most suitable ionization methods for synthetic materials and provides relevant sample preparation protocols. Most importantly, structural characterizations via one-step as well as hyphenated or multidimensional approaches are introduced and demonstrated with specific applications, including surface sensitive and imaging techniques. The aim of this tutorial review is to illustrate the capabilities of MS for the characterization of large, complex polymers and emphasize its potential as a powerful compositional and structural elucidation tool in polymer chemistry.

KEYWORDS

complex mixtures and blends, mass spectrometry, multidimensional MS techniques, polymers, surfaces

This is an open access article under the terms of the Creative Commons Attribution-NonCommercial-NoDerivs License, which permits use and distribution in any medium, provided the original work is properly cited, the use is non-commercial and no modifications or adaptations are made.

© 2023 The Authors. Mass Spectrometry Reviews published by John Wiley & Sons Ltd.

1 | INTRODUCTION TO POLYMER CHARACTERIZATION

1.1 | Applications of polymers

Over the last 50 years, synthetic polymers and polymerbased materials have experienced continuous growth in a wide range of applications. They have increased the efficiency of common, everyday tasks as well as contributed to the development of high-performance materials for technological, environmental, and biomedical applications. Plastics, polymer composites, elastomers, and artificial fibers are just a few examples of these materials which have found uses in the pharmaceutical, automobile, textile, and medicinal industries as well as many more fields (Saglam et al., 2021; Thakur et al., 2014). The ability to tailor polymers to have the desired crystallinity, tensile strength, hardness, elasticity, and permeability makes them highly desirable in all fields of industry and manufacturing (Abadie et al., 2021; Ligon et al., 2017). These properties are significantly influenced by chemical structure, architecture, and molecular weight (MW), and as such, it is crucial that accurate and precise analytical techniques exist to study and characterize these properties.

1.2 | Structure, polydispersity, repeat mass, and end groups

Polymer chain composition can be divided into two fundamental parts. The first is the backbone which is the primary chain that links the repeat units together. The second part is the side chain substituents (pendant groups) which can either be simple functionalities, such as an ethyl or hydroxy group, or longer and more complex moieties, such as shorter polymer chains with different repeat units. Since pendant groups hang off the

polymer backbone, they are often responsible for the interactions and/or reactions that can occur with other polymer chains (Boyle et al., 2019). In addition to chain composition, polymers can also be classified according to their unique architecture, including linear, cyclic, branched (hyperbranched, dendritic, tadpole, comb, brush-, or star-shaped), and crosslinked (networked), cf. Figure 1. Note that the distinct shapes of these architectures also result in substantially different numbers of end groups, which are minimized in macrocycles and maximized in branched species.

Linear polymers comprise long polymer chains with end groups at both the initiating (α) and terminating (ω) chain end. They are generally flexible in nature and can develop strong intermolecular forces between individual chains. This allows for high densities, tensile strengths, and melting points. Cyclic polymers have ring-like chains, and contrary to their counterparts, lack end groups. This topology leads to unique properties, such as a reduced degradation profile and lower hydrodynamic volume (Haque & Grayson, 2020). Branched polymers contain polymeric side chains attached to a polymer backbone. The density, chemistry, length, and uniformity of the side chains can all impact the resulting material properties but in general, these polymers are less dense than linear polymers and are often used as adhesives or coatings (Seo & Hawker, 2020). Finally, cross-linked polymers (or networks) encompass polymer chains that are interconnected intramolecularly or intermolecularly, to create a more rigid molecule with a well-defined threedimensional (3D) shape, improved chemical and mechanical stability (vs. linear polymers), and variable softness depending on the degree of crosslinking (J. Chen et al., 2020; Fortman et al., 2018). In addition to differing architectures, the chemical composition of the backbone may also vary. These types of polymers, referred to as "copolymers," contain at least two different monomers arranged in random, alternating, tapered, or block-wise

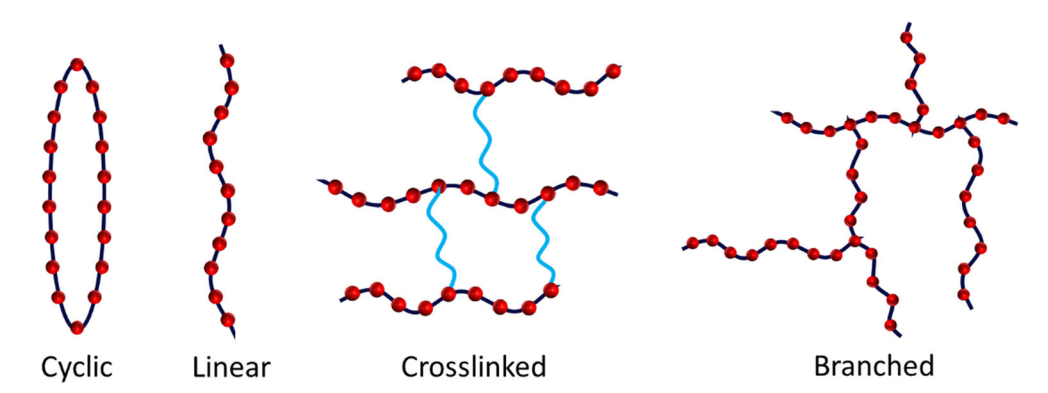


FIGURE 1 Basic polymer architecture families. End groups are minimized in macrocycles and maximized in branched polymers. [Color figure can be viewed at wileyonlinelibrary.com]

manner. These differences in architecture and sequence play a significant role in polymer properties and, thus, are important to characterize.

The length of the backbone chain is also important in defining the phase of the polymer (Wolstenholme, 1968). For instance, lower MW polymers tend to have a waxy, almost liquid composition while higher MW polymers tend to crystalize and create a more rigid and robust structure. This change is due in part to the fact that polymers can form intertwined networks, allowing for a stronger binding force between adjacent chains as the chain length increases.

Polymer synthesis generally leads to macromolecules with varying chain length and size, causing the resulting MWs to vary and form a distribution rather than have single, definite value as organic molecules and most biomolecules do. Traditionally, polymer size is classified by four main variables, viz. number-average MW (M_n) , weight-average MW (M_w) , polydispersity index (PDI), and degree of polymerization (DP). These parameters are defined in Equations (1)–(4), where N_i is the number of chains with MW M_i and M_0 is the MW of the repeat unit which is usually the monomer or its dehydration product. PDI describes how wide the MW distribution is and reflects the degree of control on molecular size provided by the synthesis process.

$$M_{\rm n} = \frac{\Sigma(N_i M_i)}{\Sigma N_i},\tag{1}$$

$$M_{\rm w} = \frac{\Sigma(N_i M_i^2)}{\Sigma(N_i M_i)},\tag{2}$$

$$PDI = \frac{M_w}{M_v},\tag{3}$$

$$DP = \frac{M_n}{M_0}. (4)$$

1.3 | Common chromatographic, spectroscopic, and thermal techniques for polymer analysis: Advantages and disadvantages

Mass analysis of polymers has been traditionally performed by size exclusion chromatography (SEC), especially the gel permeation chromatography (GPC) variant which employs a hydrophobic stationary phase and organic solvents as mobile phase; often, the terms SEC and GPC are used interchangeably in the polymer community. With this technique, polymer MW information, such as $M_{\rm n}$, $M_{\rm w}$, and PDI data, is derived based on the retention time of the sample through a packed column. The column material is a crosslinked polymer

that does not develop chemical or physical interactions with the analyte sample. Its pore sizes determine how long the macromolecules remain in the stationary phase; larger molecules do not fit easily in the pores and, thus, are eluted earlier. SEC columns are typically attached to ultraviolet (UV) or refractive index (RI) detectors. A disadvantage of conventional SEC systems is that they only provide relative MW values. The hydrodynamic volume of the unknown polymer is measured and compared to the hydrodynamic volume of polymer standards with known MW to correlate retention time with molecular size. If the relationship between hydrodynamic volume and MW is different for the unknown and standards, significant under- or overestimation errors can result (Teraoka, 2004). This problem can, however, be mitigated with multidetector methods relying on the combination of light scattering, viscometry, and refractometry (Striegel, 2005). When combined with SEC, the RI detector measures an accurate concentration profile of the sample, light scattering renders the absolute MW independent of any column calibration standards, and the viscometer reveals the intrinsic viscosity of the polymer from which structural data can be deduced, such as the hydrodynamic volume or the branching architecture (Williams, 2019).

Nuclear magnetic resonance (NMR) spectroscopy is another popular technique for characterizing polymers, as it provides information about the polymer repeat unit as well as the end groups. For smaller polymer sizes, $M_{\rm n}$ can be derived by integrating signals indicative of the repeat unit versus end groups (Izunobi & Higginbotham, 2011). A major advantage of NMR is its ability to reveal specific atom connectivities within the polymer chain, while downsides include low sensitivity and difficulties in sample preparation and data interpretation due to solubility issues and signal overlap, respectively. Solid state NMR is often used to alleviate the effects of solvent in NMR but comes with its own challenges such as peak broadening, chemical shifts, and analysis time (R. Zhang et al., 2019).

Wide and small angle X-ray scattering (WAXS and SAXS) are useful analytical techniques for gaining 3D structural and morphological information at the 0.3–0.5 and 1–200 nm scale, respectively. The variation in beam path (scattering) changes based on the internal structure of the sample, allowing for determination of the sample's chemical characteristics, such as the shape and organization of its polymer chains. Disadvantages of these techniques include radiation damage for less robust samples and weak scattering intensities (Beale et al., 2006).

In addition to these molecular analysis techniques, thermal analysis methods such as differential scanning calorimetry (DSC) and thermogravimetric analysis (TGA) are used widely in polymer characterizations. DSC measures the heat absorbed or released by a polymer versus an inert reference as a function of temperature or time, while both are maintained at nearly the same conditions. Changes in the state of the polymer are detected in this process, from which important physical properties can be determined, such as the glass transition temperature ($T_{\rm g}$), melting temperature ($T_{\rm m}$), and crystallization temperature ($T_{\rm c}$). In TGA, the weight of the polymer sample is measured as a function of temperature or time in a controlled atmosphere, which gives useful information about the thermal and oxidative stability of the polymer as well as its moisture and volatile contents (Haines, 2002).

1.4 | Benefits of mass spectrometry (MS)

While all of the previously described methods provide useful information on polymer size and architecture, they can often give unclear results, especially when dealing with questions involving molecular composition, topology, complex mixtures, and polydisperse polymers, because they all probe the average sample (i.e., the bulk).

For these reasons, MS is increasingly utilized as the optimal tool to answer these questions. The ability of MS to separate individual ions based on their mass (literally mass-to-charge ratio, m/z) makes it possible to select and examine an individual oligomer to determine crucial polymeric characteristics such as (co)monomer and end group composition, average MW, primary structure (sequence), and architecture.

When MS was first being used to analyze polymers, offline or online (within the ion source) degradation techniques were necessary to reduce the MW to a size ionizable in electron impact (EI) or chemical ionization (CI) sources (Shimizu & Munson, 1979). This was later replaced by field desorption (FD) in the late 1960s (Lattimer, 1989), followed by fast atom bombardment (FAB) in the early 1980s (Williams et al., 1981). The most significant breakthrough for the analysis of polymers via MS occurred later in the late 1980s with the inception and development of matrix-assisted laser desorption/ionization (MALDI), electrospray ionization (ESI), and atmospheric pressure CI (APCI). These revolutionary "soft" ionization sources have pioneered the way for the development of new MS-based polymer characterization techniques commonly used today. Table 1 lists representative studies utilizing these ionization methods, alone or in hyphenation, for the MS analysis of important classes of polymers.

TABLE 1 Examples of various "soft" ionization mass spectrometry techniques for the characterization of different classes of polymers.

Polymer sample(s)	Study	References
ESI		
Poly(butylene adipate)	ESI-MS analysis of low MW polymers (~800 Da)	Scionti and Wesdemiotis (2012a)
Polysaccharides (Dextran)	ESI-MS analysis of low and high MW homopolymers	Chao et al. (2022)
Polyesters	LC-ESI-MS analysis of food contact materials	Osorio et al. (2022)
MALDI		
Poly(butylene adipate)	MALDI-MS analysis of PBA and its pyrolysis products	Lattimer et al. (1998)
Polystyrene	MALDI-MS analysis of functionalized PS	Quirk et al. (2008)
Dibenzocyclooctynyl-poly(ethylene glycol)	MALDI-MS analysis of functionalized PEG	Zheng et al. (2012)
APCI		
Poly(propylene glycol) and polyisobutylene	ASAP-MS ^a of low MW polymers in engine oil deposit	Snyder and Wesdemiotis (2021)
Polymethacrylate-poly(ethylene glycol) hydrogel	ASAP-MS ^a of high MW crosslinked network	Endres et al. (2021)
Polyesters	DART-MS ^a and ASAP-MS analysis of food contact materials	Osorio et al. (2022)

Abbreviations: APCI, atmospheric pressure chemical ionization; ESI, electrospray ionization; LC, liquid chromatography; MALDI, matrix-assisted laser desorption ionization; MS, mass spectrometry.

^aAtmospheric solids analysis probe (ASAP) and direct analysis in real-time (DART) utilize APCI for ion formation (vide infra).

ditions) on Wiley Online Library for rules of use; OA articles are governed by the applicable Creative Commons

2 | IONIZATION TECHNIQUES AND SAMPLE PREPARATION FOR POLYMER ANALYSES

2.1 | Basic concepts of ESI

ESI is a soft ionization technique for dissolved samples which pass through a narrow-diameter metal or silica quartz capillary held at a high voltage (Fenn et al., 1989). The flow of analyte solution through this capillary results in the formation of a Taylor cone and subsequent fine mist of charged droplets containing analyte and solvent molecules with the same polarity as the capillary (Ho et al., 2003). A heated desolvation gas, typically nitrogen at temperatures above 80°C, causes the solvent molecules to vaporize from the droplets and produces gas-phase ions, which are attracted to the oppositely charged sampling cone of the mass analyzer (Figure 2). This process results in less fragmentation than hard ionization methods such as EI, making ESI ideal for the ionization of synthetic polymers and other types of macromolecules (Soeriyadi et al., 2013).

The ESI source was developed using a quadrupole (Q) mass analyzer (Fenn et al., 1989), but today a variety of mass analyzers can be interfaced with this device, including, but not limited to, time-of-flight (ToF), ion cyclotron resonance (ICR) trap, quadrupole ion trap (QIT), and Q/ToF analyzers. Depending on the desired information, ESI can be configured with these analyzers to elucidate the repeat unit(s), end groups, number-average MW ($M_{\rm n}$), weight-average MW ($M_{\rm w}$), and molecular architecture (via fragmentation) of polymers (Buback et al., 2007).

Despite the widespread use of ESI, the final stage by which gas-phase ions are produced from the charged

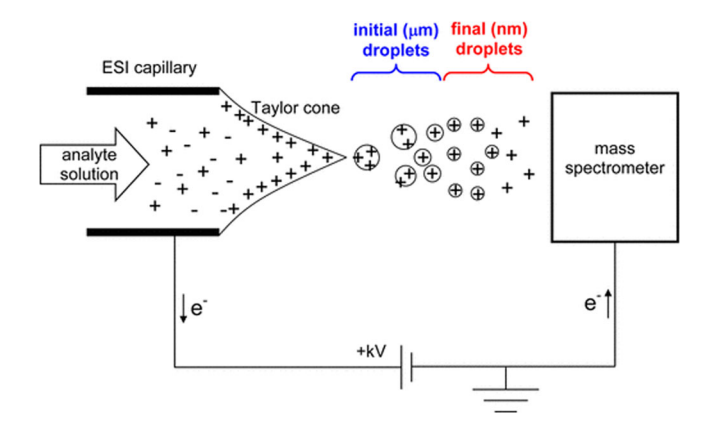


FIGURE 2 Schematic depicting ESI ionization to positive ions, where the sprayer acts as the anode and the MS inlet is the cathode. Adapted from Konermann et al. (2013) with permission from the American Chemical Society. ESI, electrospray ionization. [Color figure can be viewed at wileyonlinelibrary.com]

droplets is still debated. Three models have been extensively discussed thus far: the ion evaporation model (IEM), the charge residue model (CRM), and the chain ejection model (CEM) (Konermann et al., 2013). The IEM suggests that as the solvent molecules evaporate and the droplet radius becomes increasingly smaller the surface charge eventually becomes large enough for individual ions to desorb into the gas phase (Aliyari & Konermann, 2020). The CRM proposes that as the droplet radius decreases, a series of Coulombic explosions take place and result in the formation of single ions (Pimlott & Konermann, 2021). The CEM is typically associated with highly charged unfolded proteins and peptides as well as disordered, hydrophobic chains. It suggests that hydrophobic and electrostatic interactions force extended molecules to the droplet surface; when these molecules are ejected from the droplet, their extended conformation allows them to carry substantially more charges than a folded conformation (Metwally et al., 2018). As of now, the IEM is favored for describing the ionization of small molecules whereas the CRM is favored for describing the ionization of large macromolecules (Alivari & Konermann, 2020).

Polymers are mixtures of differently sized macromolecules and the complexity of this mixture, defined by the PDI, often has an impact on the resulting MS analysis. During ESI, some mixture constituents can experience ion suppression if they cannot be efficiently transferred from solution into the gas phase (Volmer & Jessome, 2006). Such suppression effects have been observed for the heavier chains within polydisperse polymers due to poorer solubility in the solvent used and the higher surface tension of droplets with heavier chains (X. M. Liu et al., 2003). Ion suppression may occur across the MW range of a polymer if the sample analyzed contains nonvolatile salts, which suppress solvent evaporation and analyte transfer into the gas phase, or admixtures that compete for the charges available such as contaminants with high proton or metal ion affinities (Volmer & Jessome, 2006). Suppression effects are avoided or minimized by using dilute sample solutions, purifying the analyte, switching to negative mode ESI (if possible) which is less sensitive to ion suppression than the positive mode, or utilizing a different ambient ionization technique such as APCI (Antignac et al., 2005).

Figure 3 exemplifies the results of ESI-MS analysis for a poly(butylene adipate) (pBA) sample ($M_n \approx 800 \, \text{Da}$), synthesized by condensation polymerization of adipic acid with excess of butanediol to instill hydroxy-butyl groups at both chain ends (Scionti & Wesdemiotis, 2012a).

The singly charged distribution of $[M + Na]^+$ ions dominates $(A_n \text{ labels})$ but a doubly charged $[M + 2Na]^{2+}$ distribution (*labels) is clearly discerned even at this relatively small polymer size. In addition, the spectrum

FIGURE 3 ESI-MS spectrum of poly(butylene adipate), pBA, acquired on a QIT mass spectrometer. All peaks correspond to [M + Na]⁺ ions. Adapted from Scionti and Wesdemiotis (2012a) with permission from John Wiley & Sons. ESI-MS, electrospray ionization-mass spectrometry; pBA, poly(butylene adipate); QIT, quadrupole ion trap. [Color figure can be viewed at wileyonlinelibrary.com]

provides evidence for the cogeneration of pBA macrocycles (C_n labels). Expectedly, the cyclic byproduct is most prominent at the smallest chain length, at which cyclization is entropically favored. Note that the distance between adjacent oligomers of the same distribution reveals the mass of the repeat unit (200.10 Da, $C_{10}H_{16}O_4$); whereas the m/z values of individual oligomers reveal the mass of the end groups. For example, the peak at m/z 713.37 (A_3) agrees well with the composition ($C_{10}H_{16}O_4$)₃ (600.30 Da) + $C_4H_{10}O_2$ (90.07 Da) + Na (23.00 Da) = 713.37, confirming the dihydroxy chain end nature of the main product. Conversely, peaks within the C_n distributions agree well with the composition ($C_{10}H_{16}O_4$)_n + Na, consistent with the absence of end groups in macrocycles.

The charge state of ESI-generated ions can easily be deciphered from their isotope patterns. The distance between adjacent isotopes is 1/x mass-to-charge ratio units for ions in charge state +x or -x. For example, the 13 C satellite of a polyacrylate [M + 2Na] $^{2+}$ ion will appear $\frac{1}{2} = 0.5 \ m/z$ units higher than the all- 12 C (i.e., the monoisotopic) peak. In the absence of isotopic resolution, the charge state can be determined from the distance between adjacent oligomers. For a poly(ethyl acrylate) with a $C_5H_8O_2$ repeat unit (100 Da), the n-mer and (n+1)-mer of the [M + 4Na] $^{4+}$ distribution will be $100/4 = 25 \ m/z$ units apart from each other, whereas the distance between adjacent oligomers of the [M + 3Na] $^{3+}$ distribution will be $100/3 = 33.3 \ m/z$ units.

The ESI-MS spectra of polymers with higher MW are generally more complex than the spectrum shown in Figure 3 due to the formation of multiply charged ions. As presented in Figure 4, polysaccharides such as

dextran can easily accommodate multiple charges, shifting their observed ion distributions to lower m/zvalues than the average MW of the material. The charge states of the detected ions can be determined based on the shift in m/z between adjacent *n*-mers and the isotope patterns. In the case of this dextran study (Chao et al., 2022), singly, doubly, triply, and quadruply charged oligomers with isotope spacings of 1.0, 0.5, 0.33, and 0.25 m/z units, respectively, were observed for the 5 kDa sample. Whereas for the 12 kDa sample, singly and doubly charged ions were absent, but ions with 3-6 charges were observed. For simplicity, the ions were divided into regions according to their average monomer/charge (M/C) ratio, cf. Figure 4. For example, all peaks within the highlighted M/C = 7 regions represent ions with one adducted charge (Na⁺) per seven repeat units; whereas all peaks between the highlighted M/C regions 7 and 8 have 7 < M/C < 8.

2.2 | ESI sample preparation

Solubility is vital to ESI-MS, and therefore, it constitutes one of the largest limitations for ESI-MS applications to synthetic polymers. Sample preparation for introduction to the ESI source is relatively simple and consists of selecting a suitable solvent, dilution of the sample, and optional addition of acid or salt. Due to the narrow inner diameter of the ESI emitter, filtration is often necessary to prevent capillary clogging or issues with a consistent flow. The solvent must be polarizable in the presence of an external electric field, capable of solubilizing the analyte, and have a high enough vapor pressure to facilitate desolvation and ionization. Commonly used solvents include neat methanol, 50:50 water/methanol, 50:50 water/acetonitrile, or neat acetonitrile. Occasionally, cosolvents may be added to solubilize compounds, such as tetrahydrofuran (THF), DMF (N,N-dimethylformamide), and dimethyl sulfoxide in very low quantities. Pure water is rarely ever used in ESI due to its low vapor pressure which negatively affects sensitivity (Ikonomou et al., 1991). Samples are typically diluted into the microgram-per-milliliter range, though further dilution is occasionally necessary to prevent overloading the detector or dirtying the source chamber. The addition of volatile salts and weak acids or their conjugate bases, such as ammonium acetate (NH₄OAc), formic acid (FA), trifluoroacetic acid (TFA), or sodium trifluoroacetate (NaTFA), can assist in the ionization of larger macromolecular structures. These concentrations should be kept low (<10 mM or $\sim 0.1\%$ –1% v/v) to avoid signal suppression (Constantopoulos et al., 1999).

10982787, 2024, 3, Downloaded from https://analytical

com/doi/10.1002/mas.21844 by Chrys Wesdemiotis

, Wiley Online Library on [23/07/2024]. See the Terms

nditions) on Wiley Online Library for rules of use; OA articles are governed by the applicable Creative Commons I

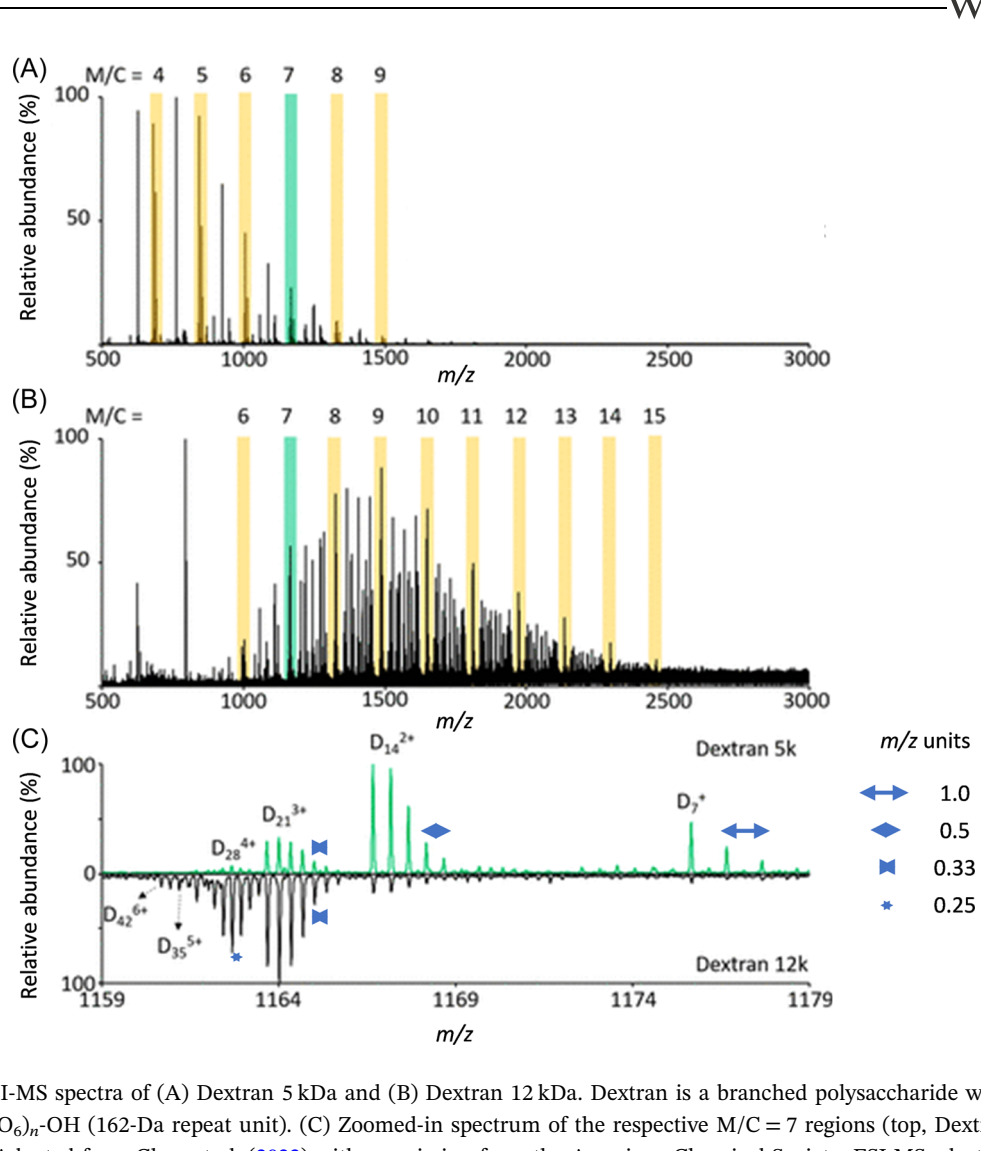


FIGURE 4 ESI-MS spectra of (A) Dextran 5 kDa and (B) Dextran 12 kDa. Dextran is a branched polysaccharide with the chemical formula $H-(C_6H_{12}O_6)_n$ -OH (162-Da repeat unit). (C) Zoomed-in spectrum of the respective M/C = 7 regions (top, Dextran 5 kDa; bottom, Dextran 12 kDa). Adapted from Chao et al. (2022) with permission from the American Chemical Society. ESI-MS, electrospray ionization-mass spectrometry. [Color figure can be viewed at wileyonlinelibrary.com]

2.3 | Advantages and disadvantages of ESI

ESI presents advantages and disadvantages dependent upon the molecule to be analyzed. A practical mass range of up to 70 kDa (contingent on the coupled mass analyzer) and sensitivity in the femtomolar to low picomolar range are positive characteristics of ESI. It is easily interfaced with liquid chromatography instrumentation and tandem MS analyzers, which is often necessary to characterize complex mixtures (Siuzdak, 2006). A further advantage of ESI is that it can produce multiply charged ions which is beneficial for analyzing high-mass molecules using a limited m/z range instrument; mass resolution and sensitivity are also generally higher at lower m/z ranges (m/z <3000). However, multiple charging also poses a disadvantage when

charge distributions overlap, producing complex and even uninterpretable spectra (Banerjee & Mazumdar, 2012). Additionally, competitive ionization can result in signal suppression of multicomponent mixtures, resulting in misleadingly simple spectra. Although competitive ionization can be overcome with separation techniques, differences among the ionization efficiencies of the various mixture species prevent direct quantitation based on peak intensities alone (see also Quantitative Analysis section). ESI is often coupled to higher mass accuracy analyzers such as Q/ToF or Orbitrap instruments, allowing for higher sensitivity of mixtures and higher selectivity when conducting tandem MS experiments. In general, higher sample purity is required for ESI than other ionization methods (vide infra), and carryover from sample to sample can be problematic (El-Aneed et al., 2009).

FIGURE 5 Schematic depicting the general MALDI ionization process. Adapted from https://commons.wikimedia.org/wiki/File:Maldi.PNG. MALDI, matrix-assisted laser desorption/ionization. [Color figure can be viewed at wileyonlinelibrary.com]

2.4 | Basic concepts of MALDI

MALDI is a versatile soft ionization technique that utilizes a laser to rapidly heat a mixture of analyte and crystalline organic matrix molecules, causing ablation and vaporization of the molecules from the sample holder, cf. Figure 5 (Karas et al., 1987; Tanaka et al., 1988). Typical laser sources used are the neodymiumdoped yttrium aluminum garnet (Nd:YAG, 266 or 355 nm), nitrogen (337 nm), erbium-doped yttrium aluminum garnet (Er:YAG, 2.94 µm), and CO₂ (10.6 µm). The vaporized matrix expands into the gas phase and pulls intact analyte molecules into the expanding matrix plume (W. C. Chang et al., 2007). According to the photochemical ionization (PI) model, matrix molecules and their fragments can be photoionized and subsequently ionize analyte molecules by proton transfer (Dreisewerd, 2003). For molecules that do not protonate easily due to low gas-phase basicity, a metal salt is added to the matrix to generate gaseous metal ions in the matrix plume, which can ionize the sample by metal ion adduction (Hanton & Owens, 2012). Another mechanism, the cluster ionization (CI) model, proposes that strong photo-absorption by the matrix causes charged particles to desorb, followed by desolvation of matrix from the clusters to produce analyte ions (Karas & Krüger, 2003). MALDI sources are typically coupled to ToF, ToF/ToF, Q/ToF, and ICR analyzers, but all other types of mass spectrometers can also be equipped with MALDI, especially MALDI sources operating at atmospheric pressure (Keller et al., 2018; Laiko et al., 2000).

2.5 | MALDI sample preparation

Preparation of samples for MALDI analysis is relatively straightforward and consists of mixing the analyte and matrix in a molar ratio of 1:1000-10,000 and adding ionization agents, such as sodium or silver salts, to promote ionization (Montaudo et al., 2006). Typical matrices used for polymer analysis are α-cyano-4hydroxycinnamic acid (CHCA), 2,5-dihydroxybenzoic dithranol (DIT), acid (DHB), trans-2-[3-(4-tert-Butylphenyl)-2-methyl-2-propenylidene] malononitrile (DCTB), and trans-3-indoleacrylic acid (IAA) (Nielen, 1999). Several strategies exist for the addition of matrix and analyte to the MALDI sample holder, though the dried droplet and sandwich methods are the most popular. In dried droplet, analyte and matrix solutions (or analyte, matrix, and salt solutions) are combined and a small amount of the mixture (~0.3 µL) is spotted onto the target plate where solvent evaporation occurs, producing crystals. This conventional dried droplet method is suitable for most soluble polymers but can result in the formation of irregular heterogenous crystals (Patil et al., 2018). Nonhomogenous crystals can hinder reproducibility and decrease mass resolution presenting the need for additional preparation methods. An alternative method is the sandwich technique, in which a drop of matrix solution (or matrix plus salt solution) is first applied onto the target plate, and the solvent is allowed to evaporate, followed by the addition of analyte solution and subsequent solvent evaporation. A final drop of matrix (or matrix plus salt) solution is then spotted onto the two layers of dried matrix and analyte, forming a "sandwich" of matrix/salt:analyte:matrix/salt (Kussmann & Roepstorff, 2000).

Unlike ESI, MALDI does not require that the sample be soluble. Solvent-free MALDI can be used with polymers that are insoluble in common organic or aqueous media (Trimpin et al., 2006). In such cases, a small amount of the polymer, ideally in pulverized form, is mechanically mixed with the solid matrix (plus salt if needed), and a few μ g of the mixture are deposited onto the target plate for analysis (Hanton & Parees, 2005; Skelton et al., 2000). Alternatively, polymer, matrix, and salt may be mixed with solvent to form a paste, before a small amount of the well-mixed paste is applied onto the target plate for analysis (Gies & Nonidez, 2004).

2.6 | Advantages and disadvantages of MALDI

MALDI is suitable for high throughput studies, as target plates contain several hundreds of sample wells for the rapid analysis of many compounds. MALDI has a practical mass range of 300 kDa, and often much higher masses can be observed with linear ToF analyzers (Kussmann & Roepstorff, 2000). These upper mass limits apply only to monodisperse macromolecules. For polymeric species, polydispersity lowers the signal-to-noise ratio as mass increases, limiting adequate mass analysis to ~50–100 kDa. The lower transmission and detection sensitivity of the larger oligomers also prevents observation of the actual MW distribution if the *PDI* surpasses ~1.7; in such cases, the MALDI mass spectra are dominated by low mass oligomers and lead to underestimated average MWs.

Fragmentation during desorption and ionization is highly limited or absent if the proper matrix is chosen and a low laser power is used (Montaudo et al., 2006). MALDI provides sensitivities in the femtomole to low picomole range, making it suitable for detecting unwanted byproducts, impurities, and degradation products. Low mass analytes (<700 Da) can be problematic due to matrix interference and detector saturation, though these issues can be resolved by using higher MW matrices, such as porphyrins, or inorganic matrices (Cohen & Gusev, 2002). Since most matrices are organic acids and laser excitation is used, the possibility of photodegradation (Diepens & Gijsman, 2007), end group modification (Charles, 2014), and acidic degradation of the analyte (Li, Guo, et al., 2011) exists with MALDI.

A major advantage of MALDI is that it generally produces singly charged ions, in which case m/z and mass scales are identical. This facilitates the analysis of mixtures, as will be illustrated with the elucidation of a chain-end functionalization reaction concerning the addition of a polymeric silvl hydride to a terminal double bond, cf. Figure 6A (Quirk et al., 2008). The MALDI-MS spectrum of the functionalization product (Figure 6B) includes three PS distributions with the expected 104-Da repeat unit (C₈H₈), labeled by 1, 2, and 3. The major distribution 1 arises from the desired trimethoxysilyl PS, confirming successful hydrosilation with a polymeric silane according to the reaction in Figure 6A. Although this polymer is the main product, two byproducts are also detected, one slightly lower in mass (2) and one at approximately twice the MW of the desired product (3). Product 2 is formed by H/vinyl exchange during the hydrosilation process, which results in a vinyl silane functionalized PS lacking the trimethoxysilyl substituent; since product 2 contains a terminal double bond, it can also undergo hydrosilation, leading to the dimeric chain 3. This MALDI-MS example clearly documents the dispersive power of MS, which makes it possible to separate byproducts from the main product, so that they can be detected and characterized with confidence, even if they are present in low concentrations. Figure 6C shows an expanded view of Figure 6B, displaying the m/z window covering the 13- and 14-mer of the main distribution 1. It provides a primer for spectral interpretation which is done based on both m/zvalues and isotope patterns. Most elements include abundant stable isotopes that contribute to the isotope cluster of the molecule in which they are contained. For the functionalized PS examined, isotope clusters are observed for each [M + Ag]⁺ ion due to the presence of ¹²C/¹³C and ²⁸Si/²⁹Si/³⁰Si in each macromolecular chain and from the silver cation added upon MALDI, which comprises two isotopes, ¹⁰⁷Ag/¹⁰⁹Ag. The lowest mass isotope of $[M + Ag]^+$ is designated as its monoisotopic mass, which is 1723.88 Da for the 13-mer and 1827.94 Da for the 14-mer. These masses differ significantly from the corresponding average masses, which are 1726.32 and 1830.47 Da, respectively. The latter are used if the isotopes become unresolved, which may occur within m/z~3000-10,000 depending on the instrument's mass resolution. A specific elemental composition is confirmed by calculating the isotope pattern of the expected composition and comparing both simulated isotope pattern and monoisotopic mass with the corresponding measured values, as shown in Figure 6C. This procedure was followed to deduce the compositions of distributions 1, 2, and 3 in Figure 6B (and all other compositions discussed in this review).

When the molecular mass surpasses ~6000 Da, the relative intensity of the lowest mass isotope may be too low to be clearly discernable above noise level. The most abundant isotope, which lies closer to the average mass value, is then used for accurate mass measurement, as illustrated in Figure 7 for a poly(ethylene glycol), PEG, derivatized with dibenzocyclooctynyl (DIBO) substituents at both chain ends (Zheng et al., 2012).

2.7 | Basic concepts of APCI

In APCI, a fine spray of analyte droplets passes through a corona discharge at ambient pressure. Reagent ions are generated in this event that ionize the vaporized analyte molecules (M) via ion-molecule reactions (Andrade et al., 2008; Waters Corporation, 2017). A pneumatic nebulizer assists in the formation of the droplets. Usually, N₂(g) serves as the nebulizing gas, causing the formation of N2++ ions that initiate a cascade of ionmolecule reactions with the spray solvent (H₂O, MeOH) to ultimately form protonated or deprotonated solvent clusters (cf. Scheme 1A and B). The sample molecules can be ionized to M⁺ by charge transfer from N₂⁺ and to $[M + H]^+$ or $[M - H]^-$ ions by proton transfer with the solvent cluster ions (Scheme 1C and D). Since ionization is performed at atmospheric pressure, the ions formed by APCI are collisionally cooled, which limits their consecutive fragmentation that usually occurs under vacuum CI

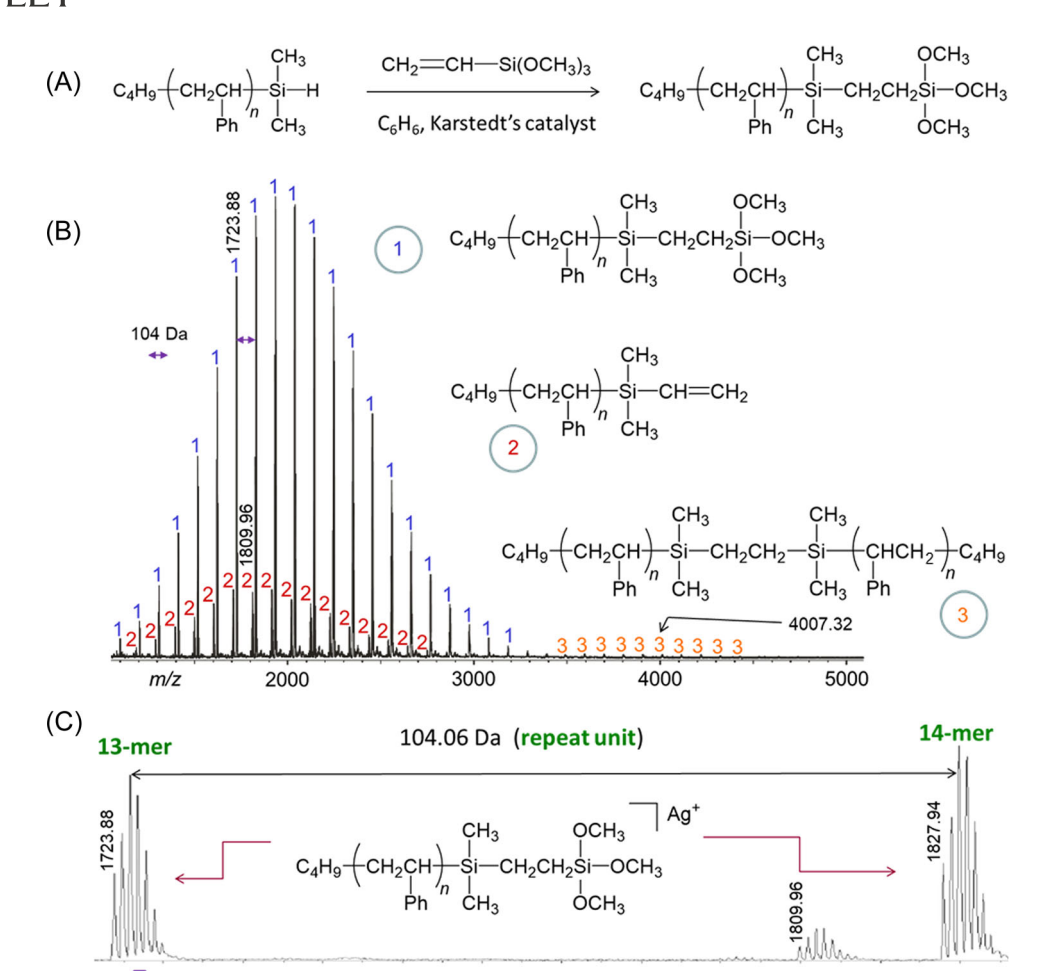


FIGURE 6 (A) Hydrosilation of vinyl trimethoxy silane with silyl hydride functionalized polystyrene (PS) to introduce a polar end group at the polymer chain end. The PS prepolymer was synthesized by living anionic polymerization using sec-butyllithium for initiation and chlorodimethylsilane for termination. (B) MALDI-MS spectrum of trimethoxysilyl functionalized polystyrene, acquired on a ToF/ToF instrument, using dithranol as matrix and silver trifluoroacetate as cationizing agent. All peaks correspond to $[M + Ag]^+$ ions; monoisotopic m/z values are given for one peak in each of the three distributions observed. (C) Zoom-in view of the m/z 1720–1835 window of the MALDI-MS spectrum, showing resolved isotope clusters. Adapted from Quirk et al. (2008) with permission from the American Chemical Society Rubber Division. MALDI-MS, matrix-assisted laser desorption/ionization-mass spectrometry; ToF, time-of-flight. [Color figure can be viewed at wileyonlinelibrary.com]

calculated

n = 13

conditions; hence, APCI counts as a soft ionization method, similar to ESI and MALDI. The APCI mechanism commonly results in singly charged ions, and the observation of intact molecular compositions is typically limited to species <1000 Da.

measured

Sample preparation is similar to that of ESI-MS; however, APCI does not require polar solvents. This provides an alternative ionization technique to species insoluble in polar organic solvents or structurally resistant to ESI, such as hydrocarbons and poly(fluoroalkyl) substances (PFAS); additionally, APCI serves as the main ionization technique in LC-MS with normal

phase chromatography. Most modern LC-MS instruments come with interchangeable ESI/APCI sources to allow for both modes of ionization coupled to chromatography (see Section 4).

Composition deduced from m/z value and isotopic

distribution

2.8 | Atmospheric solids analysis probe (ASAP)

APCI is employed in the ASAP which utilizes a nebulizing gas to pyrolyze/ionize polymeric materials under ambient pressure in the presence of a corona

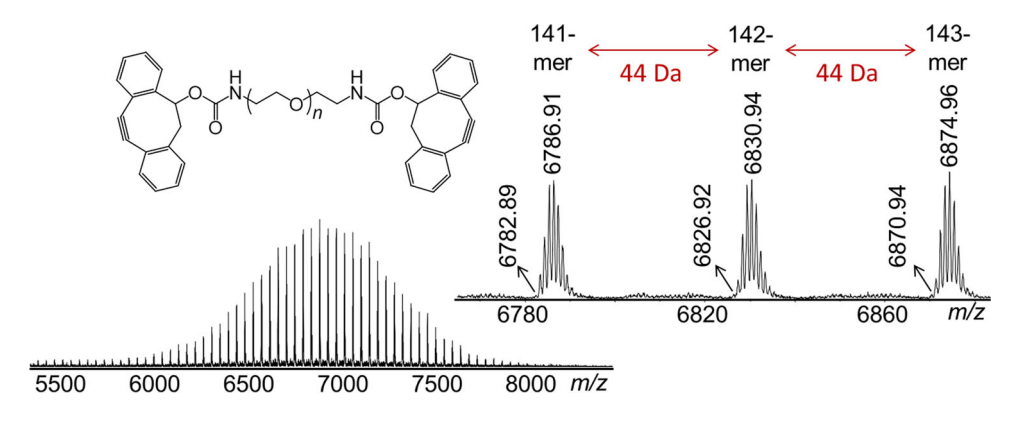


FIGURE 7 MALDI-MS spectrum of dibenzocyclooctynyl poly(ethylene glycol) (DIBO-PEG), acquired on a ToF/ToF instrument using DCTB as matrix and sodium trifluoroacetate as cationizing agent. All peaks correspond to $[M + Na]^+$ ions. The inset shows a zoom-in view of the m/z window of PEG chains with 141-143 repeat units; the m/z values marked are for the lowest mass isotope and most abundant isotope. The corresponding average masses are 6787.03, 6831.08, and 6875.13 Da, respectively. Reproduced from Zheng et al. (2012) with permission from the American Chemical Society. MALDI-MS, matrix-assisted laser desorption/ionization-mass spectrometry; ToF, time-offlight. [Color figure can be viewed at wileyonlinelibrary.com]

(A)
$$N_2 + e^- \rightarrow N_2^{+\bullet} + 2e^-$$

 $N_2^{+\bullet} + ROH \rightarrow N_2 + ROH^{+\bullet} (R = H \text{ or } CH_3)$
 $ROH^{+\bullet} + ROH \rightarrow ROH_2^+ + RO^{\bullet}$
 $ROH_2^+ + nROH \rightarrow ROH_2^+ (ROH)_n$

(B)
$$O_2 + e^- \rightarrow O_2^{-\bullet}$$

 $O_2^{-\bullet} + ROH \rightarrow RO^- + H^{\bullet} + O_2$
 $RO^- + nROH \rightarrow RO^-(ROH)_n$

(C)
$$M + N_2^{+\bullet} \to M^{+\bullet} + N_2$$

 $M + ROH_2^{+}(ROH)_n \to [M + H]^{+} + (n + 1)ROH$

(D)
$$M + RO^{-}(ROH)_{n} \rightarrow [M - H]^{-} + (n + 1)ROH$$

SCHEME 1 Reagent ions formed in the APCI source under (A) positive and (B) negative ion mode operation. Charged molecular species formed under (C) positive and (D) negative ion mode conditions. APCI, atmospheric pressure chemical ionization.

discharge, cf. Figure 8 (McEwen et al., 2005; Waters Corporation, 2017). The nebulizing gas (N_2) can be heated up to ~500-600°C to cause thermal desorption and thermal degradation of the sample, which is applied onto a glass capillary. Increasing the temperature of the nebulizing gas causes molecules to desorb from the glass capillary and offers the ability to gain boiling point profiles for volatile components (Tose et al., 2017; Waters Corporation, 2017). Thermal degradation of the nonvolatile components also occurs and is enhanced with increasing temperature of the nebulizing gas (Alawani et al., 2022). The desorbed neutral molecules and thermal degradation products are ionized in situ by APCI and

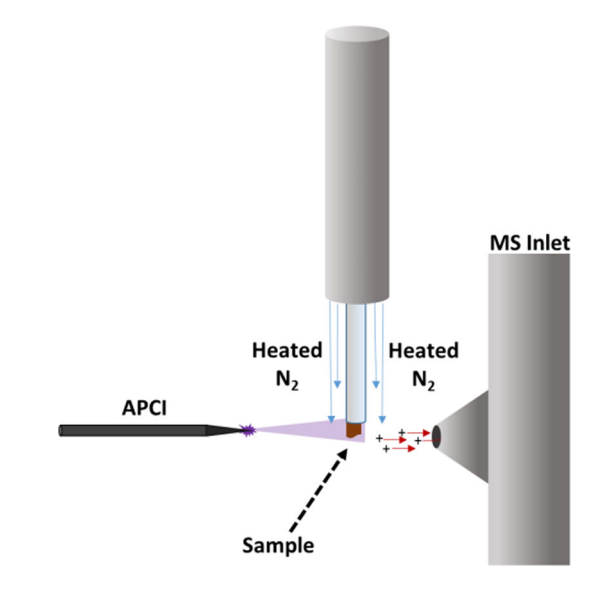


FIGURE 8 Schematic of the ASAP source. Adapted from Endres et al. (2021) with permission from the American Chemical Society. ASAP, atmospheric solids analysis probe. [Color figure can be viewed at wileyonlinelibrary.com]

sent to the mass analyzer for m/z measurement and identification. The N2 nebulizing gas and water moisture in the ASAP source give rise to $N_2^{+\bullet}$ and $(H_2O)_nH^+$ reagent ions that ionize desorbates and degradants via charge exchange (to $M^{+\bullet}$) and protonation (to $[M + H]^{+}$), respectively (Alawani et al., 2022; Endres et al., 2021).

ASAP-MS has been used in a variety of analyses, including the characterization of lipids (Pizzo et al., 2022), pesticides and agricultural pharmaceuticals in food (Fussell et al., 2010), particulate matter in vehicular engines (Snyder & Wesdemiotis, 2021), and synthetic polymers and polymer additives (Fouquet et al., 2015;

10982787, 2024, 3, Downloaded from https://analyticalsc

.com/doi/10.1002/mas.21844 by Chrys Wesdemiotis

University Of Akron Bierce Library, Wiley Online Library on [23/07/2024]. See the Terms

on Wiley Online Library for rules of use; OA articles are

Lebeau & Ferry, 2015; Smith et al., 2012; Trimpin et al., 2009). The analytical information gained by ASAP is significantly enhanced if this ionization method is interfaced with ion mobility MS (IM-MS), which will be discussed under multidimensional MS techniques (vide infra). The ASAP-IM-MS approach has been successfully used to characterize lubricants (Barrère, Hubert-Roux, et al., 2014), polymers and polymer blends (Barrère, Selmi, et al., 2012, 2014), heavy petroleum fractions (Farenc et al., 2016), hydrogels (Endres et al., 2021), and thermoplastic elastomers (Alawani et al., 2022).

2.9 | Direct analysis in realtime (DART)

DART is a sample ionization technique that can ionize gases, liquids, or solids in open air (Cody et al., 2005). Like ESI, APCI, and ASAP, DART belongs to the family of atmospheric pressure ionization or ambient pressure ionization (API) methods that operate in the open laboratory without the need of vacuum systems (Weston, 2010).

Figure 9 shows a diagram of the basic components of a DART ion source. Helium gas is introduced into a high voltage region (1-5 kV) to create a glow discharge plasma containing ions, electrons, and electronically excited (metastable) He atoms (He*). After the ions and electrons are deflected electrostatically, the metastable gas passes through a heater (≤500°C), and the hot He* atoms exit the source and collide with the sample and molecules present in the atmosphere. The energy of He* atoms (19.8 eV) is sufficient to ionize desorbed sample molecules (M) through Penning ionization, $M + He^* \rightarrow M^{+*} +$ He + e⁻. Atmospheric water is also ionized and forms $H_3O^+(H_2O)_n$ clusters (cf. Scheme 1), which can transfer a proton to sample molecules to yield [M + H]+ ions (Pavlovich et al., 2018). In negative ion mode, electrons released by Penning events are captured by atmospheric O₂, forming O₂^{-•} and HO⁻ reagent anions (cf. Scheme 1) that can deprotonate acidic analytes to [M – H]⁻ anions.

Direct e⁻ capture by sample molecules with electronegative substituents to produce M^{-*} radical anions is also possible (Pavlovich et al., 2018).

He has been the most widely used ionization gas, as the highly energized He* atoms (19.8 eV) enable efficient ionization of most types of analytes via electron or proton transfer (vide supra). N_2 (lowest metastable state at 6.2 eV), which is a cost-effective alternative gas, can successfully ionize polar organic compounds, but with lower sensitivity and higher limits of detection (Song et al., 2018). Ionizing gas temperature is the most critical parameter for maximizing DART-MS intensities (Sisco et al., 2020).

DART-MS has been applied to characterize chemical compounds in food (Hajslova et al., 2011), forensic samples (Pavlovich et al., 2018), warfare agents (Forbes & Sisco, 2018), and pharmaceuticals (Vaclavik et al., 2014). Applications to synthetic polymers are scarce and so far have been limited to the characterization of low MW standards (Bridoux & Machuron-Mandard, 2013), differentiation of nylon types (Zughaibi & Steiner, 2020), identification of polyamides in consumer products (Abe et al., 2020), and investigation of the miscibility of polymer blends in films prepared by solvent casting (AlShehri et al., 2022). The DART sources utilized for polymers were coupled to ToF or Orbitrap mass spectrometers, but the source can be attached to most commercially available mass spectrometers (Pavlovich et al., 2018).

2.10 | Sample preparation for ASAP and DART

A major benefit for both of these ionization methods is that they do not require extensive sample preparation protocols. For ASAP-MS studies of polymeric materials, a borosilicate melt point capillary is often used as a substrate for solid or liquid polymeric materials to adhere. This can be accomplished by rubbing the glass capillary onto the analyte material, dissolving the

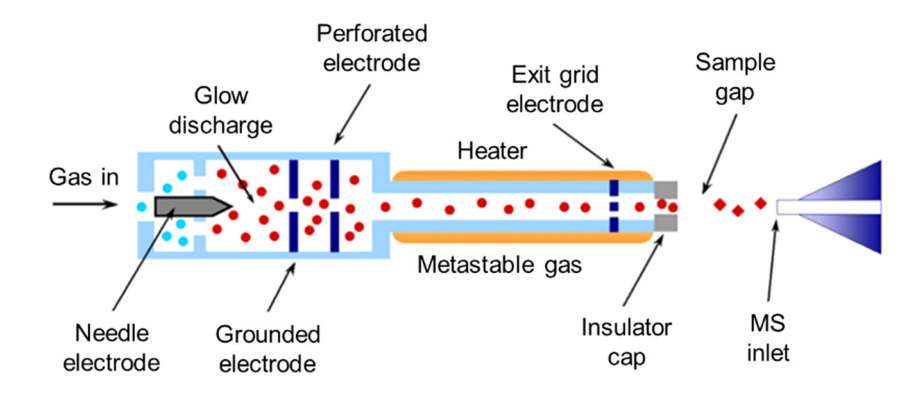


FIGURE 9 Schematic of the DART source. Reproduced from Hajslova et al. (2011) with permission from Elsevier. DART, direct analysis in real-time. [Color figure can be viewed at wileyonlinelibrary.com]

10827827820243, D. Downloaded from https://analytical circinergo-unidensing/analytical circinerg

material in a suitable solvent followed by dipping the glass capillary into the solution and allowing the solvent to evaporate (Trimpin et al., 2009), or melting the material, dipping the capillary into the melted sample, and allowing it to cool to room temperature (Alawani et al., 2022). ASAP tolerates a wide range of sample concentrations, as shown with the detection of metabolites at the ng/mL level (Zydel et al., 2012). Additionally, the open end of the glass capillary can be used to hold solid samples, thus facilitating the rapid analysis of materials (Endres et al., 2021). The glass capillary is then inserted into the probe of the ASAP source block and subjected to heating by the nebulizing gas whose temperature can be set within room temperature and 600°C and gradually increased or ramped in steps within this range. Noncrystalline, amorphic polymers can also be inserted directly into the probe if the material is too rigid to transfer to the capillaries. It should be noted that this can cause increased source contamination and will require thorough cleaning after the analysis. The physical probe used in ASAP-MS is inserted vertically, placing the sample orthogonally to the MS inlet and corona pin (cf. Figure 8). This geometry provides good proximity but can increase source contamination due to gravitational effects on loose sample crystals. The sample preparation for DART-MS is even simpler and has the advantage that the sample inlet is arranged horizontally and can simultaneously accommodate more than one sample. This allows for a cleaner analysis and high-throughput studies, unlike ASAP-MS which is limited to one capillary per analysis. DART is suitable for the analysis of solid, liquid, or gaseous samples. Solids are placed directly into the sample gap (Figure 9); liquids are analyzed by inserting a capillary or glass plate coated with the liquid into the sample gap; and vapors are introduced into the DART gas stream.

2.11 Advantages and disadvantages of ASAP and DART

A primary advantage for using the ASAP source is the potential for rapid sample analysis due to the minimal sample preparation necessary, which has contributed to expanding potential for field applications (McCullough et al., 2020). For complex polymer and additive mixtures the variable temperature ramping profile offers the potential for additives to be desorbed at lower temperatures and polymers to be desorbed at higher temperatures, which serves to remove low MW convolution in their spectra (Alawani et al., 2022; Snyder & Wesdemiotis, 2021). A disadvantage of using ASAP for the analysis of polymers is that thermal degradation can take place, which reduces the size (M_n) of the chains being analyzed. Hence the method is not suitable for MW determination of larger oligomers. However, since thermal degradation is performed under relatively mild conditions (≤600°C), end group, functional group, and connectivity information between (co)monomer units is retained in the observed products, providing important insight about the primary structure of the material under study (Alawani et al., 2022; Endres et al., 2021).

The utility of ASAP-MS will be illustrated with two examples of ASAP-MS, one involving mainly thermal desorption (Figure 10) and the other mainly thermal degradation (Figure 11). Figure 10 shows the ASAP-MS spectrum of a solid vehicular engine deposit, acquired at 325°C (Snyder & Wesdemiotis, 2021). It includes two poly (propylene glycol) (PPG) distributions with similar intensity, one with aminoethyl end groups at both chain ends (marked with red triangles) and one with H- and -OH end groups (green upside-down triangles), both of which are observed in the form of $[M + H]^+$ ions. Such low MW polyether amines and polyether alcohols are common detergent additives in motor oil packages. The third distribution (marked with purple asterisks) is accounted for by a polyisobutylene (PIB) decorated with ether and amine substituents that make it ionizable by protonation to $[M + H]^+$ ions; this family of PIB amines was recently introduced as a new detergent class of motor engine oils (Huo et al., 2017). The low MW and substitution pattern of these polymers allow for volatilization and desorption in intact form under ASAP-MS conditions. It is noteworthy that all three detected compounds are amphiphilic, containing structural features that can develop the noncovalent intermolecular interactions needed to cause particulate formation and deposition in vehicular engines.

Additionally, ASAP-MS has enabled the structural characterization of physically or chemically crosslinked materials, which are not directly amenable to other MS ionization methods and difficult to characterize by other spectroscopic methods due to infinite MW and/or insolubility. Figure 11 provides such an example for a PEG hydrogel, prepared by photochemically crosslinking PEG dimethacrylate (PEGDMA) to form polymethacrylate (PMA) chains interconnected with PEG chains (Figure 11A; Endres et al., 2021). The ASAP-MS spectrum obtained by thermal degradation at 450°C (Figure 11B) includes PMA-PEG copolymeric oligomers generated by homolytic bond cleavages in the crosslinked PMA and PEG chains (C_A, C_B, C_C, and C_D). Methacrylate substituted PEG from unreacted chain ends of the PEGDMA precursor is also observed (B₁₁ Figure 11B). The observation of copolymeric degradants confirms that the hydrogel was chemically crosslinked and not a mere noncovalent (supramolecular) aggregate of PEGDMA units. The ASAP-MS data also identify the

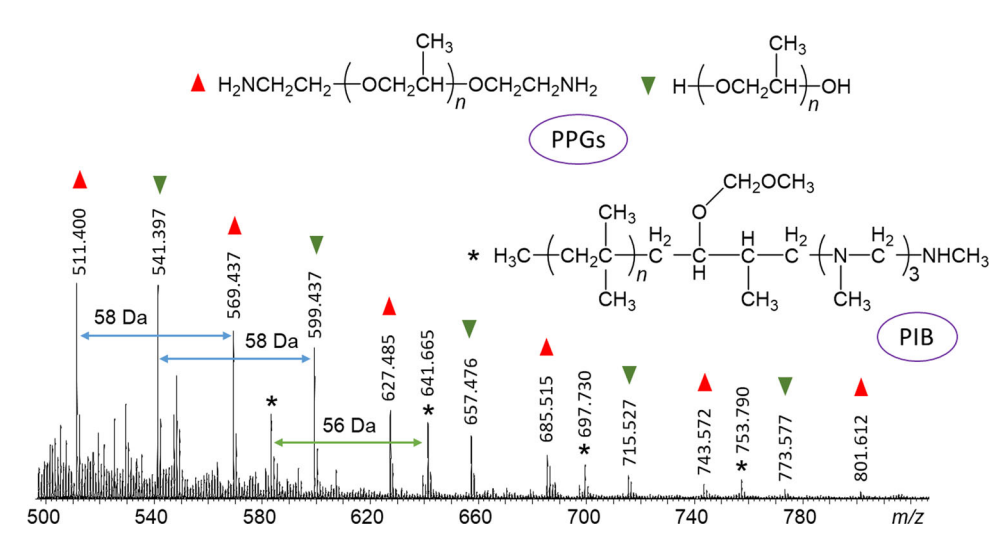


FIGURE 10 ASAP-MS spectrum of an unknown vehicular engine deposit, acquired at 325°C on a Q/ToF mass spectrometer. Reproduced from Snyder and Wesdemiotis (2021) with permission from the American Chemical Society. ASAP-MS, atmospheric solids analysis probe-mass spectrometry; ToF, time-of-flight. [Color figure can be viewed at wileyonlinelibrary.com]

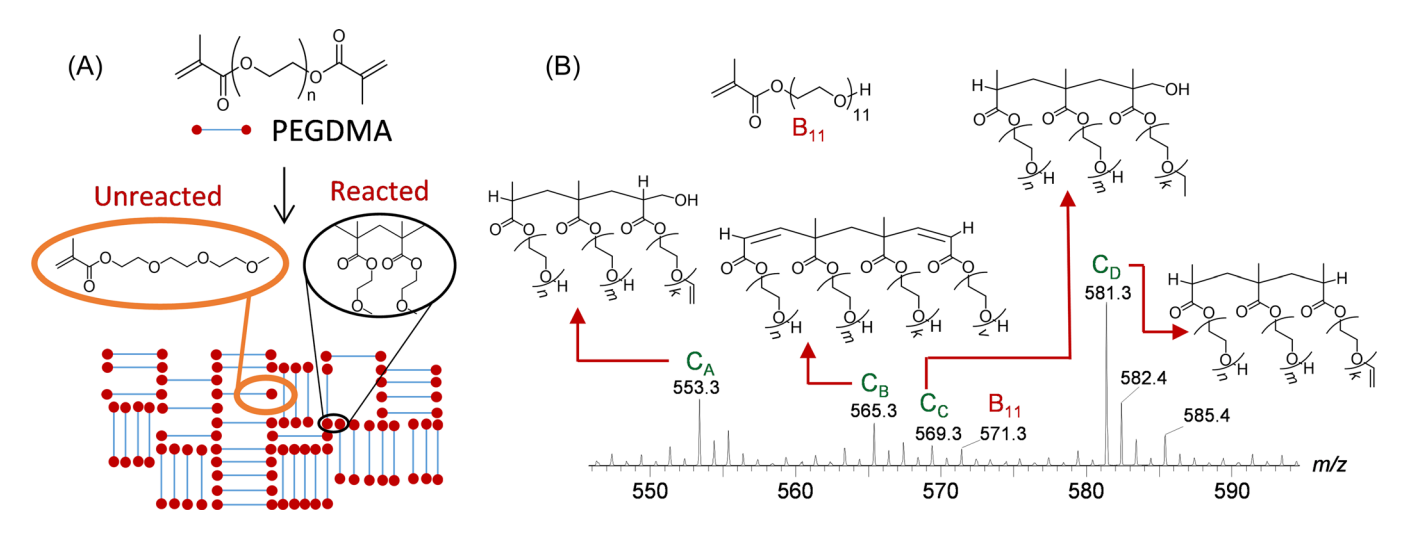


FIGURE 11 (A) Polymethacrylate (PMA)-PEG hydrogel from photoinduced radical polymerization of 4 kDa PEGDMA. (B) Partial ASAP-MS spectrum of the crosslinked hydrogel, acquired on a Q/ToF instrument. The copolymeric PMA-PEG oligomers identified within one PEG repeat unit are depicted on top of their $[M + H]^+$ ions (n + m + k + v = 6 or 7). The entire spectrum spans the m/z 350–750 range. Adapted from Endres et al. (2021) with permission from the American Chemical Society. ASAP-MS, atmospheric solids analysis probe-mass spectrometry; PEG, poly(ethylene glycol); PEGDMA, PEG dimethacrylate. [Color figure can be viewed at wileyonlinelibrary.com]

monomeric units in the hydrogel, thus allowing for deformulation of unknown materials.

Very few DART-MS studies on synthetic polymers have been reported thus far to allow for a meaningful assessment of its (dis)advantages for polymer analysis. The similarities of this ambient MS method with ASAP-MS suggests similar benefits, however. DART-MS should be particularly useful for the characterization of solid film surfaces and their headspace and, hence, could complement the available surface characterization techniques (vide supra). More studies are needed to confirm this premise.

Finally, it is noteworthy that ASAP and DART give rise to interpretable mass spectra without the need of a hyphenated separation method (cf. Figures 10 and 11). In contrast, thermal degradation with (micro)furnace or filament pyrolizers, which utilize higher temperatures (400–1000°C), yield more complicated mixtures, thus resulting in uninterpretable mass spectra (Gies, 2012; Rial-Otero et al., 2009). Typically, substituted monomers, dimers, and trimers are formed, whose identification requires online separation by gas chromatography (GC) followed by MS analysis using EI or CI (Tsuge & Ohtani, 1997). Nonetheless, this pyrolysis-GC-MS (Py-GC-MS) approach is regularly used

Wiley 44

in industrial laboratories to deformulate finished products. Py-GC-MS can provide important compositional information about (co)monomer content, thereby facilitating the interpretation of ASAP- or DART-MS spectra of industrial (co) polymers. Two limitations of Py-GC-MS are spectral irreproducibility and absence of signature peaks for products that are not suitable for GC or do not easily ionize (Analytical Methods Committee, 2018; Gies, 2012; Rial-Otero et al., 2009).

2.12 | Selecting an efficient ionization source

Choosing the best ionization source for a particular polymer sample is an essential component of method selection. Factors that must be considered include the sample solubility, polarity, thermal stability, $M_{\rm n}$, and $M_{\rm w}$. For polymers that are soluble and stable in volatile solvents (see Section 2.1) and contain polar moieties, ESI would be expected to produce efficient ionization with minimal source-induced fragmentation. Polar polymer samples with large $M_{\rm p}$ or $M_{\rm w}$ can produce convoluted spectra with multiple charge distributions in ESI, thus the MALDI source may be more appropriate for those cases in the absence of charge deconvolution algorithms (see Section 7). MALDI is not constrained by solubility requirements and typically produces only singly charged species from high MW analytes. APCI requires solubility and is limited to polymers of low MW but, unlike ESI, it can also be applied to less polar or nonpolar samples. On the other hand, the ASAP and DART variants, which utilize APCI for ion formation, are not constrained by solubility requirements and provide varying degrees of sample degradation depending on the temperature used as well as the thermal stability of the polymer. These APCI variants may be most useful for polymers with large M_n values where the mild thermal degradation of the polymer into smaller chains can provide analyzable MWs that still reveal relevant composition and connectivity information.

3 | STRUCTURAL CHARACTERIZATION VIA TANDEM MASS SPECTROMETRY (MS/MS) FRAGMENTATION

3.1 | MS/MS and multistage MS fundamentals

MS/MS involves selecting a specific ion, representative of a particular oligomer species (termed the "precursor ion"), and energetically activating this ion to dissociate into fragments that reveal structural information (Wesdemiotis, 2017). The three basic types of MS/MS scans are product ion scans, precursor ion scans, and neutral loss scans (De Hoffmann & Stroobant, 2007). Product ion scans are the most widely used variant and involve detection and identification of the fragment ions formed from a specific (mass-selected) oligomer ion (Crecelius et al., 2009; Wesdemiotis et al., 2011). Precursor ion scans and neutral loss scans are most beneficial for complex mixtures, as they identify all molecular ions in the mixture that produce a specific fragment ion or a defined neutral loss; these scans can provide quantitative information with appropriate internal standards, which are usually isotopomers of the molecules to be quantified.

Most reported polymer MS/MS studies have employed product ion scans (vide supra), which isolate an individual precursor ion to produce fragments that are structurally indicative for a single chain. Precursor ion scans and neutral loss scans are used widely in biomedical analyses via data dependent/independent acquisition (DDA/DIA) or sequential window acquisition of all theoretical masses (SWATH), to quantify or differentiate specifically derivatized metabolites (Hopfgartner et al., 2003) as well as biomolecules with similar structural features, such as the type of lipid head group and chain length (Lydic et al., 2009). Barely any applications of such scans have been reported for synthetic polymers. Applying precursor ion scans and neutral loss scans to copolymer mixtures could be a useful way to quantify the degree of repeating subunits. For example, a random copolymer with the composition A_nB_m could be scanned for the presence of A_x , B_y , or $A_x B_y$ fragments (x < n; y < m) to help characterize its sequence motifs.

Tandem mass spectrometers are classified as either tandem-in-space or tandem-in-time (Polce & Wesdemiotis, 2010; Scionti & Wesdemiotis, 2012b). Tandem-in-space (or beam) instruments are equipped with two independent mass analyzers (separated in space); the 1st is used for precursor ion selection and the 2nd for fragment ion analysis. A collision cell or other excitation section is generally placed between the two analyzers. Triple quadrupole (QqQ), Q/ToF, and ToF/ToF mass spectrometers are the most widely employed tandem-in space-instruments (q designates an RF-only quadrupole serving as collision cell). Commercial instrument configurations with more than two (Q or ToF) mass analyzers and intermediate collision cells are not available because their larger size (longer beam path) would make it difficult to maintain adequate vacuum and high ion transmission efficiencies. Finally, sector instruments, which were used in earlier MS/MS studies on synthetic polymers (Selby et al., 1994), are less common today.

MALDI-ToF mass spectrometers equipped with a reflectron allow for MS/MS experiments via the postsource decay (PSD) technique (De Hoffmann & Stroobant, 2007; Scionti & Wesdemiotis, 2012b). A higher laser power is used to produce energetically excited macromolecular ions ("metastable" ions) that dissociate after leaving the MALDI source. PSD probes the spontaneous fragmentations taking place in the fieldfree region between the ion source and the reflectron. All fragments formed in this space have the same velocity as their precursor ion; hence, an ion gate can be used to select a specific precursor ion and its fragments, as this ion family moves down the flight tube toward the reflectron. Precursor ion and fragments are separated based on their different kinetic energies inside the reflectron. The separated species are reflected back into the field-free region of the flight tube and now travel in the opposite direction to reach the detector and generate the PSD spectrum (Hanton et al., 2004). A similar concept is employed in ToF/ToF tandem mass spectrometers consisting of a linear ToF coupled to a reflectron ToF analyzer. Here, PSD takes place in the linear ToF and fragment mass analysis in the reflectron ToF device (Scionti & Wesdemiotis, 2012b). These newer instruments are also equipped with collision cells in the linear ToF region to enhance the fragmentation extent by collisionally activated dissociation, CAD (also known as collision-induced dissociation, CID). For polymers, PSD and CAD spectra are generally very similar; the extra collision may, however, promote minor, high-energy fragmentation pathways that are structurally diagnostic, yet undetectable without collisional activation (Town et al., 2019).

Tandem-in-space instruments are limited to MS/MS (MS²) experiments, unless intentional in-source dissociation is applied to cause fragmentation before mass selection, so that a fragment can be subjected to further fragmentation in the actual MS/MS step to obtain a pseudo MS³ spectrum (De Hoffmann & Stroobant, 2007). Tandem-in-time instruments, on the other hand, make it possible to repeat the isolation/fragmentation events, because they utilize a single trapping device as mass analyzer, in which several cycles of fragmentation (MS^n) can take place within a given time sequence (Scionti & Wesdemiotis, 2012b). QIT and linear ion trap (LIT) instrumentation with traditional or orbitrap detection, and Fourier transform ICR (FT-ICR) analyzers are widely used for tandem-in-time MS/MS and MSⁿ experiments.

MS/MS experiments have been used to detect and identify individual end groups, substitution and/or functionalization patterns, copolymer sequences, and macromolecular architectures and topologies (cf. Table 2).

They have also enabled the differentiation of isobars, which have different elemental compositions but very similar masses (within <0.1– $0.2\,\mathrm{Da}$), and isomers, which have identical elemental compositions but different architectures or conformations. This information is often accessible by direct sample ionization followed by MS/MS analysis of select sample ions. Complex samples may, however, require chromatographic or other type of separation before MS/MS or MSⁿ can be performed (vide infra). Table 2 lists common structural problems in polymer chemistry that have been successfully resolved with MS/MS or MSⁿ.

The fragmentation patterns in the MS/MS spectra reported thus far have led to the articulation of polymer ion fragmentation mechanisms, which provide useful guidelines for the interpretation of newly acquired spectra (Chaicharoen et al., 2008; Gies et al., 2007; Gies & Hercules, 2014; Polce et al., 2008; Snyder et al., 2019; Solak Erdem et al., 2014; Wesdemiotis et al., 2011). Briefly, polymer ions dissociate through charge-induced and charge-remote pathways, depending on their composition and functional groups and the type of charge added in the ionization step (Wesdemiotis et al., 2011). Dissociation mechanisms also depend on the activation method used to cause fragmentation, which will be discussed further in the upcoming sections.

Nomenclature of polymer fragment ions

A comprehensive description of the acronyms used to describe the backbone fragments generated from synthetic macromolecular ions has been reported (Wesdemiotis et al., 2011). This nomenclature of fragment ions follows the naming scheme previously defined for peptide fragments; examples can be seen in Figure 12 for four different types of linear homopolymers with defined initiating (α) and terminating (ω) chain end substituents. Acronyms from the beginning of the alphabet $(a_n, b_n, c_n, etc.)$ designate fragments containing the α end group; whereas acronyms from the end of the alphabet $(x_n, y_n, z_n, etc.)$ designate fragments containing the ω end group (reminiscent of the N- and C-terminal fragments from peptides, respectively). The subscripted numbers indicate the number of complete or partial repeat units within each fragment. Polymer chains with longer monomer units have more potential fragmentation sites within each repeat unit, and thus, the alphabetic nomenclature is adjusted accordingly (cf. Figure 12). Figure 13 exemplifies the nomenclature for the MS/MS fragments from the [M + Li]⁺ ion of a polystyrene with sec-C₄H₉ and H substituents at the α and ω chain end, respectively.

TABLE 2 Structural issues on macromolecular structure, architecture, and topology addressed with MS/MS.

		1 6
	Analytical information gained by MS/MS	Representative literature
1	Elucidation of individual (α and ω) end groups	Alawani et al. (2022); Jackson et al. (1996); Jedliński et al. (1998); Payne et al. (2021); Polce et al. (2008)
2	Differentiation of functionalization patterns	Wollyung et al. (2005)
3	Determination of copolymer sequences	Altuntaş and Schubert (2014); Crecelius et al. (2010); Girod et al. (2008); Snyder et al. (2019); Yol et al. (2014); Žagar et al., (2006)
4	Sequence analysis of sequence-defined polymers	Cavallo et al. (2018); Mao, Zhang, Cheng, et al. (2019); Roszak et al. (2021); Roy et al. (2015)
5	Sequence analysis of macrocyclic copolymers ^a	Alexander et al. (2018)
6	Differentiation of cyclic versus linear architectures	Gies & Hercules (2014); Yol et al. (2013)
7	Differentiation of cyclic versus tadpole architectures ^a	O'Neill et al. (2022)
8	Detection and identification of branched topologies	Chaicharoen et al. (2008); Gies et al. (2013); X. Liu et al. (2015); Mao, Zhang, Zhang, et al. (2019)
9	Isobar differentiation and identification ^a	Hilton et al. (2008); Katzenmeyer et al. (2016); Solak Erdem et al. (2014)
10	Isomer differentiation and identification ^a	O'Neill et al. (2022)
11	Bioconjugate characterization	Y. Liu et al. (2017); Sallam et al. (2018)

^aAfter separation by liquid chromatography or ion mobility.

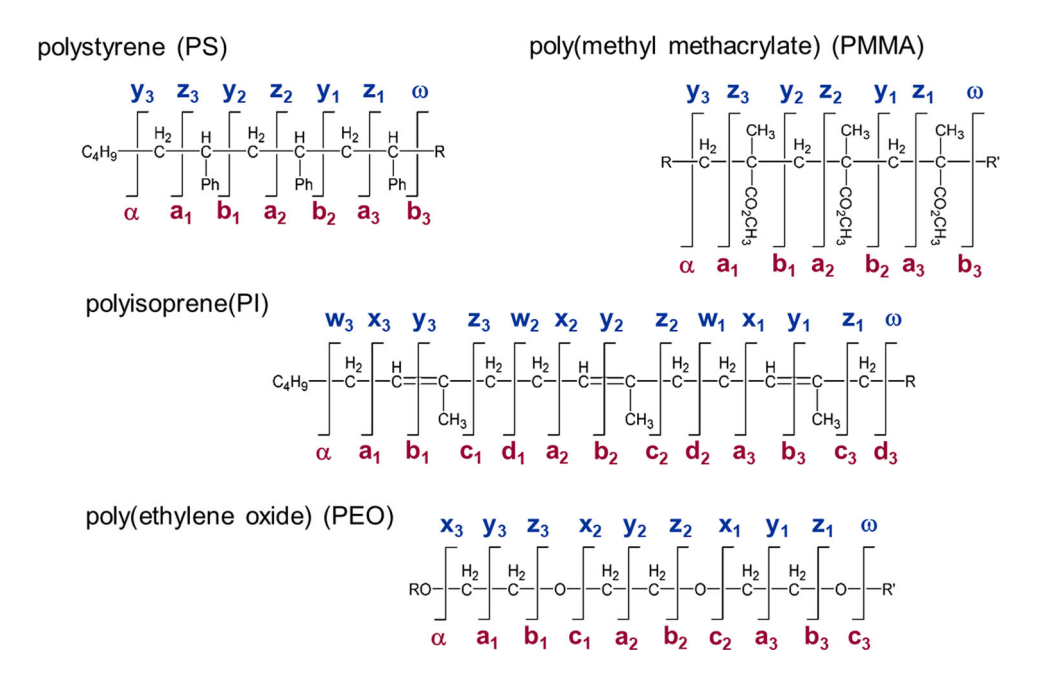


FIGURE 12 Polymer backbone nomenclature for linear homopolymers with defined α and ω chain ends. Reproduced from Polce and Wesdemiotis (2010) with permission from John Wiley & Sons, Inc. For the naming of copolymer fragments see Yol et al. (2014) and Snyder et al. (2019). [Color figure can be viewed at wileyonlinelibrary.com]

The mass (m/z ratio) of the precursor ion selected for the MS/MS spectrum in Figure 13 reflects the total end group mass of this PS chain, viz. sec-C₄H₉ (57.07 Da) + (C₈H₈)₁₇ (1769.06 Da) + H (1.01 Da) + Li (7.02 Da) = 1834.16 Da. In

contrast, the homologous a_n and y_n fragment series identify the individual α and ω end groups of this polymer, respectively. This spectrum can be used as a template for the sequence analysis of copolymer chains comprising one

10982787, 2024, 3, Downloaded from https://analytical

nelibrary.wiley.com/doi/10.1002/mas.21844 by Chrys Wesdemiotis

University Of Akron Bierce Library, Wiley Online Library on [23/07/2024]. See the Terr

meta- or one para-dimethylsilyl styrene unit (m-DMSS or p-DMSS) in addition to regular styrene (C_8H_8) repeat units, cf. Figure 14 (copolymerization via living anionic polymerization; Yol et al., 2014).

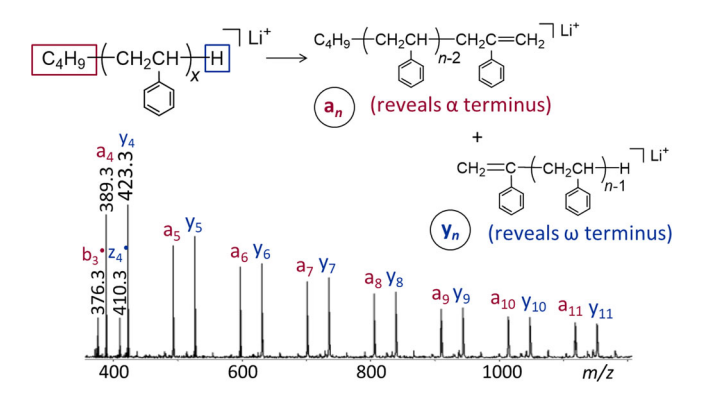


FIGURE 13 MALDI-MS/MS spectrum of the $[M + Li]^+$ ion of the 17-mer (x = 17) from a PS with sec-C₄H₉ and H end groups (m/z 1834.2), acquired on a ToF/ToF mass spectrometer using DCTB as matrix and lithium trifluoroacetate for cationization. In addition to the general polymer nomenclature system (detailed in Figure 12), a superscripted $\dot{}$ is used in this work to denote a radical ion. Reproduced from Yol et al. (2014) with permission from the American Chemical Society. DCTB, trans-2-[3-(4-tert-butylphenyl)-2-methyl-2-propenylidene] malononitrile; MALDI-MS, matrix-assisted laser desorption/ionization-mass spectrometry; PS, polystyrene. [Color figure can be viewed at wileyonlinelibrary.com]

The spectral comparison in Figure 14 provides strong evidence that PS copolymers containing either one m-DMSS or one p-DMSS unit have different sequences. The differences in sequence can be elucidated by considering that inclusion of the silylated monomer increases the mass by 58 Da; for example, a4 (which contains solely styrene units) is observed at m/z 389.3, while the congener containing one DMSS and three styrene units is observed at m/z 447.3 (marked by $^{\land}$). With a m-DMSS unit in the polymer chain, both the a_n as well as the y_n fragments are largely homopolymeric if they have small sizes (a_4-a_6, y_4-y_8) , but exclusively copolymeric at larger sizes ($\geq a_{10}$, $\geq y_{10}$). On the other hand, if a p-DMSS is incorporated in the chain, the y_n fragment series remains largely or exclusively homopolymeric at all fragment sizes, while the a_n series becomes exclusively or predominantly copolymeric except at the smallest fragment size (a₄). These trends are consistent with a random distribution of the m-DMSS comonomer in the copolymer, but incorporation of the p-DMSS comonomer near the initiator. The distinct sequence preferences for m-DMSS and p-DMSS presumably result from differences in the propagation reactivities of these monomers relative to styrene (Yol et al., 2014).

It should be mentioned at this point, that polystyrenes and polyolefins are usually ionized by Ag⁺

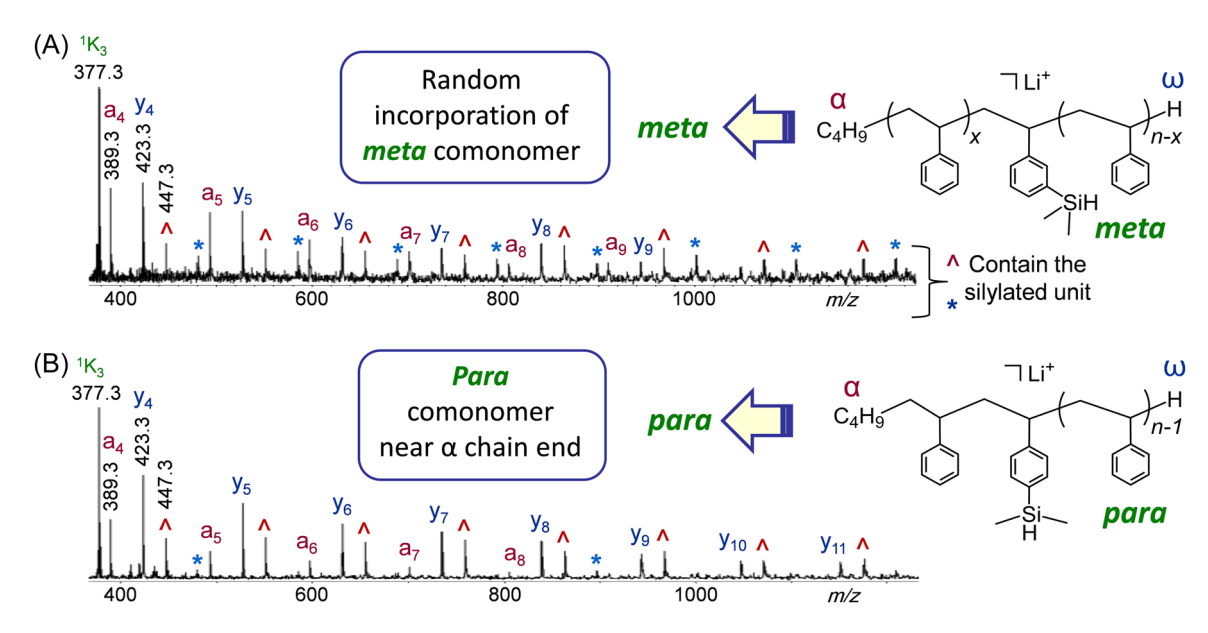


FIGURE 14 MALDI-MS/MS spectra of the $[M + Li]^+$ ions of (A) poly(m-DMSS₁-co-styrene₁₃) (m/z 1580.0) and (B) poly(p-DMSS₁-co-styrene₁₅) (m/z 1788.2), acquired on a ToF/ToF mass spectrometer using DCTB as matrix and lithium trifluoroacetate for cationization. The ^ and * signs indicate a_n and y_n ions, respectively, that contain the DMSS unit which appear 58 Da above the corresponding homopolymeric fragment ions. The 1K_3 ion (m/z 377.3) is an internal fragment with one DMSS and two styrene units. Reproduced from Yol et al. (2014) with permission from the American Chemical Society. DCTB, trans-2-[3-(4-tert-butylphenyl)-2-methyl-2-propenylidene] malononitrile; MALDI-MS, MALDI-MS, matrix-assisted laser desorption/ionization-mass spectrometry; TOF, time-of-flight. [Color figure can be viewed at wileyonlinelibrary.com]

10982787, 2024, 3, Downloaded from https://analyticalsciencejournals.onlinelibrary.wiley.com/doi/10.1002/mas.21844 by Ctrys Wesdemiotis - University Of Alron Bierce Library, Wiley Online Library on [23/07/2024]. See the Terms and Conditions (https://onlinelibra

nditions) on Wiley Online Library for rules of use; OA articles are governed by the applicable Creative Commons License

adduction, as Ag^+ ions bind strongly to π electron-containing ligands. Unfortunately, Ag^+ is also an oxidizing agent, precluding its use for polymers with easily oxidizable substituents, like silanes (which are oxidized to silanols) and thiols or thioethers (which are oxidized to sulfoxides, sulfones, or sulfonic acids). In these cases, a metal ion with low oxidation power such as Li^+ or Na^+ (Quirk et al., 2005), or an ammonium ion that induces protonation such as protonated octadecylamine (Lou et al., 2022), must be used.

3.2 | MS/MS activation methods

Ion activation methods can be categorized based on the physical or chemical process used to increase the internal energy of the precursor ion. The most widely used technique for MS/MS experiments on synthetic polymers is CAD, also known as CID. Here, ions are accelerated in the presence of an inert gas, resulting in collisions that convert a fraction of the ions' kinetic energy to internal (i.e., rovibrational) energy. The maximum internal energy that can be gained per collision is equal to the center-of-mass collision energy, $E_{\rm CM}$, defined by Equation (5), where $E_{\rm LAB}$ is the laboratory-frame kinetic energy imparted after acceleration; $m_{\rm ION}$ is the mass of the precursor ion; and $m_{\rm GAS}$ is the mass of the collision gas (typically He or Ar atoms, or N₂ molecules).

$$E_{\rm CM} = \frac{m_{\rm GAS}}{m_{\rm GAS} + m_{\rm ION}} \times E_{\rm LAB}.$$
 (5)

CAD in beam instruments (QqQ, Q/ToF) is performed in dedicated collision cells (usually RFonly quadrupoles), located between the mass analyzers and supplied with the appropriate collision gas, typically argon or nitrogen (~10⁻² mbar). Highresolution trapping instruments, like the Orbitrap or ICR trap, are normally equipped with dedicated collision cells where the fragments are formed before being conveyed to the trap for accurate m/z measurement; on the other hand, in simpler trapping equipment (QIT, LIT), fragmentation is induced inside the trap using the trap's bath gas (He, ~1 mbar) as collision gas. E_{LAB} is set at $\leq 200 \,\text{eV}$ in dedicated collision cells and ≤10 eV in trapping instruments (to prevent ejection from the trap). Under such conditions, the precursor ions generally undergo multiple collisions before enough internal energy has been accumulated to enable dissociation. E_{LAB} may be varied in steps to acquire MS/MS spectra as a function of internal energy and derive breakdown graphs and survival yield (SY) curves, which reveal information

about the dissociation energetics and stability of the precursor ion relative to the product ion fragments (Biri et al., 2012; Wesdemiotis, 2017).

In MALDI-ToF/ToF instruments, the ions' internal energy is typically increased by using a higher laser power to form energetically excited ions that dissociate spontaneously after leaving the ion source. Although higher energy dissociations can occur, this process generally produces similar fragmentation spectra as CAD in beam or trap mass spectrometers (Altuntaş et al., 2012).

The internal energy transferred to a polymer ion by collisional activation or by using higher laser power is redistributed rapidly among the rovibrational degrees of freedom of the ion before fragmentation occurs. Such energy equilibration over the entire macromolecule (ergodic process) favors cleavage of the weakest bonds. Rearrangement dissociations, which often have lower energy requirements than simple bond cleavages, are also promoted. The latter tendency may give rise to fragments incompatible with the primary structure; for example, CAD of protonated peptides has been found to produce fragments that contradict the expected sequence of amino acid units (Harrison et al., 2006). Such structural alterations have not been reported for any synthetic polymer ions; the possibility of their occurrence underscores, however, the importance of having access to alternative activation methods that avoid the slow heating by multiple collisions and facile redistribution of deposited internal energy prevalent with CAD.

Electron capture dissociation (ECD) and electron transfer dissociation (ETD) energize multiply charged precursor ions (≥2+ charges) by reducing them via electron addition to radical cations. In ECD, this is performed by allowing precursor ions trapped in an ICR cell to react with thermally excited electrons. In ETD, precursor ions and negative ions are combined in the same trap cell to cause cation-anion reactions, in which an electron is transferred from the reagent anion to the precursor cation; fluoranthene radical anions (C₁₆H₁₀^{-•}), formed in an auxiliary negative CI source, have been the most widely used ETD reagent. ETD has been performed in QIT and Q/ToF mass spectrometers as well as in hybrid instruments equipped with Orbitrap mass analyzers. ECD has been applied to polyethers (Cerda et al., 2001, 2002) and polyoxazolines (Morgan et al., 2018). ETD applications have been more widespread and so far have covered polyesters (Katzenmeyer et al., 2015; Prian et al., 2019; Scionti & Wesdemiotis, 2012a), polyacrylamides (Gerislioğlu & Wesdemiotis, 2017), and polymer-peptide bioconjugates (B. Wei et al., 2019). The consensus today is that the radical ions emerging after ECD or ETD primarily undergo radical-induced

dissociations, promoted by the newly formed radical site (Katzenmeyer et al., 2015; Prian et al., 2019). Since polymer ions are mostly formed via metal ion addition, the radical ions emerging after electron transfer usually contain salt bridges (ion pairs), such as -O-Na+ or -COO⁻Na⁺, in addition to the unpaired electron; the negative ions in these ion pairs can induce additional fragments through charge-induced dissociations (Scionti & Wesdemiotis, 2012a). Combined, the radical- and charge-induced fragmentations resulting after ECD/ETD lead to different fragment distributions as compared to CAD, thus providing complementary structure information. Also, the extent of consecutive fragmentations is significantly reduced compared to CAD of the multiply charged precursor ion, leading to simpler and more easily interpretable spectra.

For polymer ions that do not fragment efficiently, CAD can be added after ETD to improve the fragmentation yield and the formation of structurally diagnostic product ions. ETD is used first (MS^2) to create a product with structural attributes that promote fragmentation in a consecutive CAD step (MS^3), such as an unpaired electron or a stable salt bridge (Gerişlioğlu & Wesdemiotis, 2017). The efficacy of this approach will be illustrated with the sequence elucidation of a copolymer composed of N-isopropylacrylamide (NIPAM) and methacrylic acid (MAA) units, viz. p(NIPAM-co-MAA); its ESI-MS spectrum showed singly and doubly sodiated ions with NC-C(CH₃)₂- (α) and -H (ω) end

groups, cf. structure in Figure 15A. The doubly charged $[M + 2Na]^{2+}$ ion of p(NIPAM₁₁-co-MAA₃) was selected for sequence analysis via MS/MS. Upon CAD, this ion only loses propene and isopropanol from the NIPAM side chains, which reveal no sequence insight. ETD also generates a limited number of fragments (cf. Figure 15A), viz. $[M + Na]^+$ and $[M + 2Na - H]^+$, created after electron addition and consecutive loss of a Na or H atom, respectively. The $[M + 2Na - H]^+$ product carries a wellstabilized salt bridge on one MAA unit, a feature that can stimulate sequence-indicative backbone cleavages via charge-remote pathways upon successive (Gerişlioğlu & Wesdemiotis, 2017). The combined ETD-CAD (MS³) spectrum (Figure 15B) includes fragments that contain either the α - or the ω -end group (series a_n^{*}) b_n^* or y_n , respectively). All $a_n^{*\bullet}/b_n^*$ fragments include three MAA units, whereas all y_n fragments contain solely NIPAM repeat units; such a pattern is only reconciled with the block sequence depicted in Figure 15. These data demonstrate the ability of ETD-CAD (MS³) experiments to afford connectivity information when single MS/MS stages fail, a strategy that helps to expand the range of decipherable macromolecular sequences.

A serious limitation of ECD/ETD is the need for multiply charged ions, which requires the use of ESI (and, hence, solubility of the polymer) and precludes such studies on MALDI or ASAP generated ions which are singly charged. This challenge has been overcome with charge transfer dissociation (CTD), an activation

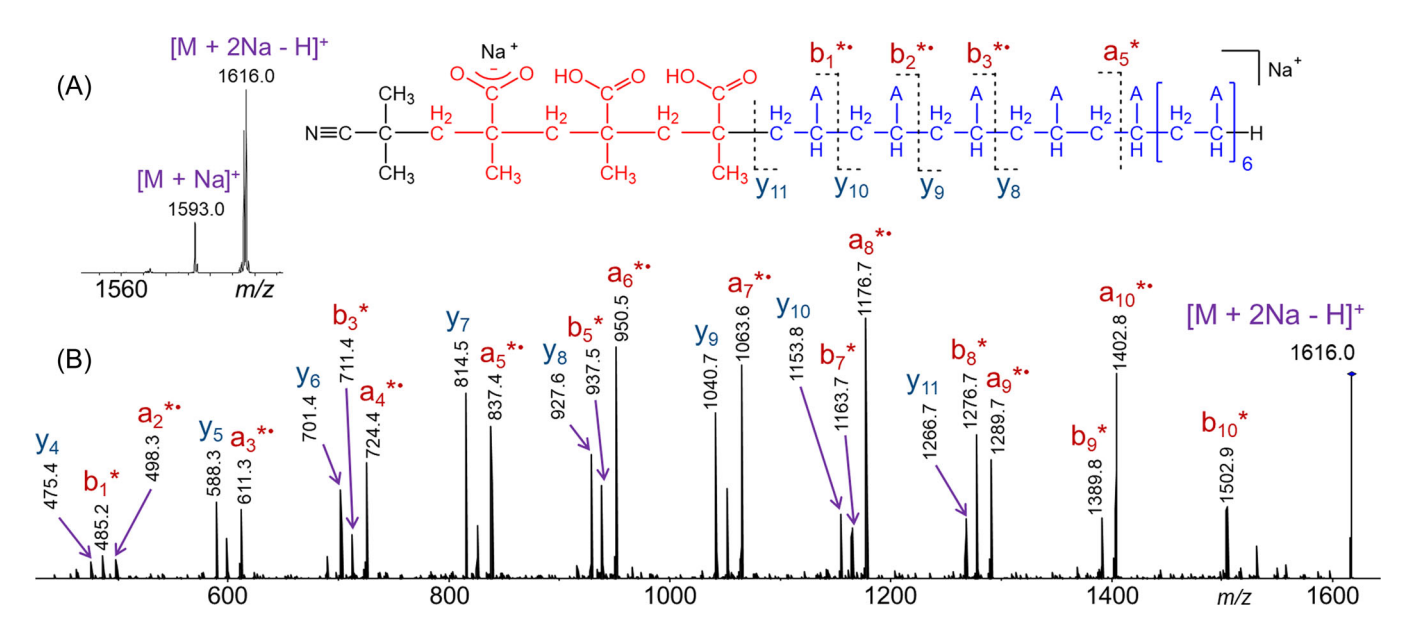


FIGURE 15 (A) MS/MS (ETD) spectrum of $[M+2Na]^{2+}$ from p(NIPAM₁₁-co-MAA₃) (m/z 808.0), acquired on a QIT mass spectrometer; (B) MS³ (ETD-CAD) spectrum of the ETD product $[M+2Na-H]^+$ (m/z 1616.0). The inset shows the sequence deduced from the MS³ fragments. "A" in the structure designates the side chain of the N-isopropylacrylamide monomer (i.e., CO-NH(CH₃)₂); * and * denote fragments with two Na⁺ ions (O⁻Na⁺ plus Na⁺) or radical ions, respectively. CAD, collisionally activated dissociation; ETD, electron transfer dissociation; MS, mass spectrometry; QIT, quadrupole ion trap. [Color figure can be viewed at wileyonlinelibrary.com]

0982787, 2024, 3, Downloaded from https

.com/doi/10.1002/mas.21844 by Chrys Wesdemiotis

- University Of Akron Bierce Library, Wiley Online Library on [23/07/2024]. See the Terms and Conditions (https://doi.org/10.1016/j.com/10.1016/j.com/10.1016/j.com/10.1016/j.com/10.1016/j.com/10.1016/j.com/10.1016/j.com/10.1016/j.com/10.1016/j.com/10.1016/j.com/10.1016/j.com/10.1016/j.com/10.1016/j.com/10.1016/j.com/10.1016/j.com/10.1016/j.com/10.1016/j.com/10.1016/j.com/10.1016/j.com/10.1016/j.com/10.1016/j.com/10.1016/j.com/10.1016/j.com/10.1016/j.com/10.1016/j.com/10.1016/j.com/10.1016/j.com/10.1016/j.com/10.1016/j.com/10.1016/j.com/10.1016/j.com/10.1016/j.com/10.1016/j.com/10.1016/j.com/10.1016/j.com/10.1016/j.com/10.1016/j.com/10.1016/j.com/10.1016/j.com/10.1016/j.com/10.1016/j.com/10.1016/j.com/10.1016/j.com/10.1016/j.com/10.1016/j.com/10.1016/j.com/10.1016/j.com/10.1016/j.com/10.1016/j.com/10.1016/j.com/10.1016/j.com/10.1016/j.com/10.1016/j.com/10.1016/j.com/10.1016/j.com/10.1016/j.com/10.1016/j.com/10.1016/j.com/10.1016/j.com/10.1016/j.com/10.1016/j.com/10.1016/j.com/10.1016/j.com/10.1016/j.com/10.1016/j.com/10.1016/j.com/10.1016/j.com/10.1016/j.com/10.1016/j.com/10.1016/j.com/10.1016/j.com/10.1016/j.com/10.1016/j.com/10.1016/j.com/10.1016/j.com/10.1016/j.com/10.1016/j.com/10.1016/j.com/10.1016/j.com/10.1016/j.com/10.1016/j.com/10.1016/j.com/10.1016/j.com/10.1016/j.com/10.1016/j.com/10.1016/j.com/10.1016/j.com/10.1016/j.com/10.1016/j.com/10.1016/j.com/10.1016/j.com/10.1016/j.com/10.1016/j.com/10.1016/j.com/10.1016/j.com/10.1016/j.com/10.1016/j.com/10.1016/j.com/10.1016/j.com/10.1016/j.com/10.1016/j.com/10.1016/j.com/10.1016/j.com/10.1016/j.com/10.1016/j.com/10.1016/j.com/10.1016/j.com/10.1016/j.com/10.1016/j.com/10.1016/j.com/10.1016/j.com/10.1016/j.com/10.1016/j.com/10.1016/j.com/10.1016/j.com/10.1016/j.com/10.1016/j.com/10.1016/j.com/10.1016/j.com/10.1016/j.com/10.1016/j.com/10.1016/j.com/10.1016/j.com/10.1016/j.com/10.1016/j.com/10.1016/j.com/10.1016/j.com/10.1016/j.com/10.1016/j.com/10.1016/j.com/10.1016/j.com/10.1016/j.com/10.1016/j.com/10.1016/j.com/10.1016/j.com/10.1016/j.com/10.1016/j.com/10.101

nditions) on Wiley Online Library for rules of use; OA articles are governed by the applicable Creative Commons Licenso

technique that employs He cations with keV kinetic energies as reagent ions (Edwards et al., 2022). Collisions of the He⁺ ions with singly charged precursor ions result in electron abstraction from the precursor ions and formation of doubly charged radical cations which then follow similar dissociation pathways as precursor ions activated by ETD, cf. equation (6). The charge transfer step in CTD is highly exothermic for

$$[M+X]^+ + He^+ \rightarrow [M+X]^{2+\cdot} + He$$

$$\rightarrow \text{fragments of } [M+X]^{2+\cdot}. \tag{6}$$

most analyte ions because of the electron affinity of He⁺ (24.6 eV). Consequently, a substantial amount of internal energy is deposited into the precursor ions in this reaction, enabling them to undergo high-energy dissociations that are not observed upon CAD. Again, fragmentation can be further enhanced if select CTD products are isolated for consecutive CAD analysis. The CTD-CAD sequence successfully distinguished a Nylon-6,6 dimer from an isobaric Nylon-6 tetramer (Edwards et al., 2022).

Photodissociation (PD) is another increasingly used ion fragmentation method in MS/MS (Brodbelt, 2014). It involves energetic activation of the sample ions by absorption of photons from mainly infrared (IR) or ultraviolet (UV) lasers. Most suitable for PD experiments are trapping mass spectrometers, in which the ions can be confined within a small volume that can be irradiated by the laser. PD in beam instruments is challenging due to difficulties in overlapping laser and ion beam and, hence, has seldomly been implemented (L. Zhang & Reilly, 2009).

Continuous CO_2 lasers are the most popular choice for IR light. Their photon wavelength (10.6 μ m) corresponds to an energy of ~0.1 eV per photon, which is insufficient to cause fragmentation. Multiple IR photons must be absorbed to reach the energy levels required for fragmentation (cf. Figure 16), resulting in IR multiphoton dissociation (IRMPD). This stepwise activation, or slow heating, is similar with the CAD activation mechanism (Figure 16). It is therefore not surprising that both CAD as well as IRMPD favor fragmentations with lower energy requirements (Brodbelt, 2014). IRMPD has been explored in the carbohydrate field (Zhou & Håkansson, 2011), but applications to synthetic materials have not yet been reported.

For ultraviolet PD (UVPD), pulsed Nd:YAG or ArF excimer lasers are typical sources of UV light. Their photon wavelengths of 355 nm (3rd harmonic of Nd:YAG laser) or 193 nm (ArF excimer laser) correspond to energies of 3.5 or 6.4 eV per photon, respectively. Such energy levels provide enough excitation to cause

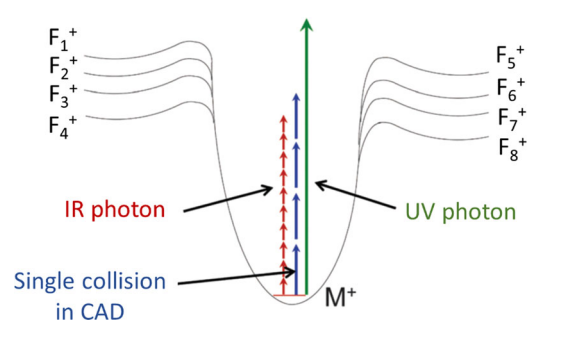


FIGURE 16 Energy diagram depicting energetic excitation of a macromolecular precursor ion (M^+) by collisional activation and absorption of IR or UV photons, to induce dissociation to fragments $F_1^+-F_8^+$. Reproduced from Brodbelt (2014) with permission from the Royal Society of Chemistry. CAD, collisionally activated dissociation; IR, infrared; UV, ultraviolet. [Color figure can be viewed at wileyonlinelibrary.com]

dissociation of a macromolecular ion after absorption of a single photon (cf. Figure 16), thereby enabling higher energy dissociation channels not accessible by CAD or IRMPD and ultimately leading to richer and more informative MS/MS spectra (Brodbelt et al., 2020; Brodbelt, 2014).

High UV photon energies are readily available from synchrotron radiation, which was recently used to study the UVPD behavior of singly cationized poly (ethylene glycol) (PEG; $M_n \approx 1$, 4, or 12 kDa) and polydimethylsiloxane (PDMS; $M_n \approx 2 \text{ kDa}$) chains (Aloui et al., 2020, 2021). The experiments were performed in a LIT at photon energies ranging from 5 eV (248 nm) to 24 eV (52 nm). UVPD led to significantly high fragmentation yields than CAD of the same polymers and produced fragments that clearly identified their end groups. With photon energies >10 eV, multiply charged fragments started appearing, which were attributed to dissociative photoionization, viz. electron detachment from the precursor ions followed by fragmentation; this event is particularly useful for the longer chains which lose the metal cation and form barely any other fragments upon CAD (Aloui et al., 2020).

UV radiation from a tunable OPO (optical parametric oscillator) Nd:YAG laser has been employed for PD experiments on multiply charged anions formed by ESI of poly(methacrylic acid) (PMAA) and poly(styrene sulfonate sodium salt) (PSS) (Girod et al., 2011 and 2012). Such polyelectrolytes do not produce end group indicative fragments in CAD experiments of their $[M-X]^-$ and $[M-2X]^{2-}$ (X=H or Na) ions. This problem is resolved by electron photodetachment dissociation (EPD) on the doubly charged anions, a method combining UV irradiation to induce $[M-2X]^{2-}$ oxidation to $[M-2X]^{-\bullet}$ (for PSS) or $[M-2X-CO_2]^{-\bullet}$ (for PMAA) and CAD

of the emerging radical anions (Antoine et al., 2014). It is noteworthy that a recurrent attribute of CAD alternatives is the formation of intermediates with unpaired electrons, which can facilitate further fragmentation through radical-catalyzed dissociations.

4 | HYPHENATED SEPARATION TECHNIQUES

While a significant number of structural questions can be answered by MS/MS and MS^n experiments (vide supra), polymeric materials with isomeric and/or isobaric components and multicomponent blends may require hyphenated separation techniques to reduce spectral complexity and achieve comprehensive sample characterization (Crotty et al., 2016). Liquid chromatography (LC), field flow fractionation (FFF), and IM spectrometry separations coupled online to MS and MS/MS analysis of the separated sample constituents can help to solve problems with complex (co)polymeric mixtures, cf. Table 3. Several variants exist for each of the three mentioned separation techniques, offering a large number of choices depending on the nature and properties of the analyte sample. The most widely used LC modes for synthetic polymers are reversed-phase LC (RP-LC) and SEC, in particular its GPC mode (T. Chang, 2018; Nielen & Buijtenhuijs Ab, 1999; Pasch, 2013; Uliyanchenko, 2017). Similarly, flow or thermal FFF can be performed for polymer separation and characterization (Toney et al., 2021; Williams & Lee, 2006); and IM dispersion can be achieved using different IM techniques, such as drift, traveling wave, trapped, and field asymmetric IM spectrometry (Dodds & Baker, 2019; May & McLean, 2015). Table 3 lists hyphenated separation-MS techniques that have been applied to various common classes of polymers over the past 20 years.

4.1 | Condensed phase separations: LC and FFF

Chromatographic techniques become imperative in polymer analysis when MS and MS/MS alone are inconclusive. Coupling these separation techniques to MS, either offline through fractionation or online using compatible ionization sources, increases analyte selectivity by reducing the overall complexity of mass spectra obtained from direct injection methods.

Offline fractionation by SEC offers a convenient means to purify (co)polymer samples and simplify mixtures and blends. The low polydispersity of the fractions enables detailed and sensitive MW and compositional analysis and the detection of minor sample components that would otherwise be invisible (Adamus et al., 2005; Fouquet et al., 2020; Montaudo et al., 2002). Moreover, the collected fractions can be used as SEC calibrants for the MW determination of polydisperse polymers if similarly structured commercial standards are unavailable (Nielen & Malucha, 1997).

Polymers ionizable via ESI and APCI can be separated using ultra/high-performance liquid chromatography (U/HPLC) (Siddhant et al., 2018), which can be interfaced online with MS analysis; the eluates are directly fed into the ESI or APCI source and the ions formed there are drawn into the mass spectrometer for MS and MS/MS characterization. U/HPLC separations are most often achieved using RP-LC mode, which employs nonpolar (hydrophobic) stationary phases and polar (hydrophilic) mobile phases. Normal phase chromatography, in which the stationary phase is polar and the mobile phase nonpolar, is usually coupled to APCI. Since RP-LC is more widespread, this tutorial focuses on RP-LC separations for polymeric mixtures coupled to ESI-MS. Typical RP stationary phases, include alkylbonded (C4, C8, C18), phenyl-bonded, or polar-modified (pentafluoro-phenyl, cyano-alkyl, amino-alkyl) resins, while typical mobile phases are mixtures of water and miscible organic solvents (Block et al., 2006; González-Manzano et al., 2006; O'Neill et al., 2022; Scionti et al., 2012). Hydrophobic oligomers interact more favorably with the stationary phase and, thus, are more strongly retained and elute later than hydrophilic oligomers. Elution/retention times are determined by the polarity, H-bonding capabilities, and π - π interaction tendencies of the analyte's components, allowing for lower MW macromolecules to be separated based on backbone, end group, and architectural differences that influence their affinity for the selected stationary phase.

SEC has also been coupled to online ESI-MS analysis to identify the end group distributions of a glycidyl methacrylate/butyl methacrylate copolymer (Aaserud et al., 1999), characterize acrylate polymers synthesized via reversible addition-fragmentation chain-transfer (RAFT) processes (Feldermann et al., 2005), and determine free radical polymerization rate coefficients (Gruendling et al., 2008). SEC of polymers is generally performed using neat THF as mobile phase (Neira-Velázquez et al., 2013). For adequate ESI efficiency of the eluates, a THF/methanol blend must be used (Feldermann et al., 2005), or methanol (plus cationizing salt if needed) can be added post column to the eluate before injection to the ESI source (Aaserud et al., 1999; Gruendling et al., 2008).

RP-LC can also be combined with SEC to generate two-dimensional (2D) separations based on both

TABLE 3 Examples of hyphenated techniques used for the separation and characterization of different classes of synthetic polymers.

Polymer sample(s)	Method	References
Polyesters and polyamides		
RAFT generated acrylates	SEC-ESI-MS	Feldermann et al. (2005)
MWD of PMMA	SEC-RI-ESI-MS	Gruendling et al. (2008)
Poly(α-peptoid)s	IM-MS	Li, Guo, et al. (2011)
Thermoresponsive polyesters	ESI-IM-MS & MS/MS	Alexander et al. (2018)
Thermoplastic elastomers	ASAP-IM-MS & MS/MS	Alawani et al. (2022)
Polyethers and glycopolymers		
PEO standards	FFF-ESI-MS	Hassellöv et al. (2006)
Nonionic surfactants	LC-MS & LC- MS/MS	Scionti et al. (2012)
Hyperbranched glycopolymers	ESI-IM-MS	X. Liu et al. (2015)
Isomeric glycans	IM-MS/MS	J. Wei et al. (2020)
Cyclic and tadpole isomers	UPLC-MS/MS	O'Neill et al. (2022)
Supramolecular polymers		
Metallo-supramacromolecules	IM-MS & MS/MS	Chan et al. (2011); Li, Chan, et al. (2011)
POSS-sorbitol self-assembly	IM-MS & MS/MS	Scionti et al. (2012)
Giant amphiphile assemblies	IM-MS & MS/MS	Shao et al. (2019)
Polyelectrolyte assemblies	IM-MS	Atakay et al. (2020)
Metallomacrocycle isomers/isobars	IM-MS	Endres et al. (2020)
Copolymers		
Polyether copolymers	LC-MS & LC- MS/MS	Scionti et al. (2012)
Polystyrene-polyether copolymers	LC-IM-MS	Shi et al. (2016)
Complex heterogeneous mixtures		
Additives in LDPE	LC-MS	Block et al. (2006)
Anthocyanidin extracts from wine	LC-MS	González-Manzano et al. (2006)
Engine oil particulate matter	LC-IM-MS	Snyder and Wesdemiotis (2021)

Abbreviations: ASAP, atmospheric solids analysis probe; ESI, electrospray ionization; FFF, field flow fractionation; IM, ion mobility; LC-MS, liquid chromatography–mass spectrometry; RAFT, reversible addition-fragmentation chain-transfer; RI, refractive index; SEC, size exclusion chromatography; UPLC, ultra-performance liquid chromatography.

molecular mass distribution and chemical composition (Schoenmakers & Aarnoutse, 2014). Commonly, RP-LC is operated in the 1st dimension, to separate the sample constituents by hydrophobicity/hydrophilicity balance, and SEC follows in the 2nd dimension to determine the MW distributions of the RP-separated species. This

procedure was applied to characterize multicomponent methacrylate (co)polymer mixtures (Uliyanchenko et al., 2012), industrial polyesters (Molenaar et al., 2022; Pretorius et al., 2015), polymeric dispersants in detergents (P. Yang et al., 2018), and commercial polystyrene/polybutadiene copolymers (Lee et al., 2018). The reverse

on Wiley Online Library for rules of use; OA articles are governed by the applicable Creative Commons Licenso

order, viz. SEC in 1st and RP-LC in 2nd dimension, has also been utilized, to determine the compositional heterogeneity of an 8-arm poly(ethylene glycol) (PEG) functionalized with maleimide for protein conjugation (S. H. Yang et al., 2020). Although optical detection was mostly used in these studies, MS analysis of the 2D-LC eluates has also been successfully implemented (Molenaar et al., 2022; S. H. Yang et al., 2020) and is preferable as a 3rd dimension of analysis, as it provides highly specific structural information about the eluting species by revealing their masses.

Figure 17 provides an example of a 2D-LC-MS analysis, involving the characterization of the impurities in a star-branched 40-kDa PEG, designed for attachment to protein therapeutics (S. H. Yang et al., 2020). SEC was performed in the 1st dimension, and the peak of interest was transferred with a loop into the 2nd dimension, consisting of a RP-LC system attached to an ESI-Q/ToF mass spectrometer. SEC separated the size variants of the polymer, but sample components of comparable size but distinct functional groups coeluted (cf. Figure 17A). The

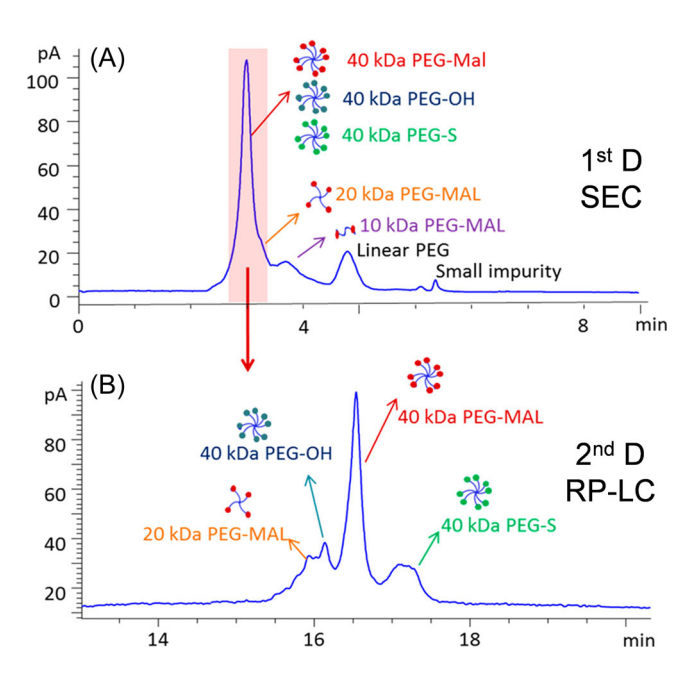


FIGURE 17 2D-LC-MS separation of a multiarm 40 kDa PEG-maleimide (PEG-MAL) reagent. (A) Separation of the size variants by SEC, which does not resolve sample components of the same size differing in end groups. (B) Separation of the coeluting species from the 1st-dimension SEC in the 2nd-dimension RP-LC according to the terminal functional groups (OH and S designate hydroxy and succinimide end groups). Reproduced from S. H. Yang et al. (2020) with permission from the American Chemical Society. 2D-LC-MS, two-dimensional liquid chromatography-mass spectrometry; RP-LC, reversed-phase liquid chromatography; SEC, size exclusion chromatography. [Color figure can be viewed at wileyonlinelibrary.com]

coeluting components (shaded peak in Figure 17A) could be resolved by RP-LC in the 2nd dimension according to end group functionality (Figure 17B). Because of the large size of the polymer (40 kDa) and the relatively small mass of the PEG repeat unit (44 Da), charge-reducing agents were added to the RP mobile phase to obtain lower charge state distributions with resolved oligomers, which allowed for the determination of their m/z ratios and derivation of the end group compositions shown in Figure 17B (S. H. Yang et al., 2020). Typical charge-reducing agents for ESI of large macromolecules include 1,8-diazabicyclo[5.4.0]undec-7-ene (DBU), 1,1,3,3-tetramethylguanidine (TMG), and triethylamine (TEA).

An alternative condensed-phase separation technique for high-mass polymers is FFF, which resembles chromatography in its dispersion potential but lacks a stationary phase. As the dissolved sample passes through the flow channel of the FFF instrument, an orthogonal field is applied (thermal, electric, gravimetric, etc.), exerting a force on the flowing molecules that affects their velocities. Smaller molecules (particles) accumulate in faster regions and bigger molecules (particles) in slower flow regions of the channel, located near the center and bottom of the channel, respectively; such distribution results in separation of the molecules (particles) by size as they travel against the applied field. Fast, gentle, and high-resolution fractionation can be achieved for molecular/particulate sizes spanning from 1 nm to 100 μm. This range encompasses larger MW analytes that cannot be adequately separated on traditional chromatographic stationary phases. Unfortunately, the inherent mass limits of MS detection have restricted FFF-MS applications to molecular sizes that can be ionized, that is, to polymers in lower MW ranges (Hassellöv et al., 2006; Kassalainen & Williams, 2003). Coupling FFF to online ESI-MS poses additional challenges due to the need to use high salt concentrations for adequate separation, which overwhelm the ESI source by generating salt clusters that reduce the ESI efficiency and detection sensitivity for the sample molecules (Crotty et al., 2016; Hassellöv et al., 2006).

4.2 | Basic concepts of IM-MS

IM-MS is a 2D technique that probes two molecular features of gas-phase ions, viz. their mobility (IM dimension) and m/z ratio (MS dimension). These parameters reveal information about two important physical properties of the ions, viz. their collision cross-section (CCS or Ω) and mass or MW, respectively (Dodds & Baker, 2019; Gabelica & Marklund, 2018; Gidden et al., 2000; May & McLean, 2015). The ions pass first

through the IM region, where they travel in a pressurized chamber under the influence of an electric field. Their mobility (K_0) or drift time (t_D) through the IM region can be converted to a CCS value which corresponds to the averaged forward-moving area of the ions through the IM chamber and reflects their 3D size and shape. After IM analysis, the ions pass through a mass analyzing device for determination of their m/z and MW.

Different variants of IM-MS exist, depending on the type of electric field (direct current or pulsed) and the gas pressure (high or low) in the IM chamber, with drift time IM (DTIM), traveling wave IM (TWIM), trapped IM (TIM), and field asymmetric IM (FAIM) being most widely employed, as they are available on commercial mass spectrometers (Dodds & Baker, 2019; May & McLean, 2015). DTIM and TIM employ low direct current fields (varied in TIM and constant in DTIM) and TWIM employs a low oscillating field, all under low pressure (<~4 mbar). FAIM is operated under atmospheric pressure with an oscillating high/low field, which precludes the measurement of CCSs. In contrast, the other three methods can be used to obtain CCS values (D'Atri et al., 2015), either directly from measured t_D data (DTIM) or after calibration with standards of known CCS (TWIM and TIM).

The mobility and drift time of an ion through the IM region depend on CCS and charge. Ions with larger CCS and lower charge state have lower mobilities and move more slowly through the IM chamber than ions with smaller CCS and higher charge state (Wesdemiotis, 2017). Overall, IM separation is completed in the millisecond timescale, as compared to minutes for chromatographic separation. For polymers, IM-MS is widely used to deconvolute ESI-MS spectra of complex polymer distributions with overlapping charge states (Charles et al., 2020; Endres et al., 2020). It also offers a much greener alternative to chromatographic separations given the absence of excessive solvent requirements.

IM-MS has made MS shape sensitive, permitting the differentiation of macromolecular isomers, provided the corresponding architectures are sufficiently distinct to render drift times and CCS values that differ beyond experimental error. Structural assignment based on observed CCS alone usually requires theoretical models to correlate experimental CCS to values predicted computationally or generated from available crystal structures (D'Atri et al., 2015). Often, geometry optimization is performed first via molecular mechanics/ dynamics simulations (or higher-level theory if tractable), and the optimized structural coordinates are input into a program that calculates the corresponding CCS, such as MOBCAL (Ieritano & Hopkins, 2021). Due to the extensive computing effort required to simulate

polymeric materials, this task can be timely and is aided by collaboration with theoretical chemists (Atakay et al., 2020). Comprehensive structural characterization of synthetic polymers can alternatively be achieved through multidimensional IM-MS and IM-MS/MS analyses (vide infra). The advantages and limitations of structural characterization using these approaches are discussed in the following sections.

4.3 | Structural characterization through CCS data

Polymers with different architectures and topologies generally have distinct hydrodynamic volumes, which makes it possible to distinguish them by GPC. Differentiation by IM-MS can also be performed if the CCS of the corresponding ions differ outside experimental error. A study on different polycaprolactone (PCL) architectures, produced via ring-opening polymerization, has shown that CCS depends strongly on both DP (i.e., macromolecular size) as well as charge state (Morsa et al., 2014). For a given DP, lightly charged ions attain compact, globular conformations with very similar CCS for linear and star-branched architectures (cf. Figure 18); this disables architectural and topological differentiation. In contrast, highly charged ions adopt elongated conformations to minimize charge repulsion, thereby giving rise to unique CCS values, representative of the corresponding architectures (cf. Figure 18); for the three topologies depicted in Figure 18, the CCS values of the 36-mers decrease with the degree of branching, in the order $\Omega(\text{linear PCL}) > \Omega(4\text{-arm star}) > \Omega(6\text{-arm star})$. This trend matches the order found for the hydrodynamic radii of the random coil conformers of these polymers (determined by GPC), which decrease in the order R(linear PCL, 3.03 nm) > R(4-arm star, 2.81 nm) > R(6-arm star,2.67 nm).

It is instructive to mention that the random coil conformations probed by GPC in solution give rise to the gas-phase compact, globular conformations observed in the IM-MS experiments after ESI (Morsa et al., 2014). The CCS (Ω_{exp}) data of these globular gas-phase structures (Figure 18) correspond to radii of 1.81-1.83 nm, which are 30%-40% smaller than the hydrodynamic radii measured in solution by GPC (vide supra). This contraction or collapse upon transfer in the gas phase has also been observed for folded proteins ionized by native ESI-MS; it has been attributed to stronger intramolecular stabilizing forces (H-bonding and hydrophobic interactions) after the solvent has been removed (Morsa et al., 2014; Rolland & Prell, 2019).

Similar results have been reported for the IM-MS separation of cyclic versus linear polymers (Hoskins

University Of Akron Bierce Library, Wiley Online Library on [23/07/2024]. See the

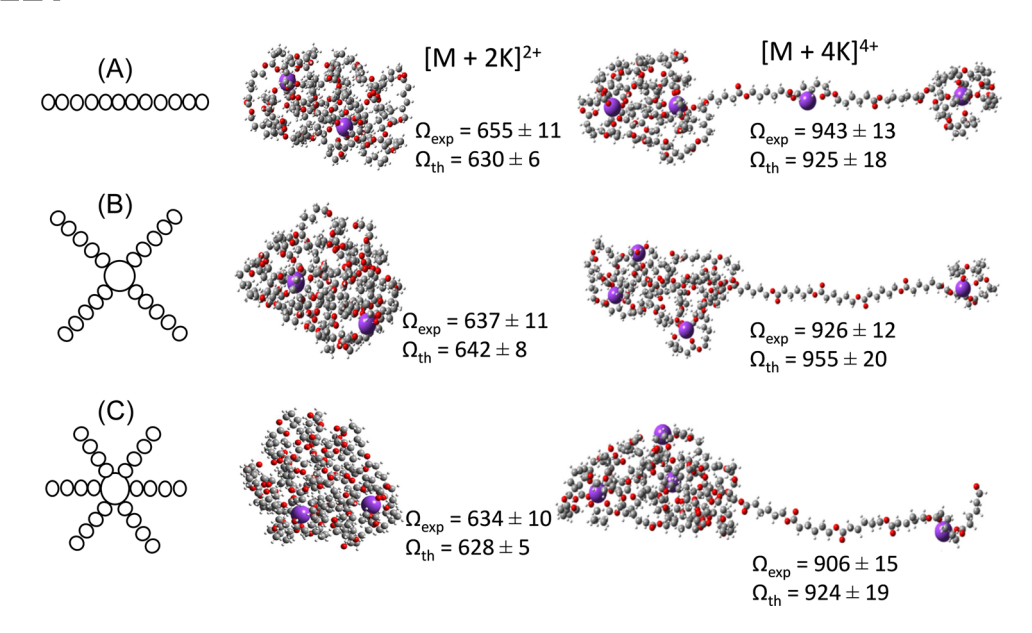


FIGURE 18 Experimental and theoretical CCS (Ω) values of the $[M + 2K]^{2+}$ and $[M + 4K]^{4+}$ ions from (a) linear, (b) 4-arm star branched, and (c) 6-arm star branched polycaprolactone (PCL) 36-mers (all in Å²). Ω_{exp} was acquired by travelling-wave IM-MS on Q/ToF instrumentation; Ω_{th} was calculated via the exact hard sphere scattering method from structures optimized by molecular dynamics computations. Reproduced from Morsa et al. (2014) with permission from the American Chemical Society. CCS, collision cross-section. [Color figure can be viewed at wileyonlinelibrary.com]

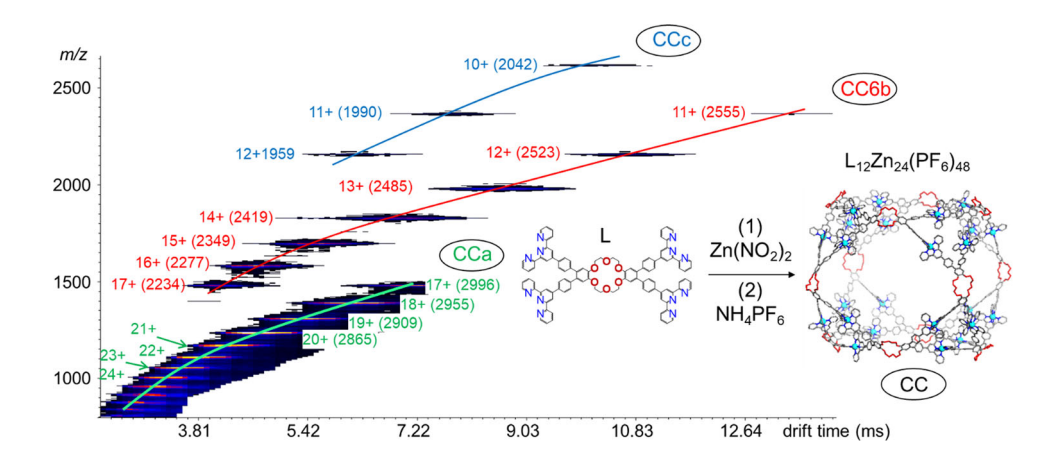


FIGURE 19 ESI-IM-MS spectrum of the coordination complex (CC) $L_{12}Zn_{24}(PF_6)_{48}$ with cuboctahedron geometry, acquired by travelling-wave IM-MS on a Q/ToF mass spectrometer. Each band represents a single charge state, given next to the band, together with its CCS in \mathring{A}^2 . Two bands with distinct CCS are observed for charge states 17+, 12+, and 11+; the other charge states show single bands. The charge states observed fall onto three different trend lines, representing three different conformers of the cuboctahedron (CCa, CCb, and CCc). Adapted from Endres (2019) with permission from the author. CCS, collision cross-section; ESI, electrospray ionization; IM, ion mobility; MS, mass spectrometry. [Color figure can be viewed at wileyonlinelibrary.com]

et al., 2011) and of branched polymers differing in the lengths of the main and side chains (Foley et al., 2015). Consistently, high charge states were necessary to obtain distinguishable IM-MS characteristics (i.e., drift times or CCS values).

The effect of charge state on macromolecular gasphase conformation can most appropriately be gauged with a monodisperse supramolecular polymer, such as the coordinatively bound complex (CC) in Figure 19, which was prepared by the self-assembly of a tetrakisterpyridine ligand (L) with $\rm Zn^{2+}$ ions and isolated as the hexafluorophosphate (PF₆⁻) salt (Endres, 2019; Xie et al., 2016). Because of the custom-made position of the four terpyridine binding sites in L, 12 L units, and 24 $\rm Zn^{2+}$ ions combine to form the organometallic complex $\rm L_{12}\rm Zn_{24}^{48+}$ whose charge is balanced by 48 PF₆⁻ anions. ESI of such supramacromolecules produces a distribution of charges, based on how many PF₆⁻ moieties are

10982787, 2024, 3, Downloaded from https://analyticalsciencejournals.onlinelibrary.wiley.com/doi/10.1002/mas.21844 by Chrys Wesdemiotis - University Of Akron Bierce Library, Wiley Online Library on [23/07/2024]. See the Terms and Conditions (https://onlinelibrar

and-conditions) on Wiley Online Library for rules of use; OA articles are governed by the applicable Creative Commons License

lost during transfer from solution to the gas phase. The ESI-IM-MS spectrum of L₁₂Zn₂₄(PF₆)₄₈ (CC) displays a distribution of ions with 10-27+ charges, arising by loss of 10-27 PF₆⁻ counterions (cf. Figure 19). Starting from the highest charge state observed (27+), drift times and CCSs gradually increase as the charge is reduced to 18+ by the addition of PF₆⁻ counterions; this trend reflects the decrease in IM as the ions carry lesser charges. Further decrease of the charge to 17+ results in two bands with unique drift time and CCS; the slower moving ion has a larger CCS than the 18+ charge state, thus continuing the described trend. The faster-moving ion is attributed to a contracted, more compact structure, arising from decreased charge repulsion in CC when its counterion shell exceeds 30 anions (there are 31 PF₆⁻ anions in the 17+ charge state of CC). Additional charge decreases (to 16+ and lower) are accompanied by CCS increases (as seen initially), until charge state 12+ is reached, when anew contraction takes place. Overall, the charge states appear to follow three trend lines, stretching from 27+ to 17+, from 17+ to 11+, and from 12+ to 10+, indicating the existence of three variously compact conformers of the cuboctahedron architecture (CCa, CCb, and CCc) depending on the extent of attractive anion-cation interactions between the positively charged supramolecule and its counterions (Figure 19).

The average CCS of all observed charge states and conformers of CC (Figure 19) is 2431 (±144) A²; this cross-sectional area agrees well with the computationally predicted value for a cuboctahedron geometry, 2380 A², calculated from the optimized counter-ion free complex by molecular mechanics/dynamics simulations. Such combined experimental/theoretical CCS data are invaluable for the elucidation of macromolecular architectures and conformations, if the polymeric product cannot be crystallized or purified for characterization by X-ray diffraction and NMR spectroscopy, respectively. This is often encountered with bioconjugates (Alalwiat et al., 2015), organometallic polymers (Endres et al., 2020), polyelectrolyte complexes (Atakay et al., 2020; Y. Chen et al., 2018), and labile or reactive materials.

4.4 | Structural characterization through IM MS/MS

The majority of commercial mass spectrometers equipped with IM-MS house the IM region behind the ion source or between two mass analyzers. In the latter configuration (e.g., in the Synapt TWIM product line), MS/MS experiments can be performed on mass-selected ions either before or after IM separation (Pringle et al., 2007). If the IM cell is located after the ion source

(e.g., in the Agilent DTIM and Bruker TIM product lines), fragmentation can be performed before IM separation by causing in-source dissociation (Gabelica & Livet, & Rosu, 2018) or by using a segmented tandem TIM cell with an intermediate ion gate (Meier et al., 2021), respectively. Separating ions before MS/MS fragmentation allows for acquisition of the fragmentation patterns of pure isomers, conformers, or isobars, that is, molecular species superimposed at the same or very similar m/zratio; such a protocol was utilized to distinguish PEG isobars (Hilton et al., 2008), isomeric organometallic complexes (Li, Chan, et al., 2011), and bioconjugate isomers (Sallam et al., 2018). Conversely, inducing fragmentation before IM separation separates the fragmentation products from the superimposed species, which can reveal information about the original overlapping architectures or sequences; this procedure has been applied to characterize linear and cyclic metallopolymers (Li, Chan, et al., 2011) and to differentiate glycan sequences (J. Wei et al., 2020).

Figure 20 exemplifies an IM-MS/MS characterization, involving separation of the random coil (compact) and helical (elongated) components of the PEGylated peptide AQK18, Ac-KAAAQAAAQAAAQAAAQK-NH-PEG (Sallam et al., 2018). IM-MS analysis of the $[AQK18-PEG_{71} + 4H]^+$ ion from this bioconjugate (Figure 20A) confirms the presence of two conformers, A and B, which were assigned to a PEGylated random coil (A, ~900 Å²) and PEGylated α -helix (B, ~1020 Å²), respectively. Subsequent MS/MS fragmentation via CAD gave rise to the 2D map depicted in Figure 20B. Extensive dissociation occurs within the peptide portion of conformer A, but barely any fragments are formed from conformer B, consistent with a higher stability of the helical conjugate and dissociation after collapse to random coil structure. The MS/MS products include N-terminal b_n/a_n and C-terminal y_n fragment ions. None of the N-terminal fragments but all of the C-terminal fragments contain the PEG chain, validating that the polymer was conjugated at the C-terminus. Figure 20C shows the computationally optimized random coil (A) and helical (B) structures, whose CCS values of \sim 968 and \sim 1040 Å² agree satisfactorily with the corresponding experimentally determined CCSs (Sallam et al., 2018).

4.5 | Coupling LC to IM-MS

IM-MS can also be interfaced with online LC to create a multidimensional method offering 2D separation by LC in the solution phase (preionization) and IM in the gaseous state (postionization) followed by MS (and, if needed, MS/MS) characterization. This approach is more

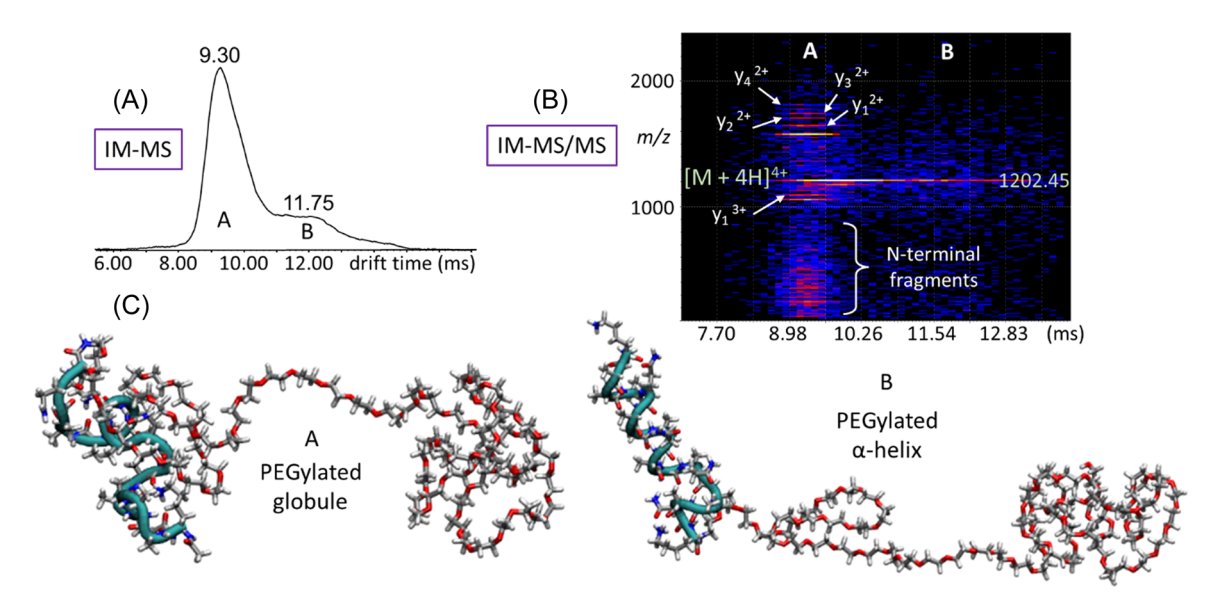


FIGURE 20 (A) ESI-IM-MS mobilogram (drift time distribution) of the $[M + 4H]^{4+}$ ion from bioconjugate AQK18-PEG₇₁, acquired on a Q/ToF mass spectrometer equipped with travelling-wave IM-MS. (B) 2D map of the IM-MS/MS spectra of the separated conformers A and B; the fragments originating from each conformer align vertically with the corresponding $[M + 4H]^{4+}$ precursor ions. (C) Computationally optimized structures of A and B. Adapted from Sallam et al. (2018) with permission from the American Chemical Society. 2D, two-dimensional; ESI, electrospray ionization; IM, ion mobility; MS, mass spectrometry; ToF, time-of-flight. [Color figure can be viewed at wileyonlinelibrary.com]

economic and environmentally friendly than connecting two LC dimensions in series (vide supra) and is applicable to a wide variety of samples by proper choice of the LC stationary phase. LC-IM-MS(/MS) has been employed to elucidate the compositional heterogeneity of nonionic surfactant blends and should be equally useful for the analysis of other multicomponent polymer mixtures (Ma et al., 2019; O'Neill et al., 2022). Figure 21 illustrates the dispersive power of orthogonal separation in LC and IM dimensions for the nonionic surfactant Chemonic CCG-6, also known as PEG-6 caprylic/capric glycerides (O'Neill et al., 2022). This amphiphilic blend is supplied with six ethoxylation (CH_2CH_2O) units (average x + y + z = 6, cf. Figure 21A), but its degree of esterification and glycerol oligomerization are unspecified.

Effective fractionation is achieved using RP-LC on a C18 column and gradient elution (Figure 21B). Orthogonal IM separation of the eluates uncovers several overlapping components which would be difficult to observe and characterize without this additional dispersion step (cf. Figure 21C). With the combined LC-IM process, 24 components of Chemonic CCG-6 could be spread sufficiently apart from each other (Figure 21C) to acquire their mass spectra and confirm their structure by accurate mass measurement via MS analysis and examination of the fragmentation patterns of select oligomers via MS/MS analysis, cf. Figure 21D. This kind

of overall 4-dimensional LC-IM-MS(/MS) analysis showed that the sample contains mono- and diglycerides that are esterified with capric (C_{10}) and/or caprylic (C_8) acids and carry 2-15 ethoxylation units. Nonesterified components and mono- and di-esterified PEG were also detected. The LC step separates the mixture by the degree of lipophilicity (hydrophobicity), revealing the presence of mono-, di-, and tri-esterified glycerides; conversely, the IM step separates by glycerol (G) content species with similar retention times (but differences in branching architecture), like the di-esterified products #11 and #12, viz. $PEO_n(C_8)_2$ and $G-PEO_n(C_8)(C_{10})$, respectively; or the tri-esterified products #20 and #21, $PEO_n(C_8)_2(C_{10})$ and G_2 - $PEO_n(C_8)(C_{10})_2$, respectively (Figure 21C,D). Such comprehensive elucidation is needed to distinguish formulations from different manufacturers or different batches. Interestingly, the sample analyzed contained no detectable dehydration products, which would produce cyclic and tadpole ether moieties.

5 | ANALYSIS AND IMAGING OF SOLID POLYMER SURFACES

In a large number of industrial applications requiring the use of synthetic polymers—such as plastics, adhesives, coatings, and medical devices—the exposed surface of the polymer is crucial to the properties, as it is the part in

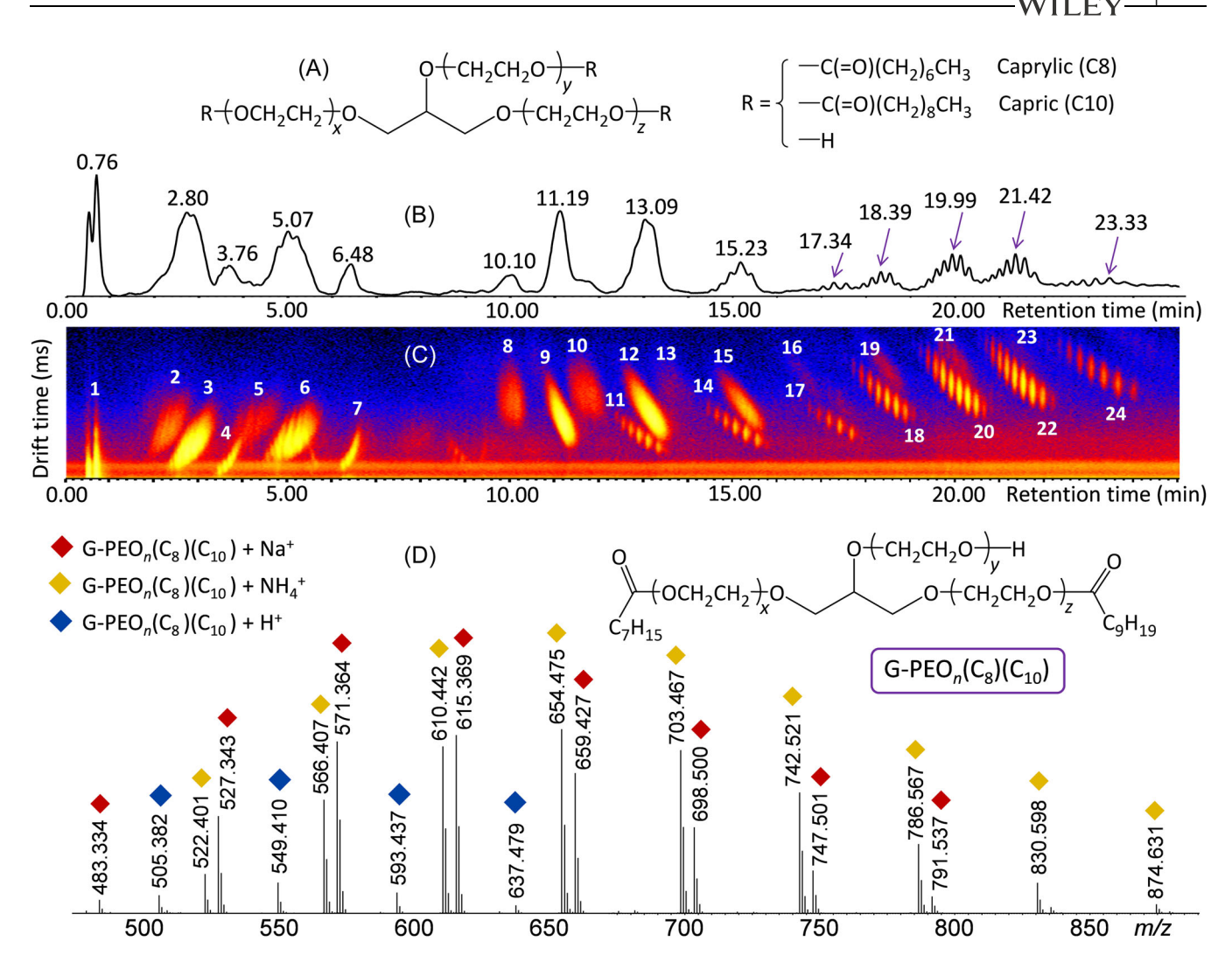


FIGURE 21 (A) Chemonic CCG-6 nonionic surfactant. (B) LC-MS total ion chromatogram and (C) LC-IM-MS total ion mobilogram of Chemonic CCG-6, acquired on a Q/ToF mass spectrometer equipped with travelling-wave IM-MS. Band #1 is unesterified G-PEG_n (G = glycerol); bands #2-7 are mono-esterified oligomers with 0 (#4, 7), 1 (#3, 6), or 2 (#2, 5) G units; bands 8-16 are di-esterified oligomers with 0 (#11, 14, 16), 1 (#9, 12, 15), or 2 (#8, 10,13) G units; bands 17-24 are tri-esterified oligomers with 1 (#18, 20, 22, 24) or 2 (#17, 19, 21, 23) G units. (D) LC-IM-MS spectrum of LC-IM band #12 (cf. Figure 21C). The m/z data of the three $[M + X]^+$ (X = Na, NH_4 , H) series observed indicate the presence of only G-PEG_n(C₈)(C₁₀) in this band. MS/MS analysis shows capric and caprylic acid losses and ions diagnostic of these fatty acids, validating the $C_8 + C_{10}$ acid content. Reproduced from O'Neill et al. (2022) with permission from the American Chemical Society. 2D, two-dimensional; ESI, electrospray ionization; IM, ion mobility; MS, mass spectrometry; ToF, time-of-flight. [Color figure can be viewed at wileyonlinelibrary.com]

direct contact with the environment. Common analytical techniques applied to synthetic polymers, like SEC/GPC and optical or NMR spectroscopy, focus on bulk properties. These can, however, differ substantially from the properties of the surface and cannot be adequately ascertained using techniques that probe the entire sample. To complement these bulk techniques, several surface-specific spectroscopic methods have been developed for the analysis of polymer surfaces, such as neutron reflectometry (NR), X-ray reflectometry (XRR), and X-ray photoelectron spectroscopy (XPS) (Vickerman & Gilmore, 2009).

5.1 | NR and XRR

NR and XRR are diffraction beam techniques that provide information based on the differences in reflectivity across the surface. With XRR, the X-ray beam probes differences in electron density to determine surface roughness and thickness. Similar analysis can be done using NR, which monitors reflectivity variations arising from different nuclei; NR is more sensitive than XRR for lighter elements or isotopes (Torikai, 2011; Zhou & Chen, 1995). Another commonly used technique for the analysis of polymer

10982787, 2024, 3, Downloaded from https://analyticals

University Of Akron Bierce Library, Wiley Online Library on [23/07/2024]. See the Terms and Condit

surfaces is XPS, which employs an X-ray beam to measure the differences in the kinetic energy of the electrons radiated from the surface. These kinetic energy values depend on the elements or functional groups emitting the electrons, thus providing elemental composition information about the surface (Vandencasteele & Reniers, 2010).

Collectively, these surface techniques have been able to identify phase segregation in block copolymers, interfacial segregation of polymer mixtures, and surface composition changes as a result of time and environment (Rymuszka et al., 2016; Thomas & Penfold, 1996; Torikai, 2011). While XRR, NR, and XPS can provide valuable information about surface composition, they have limited resolution, require isotopic labeling, and are unable to detect intact large molecules such as oligomers. To fill in the gaps left by these techniques, several MS methods have been developed which provide a more comprehensive surface analysis of polymeric materials.

5.2 | Secondary ion MS (SIMS)

In SIMS, a primary ion beam strikes a solid sample and ejects surface species (cf. Figure 22A). Only a small portion of the ejected species are charged (secondary ions) while the majority are neutral molecules. The proportion of the secondary ions is directly dependent on the amount of kinetic energy that is transferred from the primary ion beam to the surface molecules. These secondary ions are typically ionized molecules or large fragments from the surface, presenting a clear advantage over XRR, NR, and XPS which only detect certain elements. Coupling of this ionization process to mass

spectrometers, in particular ToF devices, has allowed for its broad application in the field of polymer surface research (Benninghoven, 1994; Van der Heide, 2014).

The SIMS process described above is referred to as static SIMS, as it uses a low dose of primary ions to limit damage and eject species only from the top monolayer of the sample. Conversely, dynamic SIMS employs a much higher dose of primary ions, resulting in deeper surface penetration (depth profiling) and increased yield of secondary ions. Sensitivity is much higher with dynamic SIMS than static SIMS, but the more intense primary beam also increases the fragmentation extent of the surface species. For polymers with similar structures, the additional fragmentation induced in dynamic SIMS analysis can complicate, or in some cases prevent, confident identification of the polymer species at the surface (Mei et al., 2022; Vickerman & Gilmore, 2009). Depth profiling is more conclusively performed with a dual sputter gun, in which the primary ion beam is paired with a secondary beam that successively exposes deeper layers to the surface, so that they can be characterized by the product ions ejected by the primary ion source (cf. Figure 22B).

An important factor in SIMS is the type of primary ion beam used. Most commercial ToF-SIMS instruments are equipped with liquid metal ion guns (LMIGs) based on bismuth; however, different primary beam types can be more beneficial for polymer analysis. For example, a SF_5^+ primary ion beam was found to increase secondary ion production and decrease surface damage (Kötter & Benninghoven, 1998), while a C_{60}^+ ion beam was shown to improve secondary ion intensities without increasing fragmentation (Weibel et al., 2003). Similarly, a different study documented that an argon gas cluster ion beam

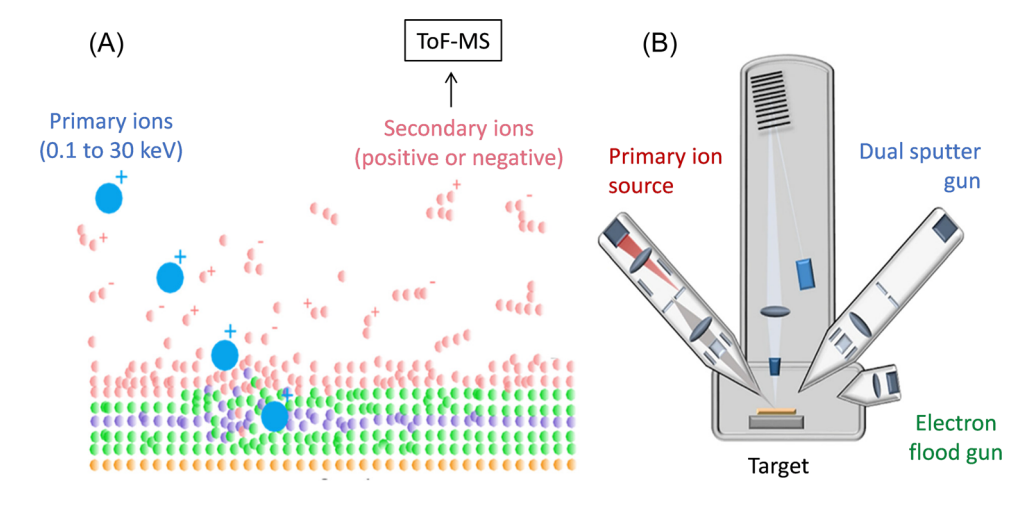


FIGURE 22 (A) SIMS process with ToF analysis of the secondary ions; (B) ToF-SIMS instrument with dual sputter gun and an electron flood gun (pulsed periodically to minimize surface charge during analysis). Reproduced from Mei et al. (2022) with permission from John Wiley & Sons, Inc. SIMS, secondary ion mass spectrometry; ToF, time-of-flight. [Color figure can be viewed at wileyonlinelibrary.com]

decreases surface damage and fragmentation, resulting in the observation of higher oligomeric species (Rabbani et al., 2011). These findings underscore the importance of selecting the appropriate primary beam type and correct beam intensity for achieving an optimal analysis.

Specific peaks in ToF-SIMS mass spectra can be used to create surface images or perform depth profiling (Mei et al., 2022). Figure 23A shows the image of ATRP-TAD, a triazolinedione (TAD) substituted with an initiator for atom transfer radical polymerization (ATRP), which was printed onto an indole functionalized glass substrate in 5 μm stripes spaced by 10 μm (Roling et al., 2015). PMA brushes could be grown from these patterned regions. TAD and indole form an adduct at room temperature that is cleaved at elevated temperature; this reversibility allows one to erase the printed sections and reprint a different pattern (Roling et al., 2015).

Figure 23B shows the depth profile of a polymer film acquired using a dual sputter gun. The film was prepared on a Si wafer from a blend of linear PMMA and a PS-PMMA brush copolymer (Mei et al., 2019). $C_2H_3O_2^+$, $C_7H_7^+$, and Si⁺ secondary ions served as signatures for PMMA, PS-PMMS, and the wafer, respectively. The ToF-SIMS data clearly show complete segregation of the bottlebrush polymer from the interior of the film and enrichment at the interfaces, which was primarily at the top of the film and to a lesser extent at the wafer surface.

ToF-SIMS imaging has been used to determine the influence of end group polarity in the formation of ordered structures during film formation (Yunus et al., 2007) and to identify polymer orientation on the surface of films (Karar & Gupta, 2015). In dynamic mode or with dual beam instrumentation, this technique can reveal the 3D phase domain structure of films prepared from polymer blends, cf. Figure 23B (Bernasik et al., 2001; Mei et al., 2019, 2022).

In general, SIMS has several advantages over XRR, NR, and XPS by providing direct surface composition information and high-depth resolution without the need for isotopic labeling. These characteristics make SIMS valuable for polymer surface analysis. Unfortunately, it usually leads to complex spectra, which can be difficult to interpret, and generates intense noise signal from the production of positive, negative, and neutral species during the sputtering and ejection processes. Furthermore, the SIMS technique can only probe fragment species and small oligomers but rarely intact polymers, thus posing the need for alternative methods for polymer surface analysis.

5.3 | Surface-layer (SL) MALDI-MS

MALDI-MS is known as a widely applicable analytical tool for synthetic polymers for a variety of reasons: (a) MALDI is a soft ionization method that enables the observation of intact macromolecules, as opposed to their fragments, which is a common problem with the previously mentioned SIMS technique. (b) Coupling a MALDI source to a ToF mass analyzer allows for detection of high MW polymers and calculation of their average MWs and polydispersities according to Equations (1)-(3). (c) Unlike GPC, which also reveals MW information, MALDI-MS can resolve individual oligomers within specific mass ranges (determined by sample complexity and composition), thus permitting measurement of their masses to derive repeat unit and chain end group information not available by GPC (Räder & Schrepp, 1999).

The SL variant of MALDI-MS has extended the applicability and advantages of this method to solid polymer surfaces (Wang et al., 2012). SL-MALDI-MS

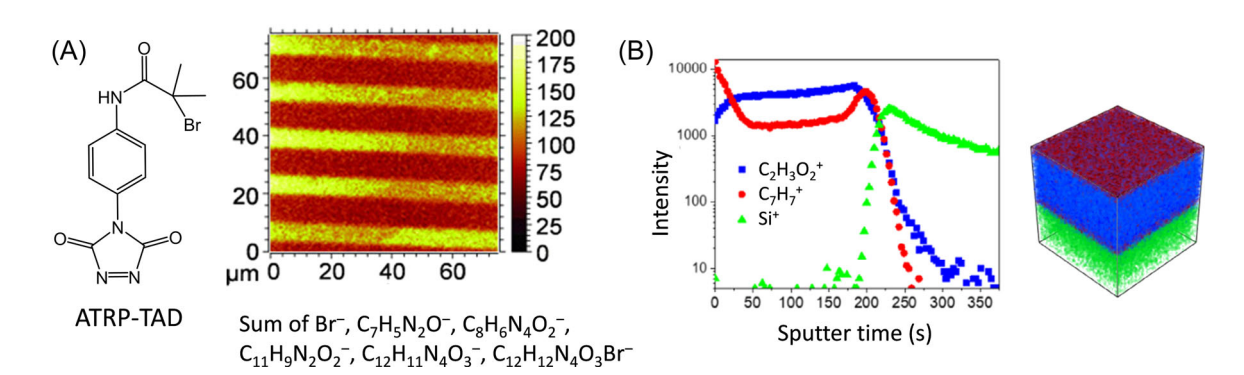


FIGURE 23 (A) ToF-SIMS image of ATRP-TAD printed in 5 μ m stripes spaced by 10 μ m; reproduced from Roling et al. (2015) with permission from Wiley-VCH Verlag GmbH & Co. KGaA. (B) Depth profiling of a blend containing linear PMMA (blue) and surface-active bottlebrush copolymer with PS and PMMA side chains (red); reproduced from Mei et al. (2019) with permission from the American Chemical Society. [Color figure can be viewed at wileyonlinelibrary.com]

achieves surface specificity by utilizing a solvent-free sample preparation protocol, in which the matrix and auxiliary ionization salt are applied via mechanical (dusting) or sublimation means (vide infra). By avoiding solvent during matrix/salt application, a depth resolution of <2 nm (top 1–2 molecular layers) has been demonstrated by the analysis of bilayer films with different polymers on the top and bottom layers (Wang et al., 2012).

The SL-MALDI-MS technique has been used to investigate segregation phenomena during the preparation (via spin casting) of films from polymer blends with components differing in MW, polarity, or architecture. Shorter linear PS and PMMA oligomers were entropically driven to the surface resulting in a decrease of the observed $M_{\rm n}$ and $M_{\rm w}$ (Hill, Endres, Mahmoudi, et al., 2018; Wang et al., 2012); whereas the surfaces of films made from blends differing in chain end chemistry were completely depleted of the polar constituent due to enthalpic factors (Hill, Endres; Meyerhofer, et al., 2018), cf. Figure 24. On the other hand, films prepared from a blend of cyclic PS and linear PS showed entropically driven enrichment of the linear chains at the surface (Wang et al., 2012). It is evident from these results that the bulk and surface can have distinct compositions. Knowledge of the surface composition is particularly important for understanding the physicochemical, mechanical, and electrical properties of the material under investigation, as the surface is the first point of contact with the material's environment.

If SL-MALDI-MS is used in conjunction with etching, depth profiling can be implemented. This procedure was applied to investigate a PS bilayer film and characterize its top, bottom, and interfacial regions (Fouquet et al., 2014). SL-MALDI-MS is also suitable for imaging

defects on polymer surfaces; this mass spectrometry imaging (MSI) capability has been recently demonstrated with the acquisition of images of defects from foreign materials, material absence, mechanical scribing, and solvent perturbation at the surface of PMMA and PS thin films (Endres et al., 2018); Figure 25 exemplifies a SL-MSLDI-MSI analysis of a solvent-damaged surface.

SL-MALDI requires a solventless sample preparation procedure, so that the chemical environment and (macro)molecular characteristics of the surface are not disrupted. Dry matrix and salt powders that have been mixed with a mortar and pestle can be mechanically applied on the top of the sample with a spatula (Wang et al., 2012). This preparation method is quick and convenient, but it can cause increased noise during analysis if the powder does not completely adhere to the surface. A more uniform surface coverage by matrix/salt and more reproducible results are obtained by sublimation; where the sample is attached to a cold plate above the matrix/salt powders which are heated. The matrix and salt molecules sublime into the gas phase and deposit onto the cold sample surface. Matrix/salt coating by sublimation has also been used in regular MALDI imaging (Hankin et al., 2007) and enhances considerably the analysis specificity (Endres et al., 2018).

The detection sensitivity of SL-MALDI-MS is low, since only a very small part of the sample, viz. the surface, is probed. Substantial improvement is possible with MALDI lasers operating at frequencies ≥2 kHz, as compared to the ~100 Hz in the equipment of the studies reported thus far (Endres et al., 2018) due to markedly improved signal averaging. The current upper mass limit is around 20 kDa (Yao, 2014), making the SL-MALDI-MS method most suitable for the analysis of low to medium MW samples and of additives (such as drugs or unwanted

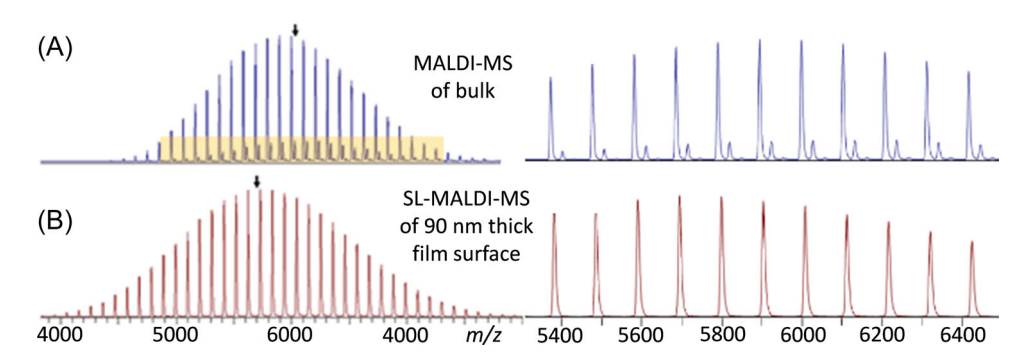


FIGURE 24 (A) MALDI-MS spectrum of a PS blend composed of 91% C_4H_9 - $(C_8H_8)_n$ -H and 9% C_4H_9 - $(C_8H_8)_n$ -CH₂OH. (B) SL-MALDI-MS spectrum of a film prepared by spin casting this blend. DCTB matrix and silver trifluoroacetate cationizing salt were (A) mixed with the bulk sample and (B) applied to the surface by mechanical dusting. All peaks correspond to $[M + Ag]^+$ ions detected in a MALDI-ToF mass spectrometer. The blue arrows indicate the M_n in each spectrum. Shorter chains are enriched at the surface and polar chains are depleted from the surface. Reproduced from Hill, Endres; Meyerhofer, et al. (2018) with permission from the American Chemical Society. MALDI-MS, matrix-assisted laser desorption/ionization-mass spectrometry; SL, surface-layer. [Color figure can be viewed at wileyonlinelibrary.com]

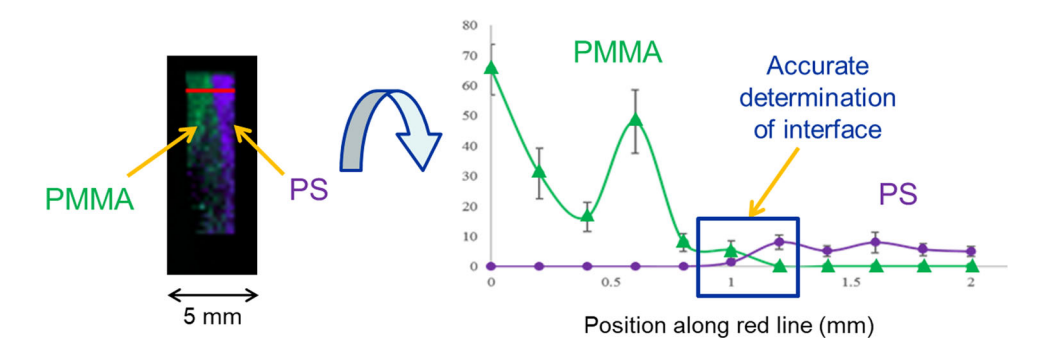


FIGURE 25 SL-MALDI-MS image of a bilayer film prepared by spin casting a 6 kDa PS layer onto a spun cast 7 kDa PMMA film, then removing (from the left side) half the top PS layer by dissolving it in cyclohexane (acquired with a MALDI-ToF mass spectrometer). A mixture of matrix and silver salt was sublimated onto the film. The intensity profile of PMMA and PS ions across the red line is shown at right. Reproduced from Endres et al. (2018) with permission from the American Chemical Society. MALDI-MS, matrix-assisted laser desorption/ionization-mass spectrometry; SL, surface-layer. [Color figure can be viewed at wileyonlinelibrary.com]

contaminants) on the surface of very high-mass polymers (Williams-Pavlantos & Wesdemiotis, 2021).

5.4 | Solvent-based MALDI MSI

In conventional MALDI-MSI, a solution of matrix and auxiliary ionization salt (if needed) is used to add matrix/salt to the sample, either dropwise or through a sprayer. This sample preparation protocol is widely utilized for imaging biological tissues to track lipid, protein, and metabolite distributions (Cornett et al., 2007; Vaysse et al., 2017). Depth profiling is obtained by analyzing thin slices of the tissue to reconstruct a 3D profile of the desired substance. Such multilayer imaging has not been performed yet with polymers but could be beneficial for the analysis of additive distributions in polymeric materials.

Coating a polymer film with a matrix/salt solution would remove surface specificity, as the solvent can cause mixing of surface and bulk molecular layers. Nevertheless, the resulting spectra and/or images can unveil valuable information about the polymer sample being analyzed or the changes it has undergone after chemical treatment (Crecelius et al., 2014). Solvent-based MALDI-MSI has been performed on polymer samples prepared for MALDI-MS analysis using the dried droplet method to determine polymer/matrix distributions; matrix accumulation in the periphery of the sample spot and segregation of polymer and matrix were observed for some matrix/analyte combinations (Weidner & Falkenhagen, 2009). A MALDI-MSI study of PS films irradiated by UV light for variable time intervals showed the occurrence of significant crosslinking in the irradiated areas (Crecelius et al., 2011). Similarly, the degradation of low MW PCL under aerobic and denitrifying conditions could be monitored by the corresponding MALDI-MSI scans, which showed significant differences between these two degradation modes; only the denitrifying (bacteria containing) environment led to major changes in composition (Rivas et al., 2016). Meanwhile, MALDI-MSI analysis of a dialysis membrane composed of polysulfone (PSu) and polyvinylpyrrolidone (PVP) indicated different compositions at the luminal and abluminal sides of the membrane: the abluminal surface comprised more PSu than PVP, while the reverse was true for the luminal surface, cf. Figure 26 (Krueger et al., 2013).

5.5 | Desorption electrospray ionization (DESI)-MS

DESI is an ambient ionization MS technique introduced by Cooks et al. in the early 2000s. It combines the characteristics of ESI and desorption ionization and can be used to analyze solid materials, frozen solutions, liquids, and adsorbed gases (Takáts et al., 2004, 2005). With this technique, an electrospray system is used to form solvent ions and charged microdroplets which are directed, at an angle, to the surface containing the sample. The charged droplets extract and desorb sample molecules from the surface, which are ionized within the droplet. The secondary ions formed are drawn with appropriate potentials to the entrance of the mass spectrometer for mass and structural analysis. Two major advantages of DESI-MS are that it is performed under ambient conditions and requires minimal sample preparation. This ease of use and the surface specificity of DESI-MS have made it widely applicable in both forensics and biology studies (Bodzon-Kulakowska et al., 2015; Wójtowicz & Wietecha-Posłuszny, 2019).

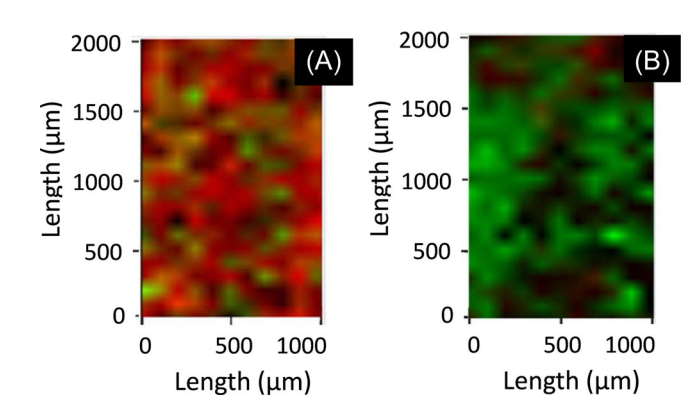


FIGURE 26 MALDI-MSI distributions of polysulfone (PSu; red color) and polyvinylpyrrolidone (PVP; green color) signature ions from (A) the abluminal and (B) luminal surface of a polymeric dialyzer membrane, acquired on a LTQ Orbitrap-XL mass spectrometer equipped with a nitrogen laser. Adapted from Krueger et al. (2013) with permission from the American Chemical Society. MALDI-MSI, matrix-assisted laser desorption/ionization-mass spectrometry imaging. [Color figure can be viewed at wileyonlinelibrary.com]

The applicability and advantages of DESI-MS were initially demonstrated for the investigation of biological samples and pharmaceuticals (Takáts et al., 2004, 2005), but this method has also shown promise for the analysis of more complex systems such as protein complexes (Hale & Cooper, 2020) and polymers. The first DESI-MS study on polymeric materials concerned industrial polymers, viz. poly(ethylene glycol) (PEG), poly(tetramethylene glycol) (PTMG), and polyacrylamide (PAM), which were examined on a LIT mass spectrometer (Nefliu et al., 2006). DESI-MS of PEG gave rise to several multiply charged distributions, from which average MW data could be derived that were in good agreement with the sample's expected MW. The more hydrophobic PTMG and PAM, however, showed reduced multiple charging, overlapping isobaric peaks, and reduced ionization efficiency for the longer chains, indicating that sample preparation and spectral acquisition conditions may need to be optimized for each type of polymer under investigation (Nefliu et al., 2006). A newer study, utilizing DESI-Orbitrap-MS, looked at polymers and copolymers with a wider range of polarities and MWs spanning from 500 Da to 20 kDa (Friia et al., 2012). With the use of a deconvolution software for the multiple charge states observed, average MWs and polydispersity could be deduced for homopolymers up to 7000 Da that were in fairly good agreement with similar data obtained by MALDI-ToF-MS or GPC. On the other hand, the DESI-MS spectra of larger homopolymers (>10 kDa) were too complex to be processed. Similarly, the spectral complexity was high for the copolymers due to

overlapping charge states and superimposed isobaric ions with different comonomer units or different metal adducts. Given the high resolving power of Orbitrap mass analyzers, it was concluded that successful DESI-MS analysis of copolymers and complex mixtures requires more powerful deconvolution software (Friia et al., 2012).

One of the difficulties in DESI-MS is that some molecules, particularly nonpolar species, do not ionize well. To overcome this issue, a variant of traditional DESI, termed reactive DESI, has been developed (Nyadong et al., 2009). With reactive DESI, different reagents are added to the spray solution that specifically target the sample molecules to assist with their ionization and detection. Reactive DESI has been shown to overcome the sensitivity issues encountered in traditional DESI-MS, thus increasing this method's robustness as an analytical tool. The reactive DESI process has been successfully applied to detect and characterize fatty acids, algae extracts, and polymers (Fouquet et al., 2021; Nyadong et al., 2009).

DESI and the reactive DESI variant are also suitable for MS imaging studies; here, the sample is rastered to allow the charged microdroplet stream coming from the ESI source to strike different sample spots. The secondary ions produced at each spot are then sent to the mass spectrometer for analysis and image generation (Eberlin et al., 2011; Neumann et al., 2020). The lack of laborious sample preparation and the ability to perform experiments at ambient conditions have quicky led to an influx of DESI-MSI applications. In the past 5 years, DESI-MSI has been utilized to detect and characterize small molecules and oligomers on synthetic polymer surfaces. In one such study, DESI-MSI was used to identify the presence of biodiesel in rubber (Silva et al., 2017); these experiments showed that biodiesel compounds and their oxidized species become trapped in the rubber networks, posing a risk for potential degradation of the rubber over time. A second example of a successful application of DESI-MSI to polymers includes determination of the drug distribution in the interior and exterior of cylindrical polymeric materials before and after exposure to release media (Pierson et al., 2020); the drug was localized mainly in the core of implants exposed to methanolic water but uniformly distributed through the implants exposed to acidic buffer. The most recent DESI-MSI study uncovered and mapped the picture "01" (cf. Figure 27), which was imprinted on a piece of satin fabric using isomeric monodisperse poly(alkoxyamine phosphodiester)s with different sequences for each character (Amalian et al., 2021); the oligomer sequences representing 0 and 1 were decoded by DESI-MS/MS, affirming the ability of this imaging technique to read digital labels written with polymeric inks (cf. Figure 27).

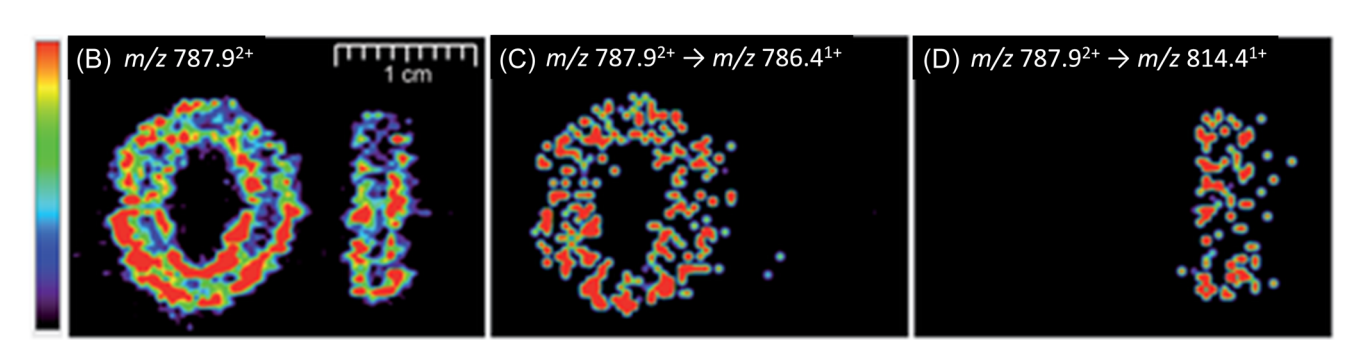


FIGURE 27 (A) Isomeric oligo(alkoxyamine phosphodiester)s used to print picture "01"; the sequence 100110 (P7, 1563.9 Da) denotes the circular character "0" and the sequence 101100 (P8, 1563.9 Da) the linear character "1." The tip of a pipette was employed as a pen to draw "0" and "1" with methanolic solutions of P7 and P8, respectively. (B) DESI image of "01", generated by monitoring the $[M - 2H]^{2-}$ (m/z 787.9) ion. (C) The MS/MS fragmentation $[M - 2H]^{2-} \rightarrow m/z$ 786.4¹⁻ (c_2^-) is only observed from "0", while (D) the MS/MS fragmentation $[M - 2H]^{2-} \rightarrow m/z$ 814.4¹⁻ (c_2^-) is only observed from "1", unveiling the corresponding sequences (the c_2^- series arises by C(CH₃)₂O-N bond cleavages, leading to fragment anions with C(CH₃)₂O- end groups). Adapted from Amalian et al. (2021) with permission from John Wiley & Sons, Inc. DESI, desorption electrospray ionization; MS, mass spectrometry. [Color figure can be viewed at wileyonlinelibrary.com]

For easy reference to the desired surface analysis and imaging technique, Table 4 details representative studies using SIMS, DESI, and MALDI (or SL-MALDI) for the characterization of polymeric materials.

6 | QUANTITATIVE ANALYSIS

Quantitative analysis of synthetic polymers is rarely performed by MS techniques due to inherent uncertainties in ionization efficiencies and the occurrence of ionization suppression (vide supra). Pure polymers can be quantified by MS analysis if calibration standards of the same polymer type are available. An isotopically labeled internal standard would provide the highest accuracy. For mixtures of polymers differing only in their end groups, the corresponding relative intensities provide adequate relative quantitation if the end groups do not affect the ionization efficiency. This has been documented for PS and PEG polymers with distinct end groups (H. Chen et al., 2003; Quirk et al., 2002). On the other hand, for blends of different MW ranges or different polymer types and complex mixtures, mass discrimination resulting from differences in solubility, polarity, desorption efficiency, and/or ionization efficiency preclude quantitation without tedious and costly separation techniques and appropriate standards for each mixture component (Shimada et al., 2001). In such cases, the use of other analytical/detection techniques, such as SEC and NMR spectroscopy, is recommended.

7 | ADVANCEMENTS IN DATA PROCESSING

As polymeric materials and their respective formulations and products become more complex to analyze, predictive software, machine learning, and mass defect computations may be required to deconvolute the data. Kendrick analysis (Kendrick, 1963) and mass remainder analysis have become vital tools for mass spectrometric interpretation as they can convert spectra containing overlapping distributions as a result of multiple end groups, adduct ions, and variably charged species into a simple and easy-to-interpret 2D plot (Fouquet & Sato, 2017; Fouquet, 2019; Nagy et al., 2018). This type of data treatment is crucial for complex samples like crude oil (Marshall & Rodgers, 2008), mixtures of polymeric additives (Lacroix-Andrivet et al., 2022), lignans (Mikhael et al., 2021), and other complex samples with superimposed isobaric and/or isomeric constituents (Fouquet, 2019). Examples of simplified data representation using Kendrick analysis on polymeric materials and mixtures are provided in Figure 28. These plots were constructed using CH2 (methylene) as base unit and display the Kendrick mass defect (KMD) of the observed

10982787, 2024, 3, Downloaded from https

Wiley Online Library on [23/07/2024]. See the Tern

TABLE 4 Examples of mass spectrometry techniques used for the surface analysis and imaging of various types of polymers.

Polymer sample(s)	Method	References
SIMS		
Honeycomb-like polystyrene films	Static SIMS	Yunus et al. (2007)
Plastic solar cells	Dynamic SIMS	Treat et al. (2011)
Polymer brush micropatterns	Static SIMS	Roling et al. (2015)
Polyurethane-carbon nanotube composites	Static SIMS	Karar and Gupta (2015)
DESI		
Polyacrylamide and polyethers	DESI-MS	Nefliu et al. (2006)
Macrolides on algal soft tissue	Reactive DESI-MS	Nyadong et al. (2009)
Biodiesel in commercial rubbers	DESI-MSI	Silva et al. (2017)
Drug distributions on polymeric implants	DESI-MSI	Pierson et al. (2020)
Sequence-encoded (digital) polymers	DESI-MSI	Amalian et al. (2021)
MALDI		
Polystyrene films	SL-MALDI-MS	Hill, Endres, Mahmoudi, et al. (2018), Hill, Endres, Meyerhofer, et al. (2018); Wang et al. (2012)
Polysulfone and polyvinylpyrrolidone membranes	MALDI-MSI	Krueger et al. (2013)
Degraded polycaprolactone films	MALDI-MSI	Rivas et al. (2016)
Defects on polymers surfaces	SL-MALDI-MSI	Endres et al. (2018)

Abbreviations: DESI, desorption electrospray ionization; MALDI, matrix-assisted laser desorption/ionization; SIMS, secondary ion mass spectrometry.

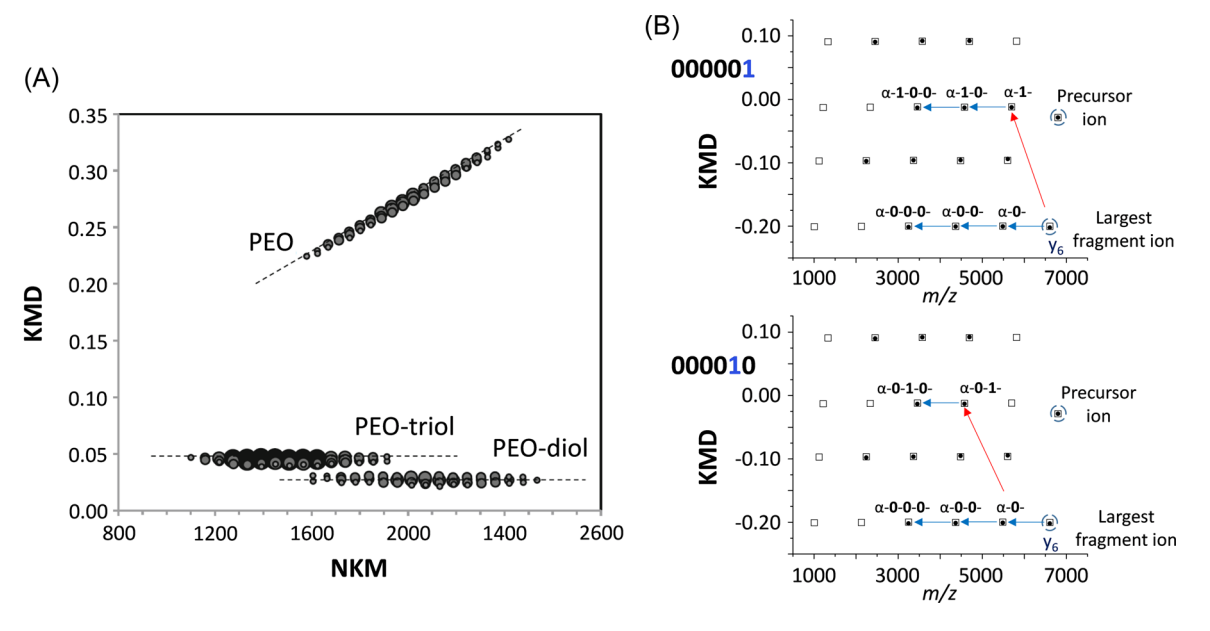


FIGURE 28 (A) Kendrick plot of the MALDI-MS spectrum of a blend of PEO, poly(propylene oxide) diol (PPO-diol), and poly (propylene oxide) triol (PPO-triol); all three polymers are clearly discerned in separate regions of the plot, whereas these distributions overlap in the MALDI-MS spectrum. Reproduced from Sato et al. (2014) with permission from the American Chemical Society. (B) Kendrick plots of the MS/MS fragments from two monodisperse polyester copolymers with different sequences (denoted 000001 and 000010); sequence differentiation is more clearly visible in the plots than in the MS/MS spectra. Adapted from Mao, Zhang, Cheng, et al. (2019) with permission from Sage Publications. See Fouquet (2019) for a tutorial on Kendrick analysis. MALDI-MS, matrix-assisted laser desorption/ionization-mass spectrometry. [Color figure can be viewed at wileyonlinelibrary.com]

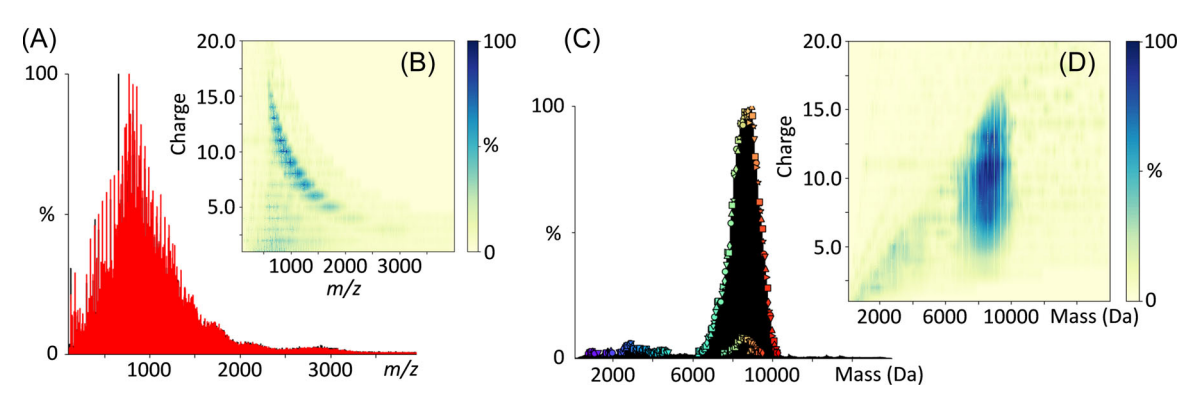


FIGURE 29 (a) Raw ESI-MS spectrum of PEG 7000 entered in the UniDec program; (B) Bayesian deconvolution output of the raw data, depicted as a 2D heat map of the average charge states observed for a given m/z. (C) Charge deconvoluted mass spectrum and (D) heat map, showing the molecular weight distribution of the polymer. $M_n = 8200$ Da based on the exported peak list of deconvoluted masses in part (C). Adapted from Keating and Wesdemiotis (2023) with permission from John Wiley & Sons. 2D, two-dimensional; ESI-MS, electrospray ionization-mass spectrometry; PEG, poly(ethylene glycol). [Color figure can be viewed at wileyonlinelibrary.com]

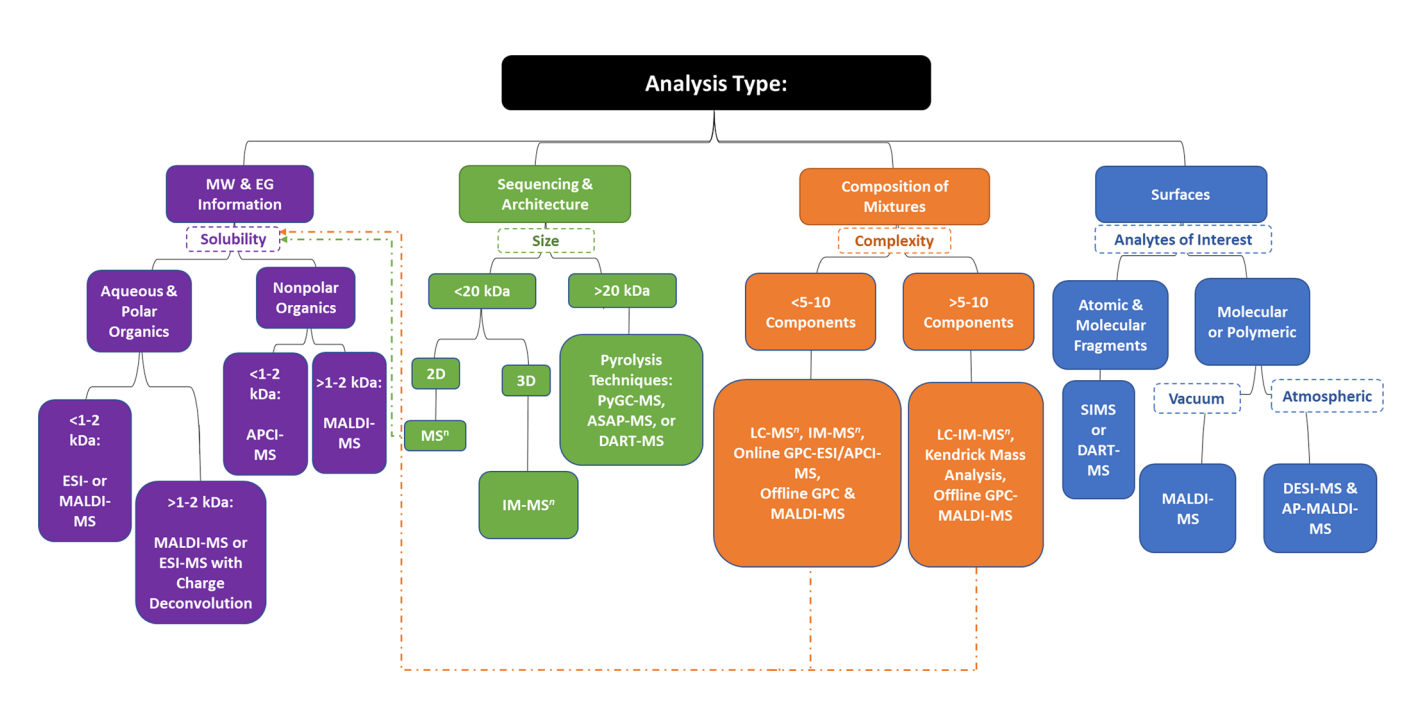


FIGURE 30 Flow chart separated into four distinct categories of information or data sought, including molecular weight and end group, sequencing and architecture, mixture/blend composition, and surface analysis. Subcategories within each analysis type facilitate determination of the proper MS method(s). MS, mass spectrometry. [Color figure can be viewed at wileyonlinelibrary.com]

ions versus the corresponding nominal Kendrick mass (NKM) or the corresponding m/z; Kendrick mass (KM), KMD, and NKM with CH₂ as the base unit are defined in Equations (7)–(9).

$$KM = observed \frac{m}{z} \times \frac{\text{nominal mass of CH}_2(14.00000)}{\text{IUPAC mass of CH}_2(14.01565)},$$
(7)

$$NKM = integer of KM, (8)$$

$$KMD = integer of KM - KM.$$
 (9)

For analyses involving copolymers and homopolymer mixtures, commercial programs like PolyToolsTM (Bruker Inc.) and Polymerix (Sierra Analytics) are available that allow for end group and MW data determination and copolymer sequence differentiation, although licenses to such software are required and can become pricy. Opensource programs such as Polymerator (Thalassinos et al., 2007) and PLUMS (Baumgaertel et al., 2011) are extremely useful for the interpretation and elucidation of MS/MS data and fragmentation patterns, while UniDec (Marty, 2022) allows for charge deconvolution of mass

10982787, 2024, 3, Downloaded from https://analyticalsciencejournals onlinelibrary.wileje.com/doi/10.1002/mas.21844 by Chrys Wesdemiotis - University Of Akron Bierce Library, Wiley Online Library on [23/07/2024]. See the Terms and Conditions (https://analyticalsciencejournals onlinelibrary.wileje.com/doi/10.1002/mas.21844 by Chrys Wesdemiotis - University Of Akron Bierce Library, Wiley Online Library on [23/07/2024]. See the Terms and Conditions (https://analyticalsciencejournals.onlinelibrary.wileje.com/doi/10.1002/mas.21844 by Chrys Wesdemiotis - University Of Akron Bierce Library, Wiley Online Library on [23/07/2024]. See the Terms and Conditions (https://analyticalsciencejournals.onlinelibrary.wileje.com/doi/10.1002/mas.21844 by Chrys Wesdemiotis - University Of Akron Bierce Library, Wiley Online Library on [23/07/2024]. See the Terms and Conditions (https://analyticalsciencejournals.onlinelibrary.wileje.com/doi/10.1002/mas.21844 by Chrys Wesdemiotis - University Of Akron Bierce Library, Wiley Online Library on [23/07/2024]. See the Terms and Conditions (https://analyticalsciencejournals.onlinelibrary.wileje.com/doi/10.1002/mas.21844 by Chrys Wesdemiotis - University Of Akron Bierce Library, Wiley Online Library on [23/07/2024]. See the Terms and Conditions (https://analyticalsciencejournalsciencejournalsciencejournalsciencejournalsciencejournalsciencejournalsciencejournalsciencejournalsciencejournalsciencejournalsciencejournalsciencejournalsciencejournalsciencejournalsciencejournalsciencejournalsciencejournalsciencejournalsciencejournalsciencejournalsciencejournalsciencejournalsciencejournalsciencejournalsciencejournalsciencejournalsciencejournalsciencejournalsciencejournalsciencejournalsciencejournalsciencejournalsciencejournalsciencejournalsciencejournalsciencejournalsciencejournalsciencejournalsciencejournalsciencejournalsciencejournalsciencejournalsciencejournalsciencejournalsciencejournalsciencejournalsciencejournalsciencejournalsciencejournalsciencejournalsciencejournalsciencejournalsciencejournalsci

und-conditions) on Wiley Online Library for rules of use; OA articles are governed by the applicable Creative Commons License

WESDEMIOTIS ET AL. broaden MS's applicability in polymer science and engineering. On the instrumental platform, charge detection MS coupled with high mass resolving power could pave the way for characterizing macromolecules in the megadalton range and even entire particles of the size of viruses or micelles (Jarrold, 2022). Meanwhile, the applicability of IM techniques to polymer science and engineering would be significantly expanded with the availability of a universal algorithm for the calculation of collision cross sections that is compatible with all possible collision gases and analyte elemental compositions. Similarly, the development of new data processing software and supervised machine learning training sets would assist in the postacquisition treatment of MS results and the interpretation of complex spectra. Advancements in artificial intelligence and image recognition for rapid data analysis of mixtures are in the early stages; however, increasing the sample sets of published polymer spectra through the creation of appropriate databases, similar to those available for biopolymers, would greatly accelerate practical applications of MS in all phases of polymer/materials characterization. Similarly beneficial would be an MS/MS data analysis program for (co)polymers and an extended fragment naming scheme applicable to diverse macromolecular architectures and topologies. **ACKNOWLEDGMENTS**

spectra containing overlapping charge states. Although the UniDec software was developed for the analysis of large biomolecules (Marty et al., 2015), specific features allow the user to define mass regions of interest and input oligomer mass information for predictive peak identification, thus opening the door to larger synthetic material characterization by ESI and other methods producing multiply charged ions. Figure 29 illustrates the improved information gained using this algorithm.

| CONCLUSIONS AND FUTURE OUTLOOK

Synthetic polymers have become a crucial component of many manufacturing processes and a pivotal aspect of macromolecular chemistry research. As a result of these activities, new analytical methods and techniques have been developed for the investigation and elucidation of important chemical properties of these substances, such as their size/MW, chemical composition, microstructure, architecture, and topology.

As with all analytical techniques, there is no universal mass spectrometer capable of analyzing all synthetic materials under a variety of physical states, so understanding the role of mass analysis in the overall materials' characterization is vital to selecting the proper method(s). The flow chart in Figure 30 provides a guide for selecting the appropriate MS method based on the question/problem being addressed.

This tutorial review detailed and exemplified various MS techniques that can be applied to the study of both single polymers as well as complex (co)polymer mixtures, including ESI-MS, MALDI-MS, and ASAP-MS which are essential in an analytical polymer laboratory. Multidimensional approaches, in particular MS/MS, LC-MS, and IM-MS, enhance the accessible analytical capabilities by providing complementary structural and composition information about major and, especially, minor products that are undetectable by methods probing the bulk as a whole. Additionally, surface analysis and imaging methods, like SIMS, DESI-MS, and SL-MALDI-MS can provide surface-specific information not obtainable with bulk techniques but are of great importance as they impact the applications and properties of the polymeric product being investigated. The discussion of all these subjects in this tutorial review clearly documents that MS has become a valuable analytical technique with numerous potentials for the study of polymer systems and should be an integral part of a polymer characterization facility.

In spite of this progress, further advancements are desired to augment the described capabilities and

Financial support from the National Science Foundation (CHE-1308307, CHE-1808115, and DMR-2215940). Sherwin-Williams, Lubrizol Corp., and Omnova Solutions Foundations is gratefully acknowledged.

REFERENCES

Aaserud, D.J., Prokai, L., Simonsick, W.J., Jr. 1999. Gel permeation chromatography coupled to Fourier transform mass spectrometry for polymer characterization. Anal. Chem. 71(21): 4793-4799. https://doi.org/10.1021/ac990722c

Abadie, M.J.M., Pinteala, M., Rotaru, A. (Eds.). 2021. New Trends in Macromolecular and Supramolecular Chemistry for Biological Applications, Springer Nature, Cham, Switzerland. https://doi. org/10.1007/978-3-030-57456-7

Abe, Y., Ackerman, L.K., Mutsuga, M., Sato, K., Begley, T.H. 2020. Rapid identification of polyamides using direct analysis in real-time mass spectrometry. Rapid Commun. Mass Spectrom. 34(S2): e8707. https://doi.org/10.1002/rcm.8707

Adamus, G., Rizzarelli, P., Montaudo, M.S., Kowalczuk, M., Montaudo, G. 2005. Matrix-assisted laser desorption/ionization time-of-flight mass spectrometry with size-exclusion chromatographic fractionation for structural characterization of synthetic aliphatic copolyesters. Rapid Commun. Mass Spectrom. 20(5):804-814. https://doi.org/10.1002/rcm.2365

Alalwiat, A., Grieshaber, S.E., Paik, B.A., Kiick, K.L., Jia, X., Wesdemiotis, C. 2015. Top-down mass spectrometry of hybrid materials with hydrophobic peptide and hydrophilic or

- hydrophobic polymer blocks. *Analyst* 140(22):7550–7564. https://doi.org/10.1039/c5an01600b
- Alawani, N., Barrère-Mangote, C., Wesdemiotis, C. 2022. Analysis of thermoplastic copolymers by mild thermal degradation coupled to ion mobility mass spectrometry. *Macomol. Rapid Commun.* 44:e2200306. https://doi.org/10.1002/marc. 202200306
- Alexander, N.E., Swanson, J.P., Joy, A., Wesdemiotis, C. 2018. Sequence analysis of cyclic polyester copolymers using ion mobility tandem mass spectrometry. *Int. J. Mass Spectrom.* 429:151–157. https://doi.org/10.1016/j.ijms.2017.07.019
- Aliyari, E., Konermann, L. 2020. Formation of gaseous proteins via the ion evaporation model (IEM) in electrospray mass spectrometry. *Anal. Chem.* 92(15):10807–10814. https://doi.org/10.1021/acs.analchem.0c02290
- Aloui, I., Legros, V., Giuliani, A., Buchmann, W. 2020. Synchrotron UV photoactivation of trapped sodiated ions produced from poly(ethylene glycol) by electrospray ionization. *Rapid Commun. Mass Spectrom.* 34(S2):e8773. https://doi.org/10. 1002/RCM.8773
- Aloui, I., Legros, V., Giuliani, A., Buchmann, W. 2021. Ultraviolet photoactivation using synchrotron radiation for tandem mass spectrometry of polysiloxanes. *J. Am. Soc. Mass Spectrom*. 32(4):901–912. https://doi.org/10.1021/JASMS.0C00392
- AlShehri, M.M., ALOthman, Z.A., Bedjah, A.Y., Ahmed, H., Aouak, T. New method based on direct analysis in real-time coupled with time-of-flight mass spectrometry (DART-ToF-MS) for investigation of the miscibility of polymer blends. 2022. Polymers 14(9):1644. https://doi.org/10.3390/polym14091644
- Altuntaş, E., Knop, K., Tauhardt, L., Kempe, K., Crecelius, A.C., Jäger, M., Hager, M.D., Schubert, U.S. 2012. Tandem mass spectrometry of poly(ethylene imine)s by electrospray ionization (ESI) and matrix-assisted laser desorption/ionization (MALDI). J. Mass Spectrom. 47(1):105–114. https://doi.org/ 10.1002/jms.2032
- Altuntaş, E., Schubert, U.S. 2014. "Polymeromics": Mass spectrometry-based strategies in polymer science toward complete sequencing approaches: A review. *Anal. Chim. Acta* 808:56–69. https://doi.org/10.1016/J.ACA.2013.10.027
- Amalian, J.-A., Mondal, T., Konishcheva, E., Cavallo, G., Petit, B.E., Lutz, J.-F., Charles, L. 2021. Desorption electrospray ionization (DESI) of digital polymers: Direct tandem mass spectrometry decoding and imaging from materials surfaces." *Adv. Mater. Technol.* 6(4):2001088. https://doi.org/10.1002/ADMT. 202001088
- Analytical Methods Committee, AMCTB No. 85. 2018. Analytical pyrolysis in cultural heritage. *Anal. Meth.* 10:5463–5467. https://doi.org/10.1039/C8AY90151A
- Andrade, F.J., Shelley, J.T., Wetzel, W.C., Webb, M.R., Gamez, G., Ray, S.J., Hieftje, G.M. 2008. Atmospheric pressure chemical ionization source. 1. Ionization of compounds in the gas phase. *Anal. Chem.* 80(8):2646–2653. https://doi.org/10.1021/ ac800156y
- Antignac, J.P., de Wasch, K., Monteau, F., De Brabander, H., Andre, F., Le Bizec, B. 2005. The ion suppression phenomenon in liquid chromatography-mass spectrometry and its consequences in the field of residue analysis. *Anal. Chim. Acta* 529(1-2):129–136. https://doi.org/10.1016/j.aca. 2004.08.055

- Antoine, R., Lemoine, J., Dugourd, P. 2014. Electron photodetachment dissociation for structural characterization of synthetic and bio-polymer anions. *Mass Spectrom. Rev.* 33(6):501–522. https://doi.org/10.1002/mas.21402
- Atakay, M., Aksakal, F., Bozkaya, U., Salih, B., Wesdemiotis, C. 2020. Conformational characterization of polyelectrolyte oligomers and their noncovalent complexes using ion mobility-mass spectrometry *J. Am. Soc. Mass Spectrom. 31*(2): 441–449. https://doi.org/10.1021/JASMS.9B00135
- Banerjee, S., Mazumdar, S. 2012. Electrospray ionization mass spectrometry: A technique to access the information beyond the molecular weight of the analyte. *Int. J. Anal. Chem.* 2012:282574. https://doi.org/10.1155/2012/282574
- Barrère, C., Hubert-Roux, M., Afonso, C., Racaud, A. 2014. Rapid analysis of lubricants by atmospheric solid analysis probe–ion mobility mass spectrometry. *J. Mass Spectrom.* 49(8):709–715. https://doi.org/10.1002/jms.3404
- Barrère, C., Maire, F., Afonso, C., Giusti, P. 2012. Atmospheric solid analysis probe–Ion mobility mass spectrometry of polypropylene. *Anal. Chem.* 84(21):9349–9354. https://doi.org/10. 1021/ac302109q
- Barrère, C, Selmi, W., Hubert-Roux, M., Coupin, T., Assumani, B., Afonso, C., Giusti, P. 2014. Rapid analysis of polyester and polyethylene blends by ion mobility-mass spectrometry. *Polym. Chem.* 5:3576–3582. https://doi.org/10.1039/C4PY00164H
- Baumgaertel, A., Scheubert, K., Pietsch, B., Kempe, C., Crecelius, A.C., Böcker, S, Schubert, U.S. 2011. Analysis of different synthetic homopolymers by the use of a new calculation software for tandem mass spectra. *Rapid Commun. Mass Spectrom.* 25(12):1765–1778. https://doi.org/ 10.1002/rcm.5019
- Beale, A.M, van Der Eerden, A.M.J., Jacques, S.D.M., Leynaud, O., O'Brien, M.G., Meneau, F., Nikitenko, S., Bras, W., Weckhuysen, B.M. 2006. A combined SAXS/WAXS/XAFS setup capable of observing concurrent changes across the nano-to-micrometer size range in inorganic solid crystallization processes. *J. Am. Chem. Soc.* 128(38):12386–12387. https://doi.org/10.1021/ja062580r
- Benninghoven, A. 1994. Surface analysis by secondary ion mass spectrometry (SIMS). *Surf. Sci.* 299:246–260. https://doi.org/10.1016/0039-6028(94)90658-0
- Bernasik, A., Rysz, J., Budkowski, A., Kowalski, K., Camra, J., Jedliński, J. 2001. Three-dimensional information on the phase domain structure of thin films of polymer blends revealed by secondary ion mass spectrometry. *Macromol. Rapid Commun. 22*(11):829–834. https://doi.org/10.1002/1521-3927(20010701)22:11<829::AID-MARC829>3.0.CO;2-8
- Biri, B., Nagy, L., Kuki, Á., Tőke, E.R., Deák, G., Zsuga, M., Kéki, S. 2012. Collision-induced dissociation study of poly(2-ethyl-2-oxazoline) using survival yields and breakdown curves. *J. Mass Specttrom.* 48(1):16–23. https://doi.org/10.1002/jms.3105
- Block, C, Wynants, L., Kelchtermans, M., De Boer, R., Compernolle, F. 2006. Identification of polymer additives by liquid chromatography-mass spectrometry. *Polym. Degrad. Stab.* 91(12):3163-3173. https://doi.org/10.1016/j.polymdegr adstab.2006.07.015
- Bodzon-Kulakowska, A., Cichon, T., Golec, A., Drabik, A., Ner, J., Suder, P. 2015. DESI-MS as a tool for direct lipid analysis in

- cultured cells. *Cytotechnology 67*(6):1085–1091. https://doi.org/10.1007/S10616-014-9734-Z
- Boyle, B.M., Heinz, O., Miyake, G.M., Ding, Y. 2019. Impact of the pendant group on the chain conformation and bulk properties of norbornene imide-based polymers. *Macromolecules 52*(9): 3426–3434. https://doi.org/10.1021/acs.macromol.9b00020
- Bridoux, M.C., Machuron-Mandard, X. 2013. Capabilities and limitations of direct analysis in real-time orbitrap mass spectrometry and tandem mass spectrometry for the analysis of synthetic and natural polymers. *J. Mass Spectrom. 27*(18): 2057–2070. https://doi.org/10.1002/rcm.6664
- Brodbelt, J.S. 2014. Photodissociation mass spectrometry: New tools for characterization of biological molecules. *Chem. Soc. Rev.* 43:2757–2783. https://doi.org/10.1039/c3cs60444f
- Brodbelt, J.S., Morrison, L.J., Santos, I. 2020. Ultraviolet photodissociation mass spectrometry for analysis of biological molecules. *Chem. Rev.* 120(7):3328–3380. https://doi.org/10. 1021/acs.chemrev.9b00440
- Buback, M., Frauendorf, H., Günzler, F., Vana, P. 2007. Electrospray ionization mass spectrometric end-group analysis of PMMA produced by radical polymerization using diacyl peroxide initiators. *Polymer 48*(19):5590–5598. https://doi.org/10.1016/j.polymer.2007.07.041
- Cavallo, G., Poyer, S., Amalian, J.-A., Dufour, F., Burel, A., Carapito, C., Charles, L., Lutz, J.-F. 2018. Cleavable binary dyads: Simplifying data extraction and increasing storage density in digital polymers. *Angew. Chem. Int. Ed.* 57(21): 6266–6269. https://doi.org/10.1002/anie.201803027
- Cerda, B.A., Breuker, K., Horn, D.M., McLafferty, F.W. 2001. Charge/radical site initiation versus coulombic repulsion for cleavage of multiply charged ions. Charge solvation in poly (alkene glycol) ions. *J. Am. Soc. Mass Spectrom.* 12(5):565–570. https://doi.org/10.1016/S1044-0305(01)00209-4
- Cerda, B.A., Horn, D.M., Breuker, K., McLafferty, F.W. 2002. Sequencing of specific copolymer oligomers by electron-capture-dissociation mass spectrometry. *J. Am. Chem. Soc.* 124(31):9287–9291. https://doi.org/10.1021/ja0123756
- Chaicharoen, K., Polce, M.J., Singh, A., Pugh, C., Wesdemiotis, C. 2008. Characterization of linear and branched polyacrylates by tandem mass spectrometry. *Anal. Bionanl. Chem.* 392(4): 595–607. https://doi.org/10.1007/S00216-008-1969-0
- Chan, Y.-T., Li, X., Carri, G.A., Moorefield, C.N., Newkome, G.R., Wesdemiotis, C. 2011. Design, synthesis, and traveling wave ion mobility mass spectrometry characterization if iron(II)-and ruthenium(II)-terpyridine metallomacrocycles. *J. Am. Chem. Soc.* 133(31):11967–11976. https://doi.org/10.1021/ja107307u
- Chang, T. 2018. Chromatographic separation of polymers. In: Wang, Y., Gao, W., Orski, S., Liu, X.M. (Eds.). Recent Progress in Separation of Macromolecules and Particulates. ACS Symposium Series, American Chemical Society, Washington, DC, chapter 1, pp. 1–17. https://doi.org/10.1021/bk-2018-1281.ch001
- Chang, W.C., Huang, L.C.L., Wang, Y.-S., Peng, W.-P., Chang, H.C., Hsu, N.Y., Yang, W.B., Chen, C.H. 2007. Matrix-assisted laser desorption/ionization (MALDI) mechanism revisited. *Anal. Chim. Acta* 582(1):1–9. https://doi.org/10.1016/j.aca.2006.08.062
- Chao, H.C., Lee, K.W., Shih, M., McLuckey, S.A. 2022. Characterization of homopolymer distributions via direct infusion ESI-MS/MS using wide mass-to-charge windows and gas-phase

- ion/ion reactions. *J. Am. Soc. Mass Spectrom. 33*(4):704–713. https://doi.org/10.1021/jasms.2c00001
- Charles, L. 2014. MALDI of synthetic polymers with labile endgroups. Mass Spectrom. Rev. 33(6):523-543. https://doi.org/10. 1002/mas.21403
- Charles, L., Chendo, C., Poyer, S. 2020. Ion mobility spectrometry–Mass spectrometry coupling for synthetic polymers. *Rapid Commun. Mass Spectrom.* 34(S2):e8624. https:// doi.org/10.1002/rcm.8624
- Chen, H., He, M., Pei, J., He, H. 2003. Quantitative analysis of synthetic polymers using matrix-assisted laser desorption/ionization time-of-flight mass spectrometry. *Anal. Chem.* 75(23):6531–6535. https://doi.org/10.1021/ac0344034
- Chen, J., Garcia, E.S., Zimmerman, S.C. 2020. Intramolecularly cross-linked polymers: From structure to function with applications as artificial antibodies and artificial enzymes. *Acc. Chem. Res.* 53(6):1244–1256. https://doi.org/10.1021/acs.accounts.0c00178
- Chen, Y., Zuo, Z., Dai, X., Xiao, P., Fang, X., Wang, X., Wang, W., Ding, C.-F. 2018. Gas-phase complexation of α-/β-cyclodextrin with amino acids studied by ion mobility-mass spectrometry and molecular dynamics simulations. *Talanta* 186:1–7. https://doi.org/10.1016/j.talanta.2018.04.003
- Cody, R.B., Laramée, J.A., Durst, H.D. 2005. Versatile new ion source for the analysis of materials in open air under ambient conditions. *Anal. Chem.* 77(8):2297–2302. https://doi.org/10.1021/ac050162j
- Cohen, L.H., Gusev, A.I. 2002. Small molecule analysis by MALDI mass spectrometry. *Anal. Bional. Chem.* 373(7):571–586. https://doi.org/10.1007/s00216-002-1321-z
- Constantopoulos, T.L., Jackson, G.S., Enke, C.G. 1999. Effects of salt concentration on analyte response using electrospray ionization mass spectrometry. *J. Am. Soc. Mass Spectrom.* 10(7):625–634. https://doi.org/10.1016/S1044-0305(99)00031-8
- Cornett, D.S., Reyzer, M.L., Chaurand, P., Caprioli, R.M. 2007.
 MALDI imaging mass spectrometry: Molecular snapshots of biochemical systems. *Nat. Methods* 4:828–833. https://doi.org/10.1038/nmeth1094
- Crecelius, A.C., Alexandrov, T., Schubert, U.S. 2011. Application of matrix-assisted laser desorption/ionization mass spectrometric imaging to monitor surface changes of UV-irradiated poly (styrene) films. *Rapid Commun. Mass Spectrom.* 25(19): 2809–2814. https://doi.org/10.1002/rcm.5164
- Crecelius, A.C., Baumgaertel, A., Schubert, U.S. 2009. Tandem mass spectrometry of synthetic polymers. *J. Mass Spectrom*. 44(9):1277–1286. https://doi.org/10.1002/jms.1623
- Crecelius, A.C., Becer, R., Knop, K., Schubert, U.S. 2010. Block length determination of the block copolymer mPEG-b-PS using MALDI-TOF MS/MS. *J. Polym. Sci. A: Polym. Chem.* 48(20): 4375–4384. https://doi.org/10.1002/pola.24223
- Crecelius, A.C., Vitz, J., Schubert, U.S. 2014. Mass spectrometric imaging of synthetic polymers. *Anal. Chim. Acta* 808:10–17. https://doi.org/10.1016/J.ACA.2013.07.033
- Crotty, S., Gerişlioğlu, S., Endres, K.J., Wesdemiotis, C., Schubert, U.S. 2016. Polymer architectures via mass spectrometry and hyphenated techniques: A review. *Anal. Chim. Acta* 932:1–21. https://doi.org/10.1016/j.aca.2016.05.024
- D'Atri, V., Porrini, M., Rosu, F., Gabelica, V. 2015. Linking molecular models with ion mobility experiments. Illustration

- with a rigid nucleic acid structure. *J. Mass Spectrom.* 50(5): 711–726. https://doi.org/10.1002/JMS.3590
- De Hoffmann, E., Stroobant, V. 2007. Mass Spectrometry Principles and Applications, 3rd ed., John Wiley & Sons Ltd., Chichester, UK, pp. 189–216. https://www.wiley.com/en-us/Mass+Spectrometry%3A+Principles+and+Applications%2C+3rd+Editionp-9781118681947
- Diepens, M., Gijsman, P. 2007. Photodegradation of bisphenol A polycarbonate. *Polym. Degrad. Stabil.* 92(3):397–406. https://doi.org/10.1016/j.polymdegradstab.2006.12.003
- Dodds, J.N., Baker, E.S. 2019. Ion mobility spectrometry: Fundamental concepts, instrumentation, applications, and the road ahead. *J. Am. Soc. Mass Specttrom.* 30(11):2185–2195. https://doi.org/10.1007/s13361-019-02288-2
- Dreisewerd, K. 2003. The desorption process in MALDI. *Chem. Rev.* 103(2):395–426. https://doi.org/10.1021/cr010375i
- Eberlin, L.S., Ferreira, C.R., Dill, A.L., Ifa, D.R., Cooks, R.G. 2011. Desorption electrospray ionization mass spectrometry for lipid characterization and biological tissue imaging. *Biochim. Biophys. Acta* 1811(11):946–960. https://doi.org/10.1016/j. bbalip.2011.05.006
- Edwards, H.M., Sasiene, Z.J., Mendis, P.M., Jackson, G.P. 2022. Structural characterization of natural and synthetic macrocycles using charge-transfer dissociation mass spectrometry. J. Am. Soc. Mass Spectrom. 33(4):671–680. https://doi.org/10.1021/JASMS.1C00369
- El-Aneed, A., Cohen, A., Banoub. J. 2009. Mass spectrometry, review of the basics: Electrospray, MALDI, and commonly used mass analyzers. *Appl. Spectrosc. Rev.* 44(3):210–230. https://doi.org/10.1080/05704920902717872
- Endres, K.J., Barthelmes, K., Winter, A., Antolovich, R., Schubert, U.S., Wesdemiotis, C. 2020. Collision cross-section analysis of self-assembled metallomacrocycle isomers and isobars via ion mobility mass spectrometry. *Rapid Commun. Mass Spectrom.* 34(S2):e8717. https://doi.org/10.1002/RCM.8717
- Endres, K.J., Dilla, R.A., Becker, M.L., Wesdemiotis, C. 2021. Poly (ethylene glycol) hydrogel crosslinking chemistries identified via atmospheric solids analysis probe mass spectrometry. *Macromolecules* 54(17):7754–7764. https://doi.org/10.1021/acs.macromol.1c00765
- Endres, K.J., Hill, J.A., Lu, K., Foster, M.D., Wesdemiotis, C. 2018. Surface layer matrix-assisted laser desorption ionization mass spectrometry imaging: A surface imaging technique for molecular-level analysis of synthetic material surfaces. *Anal. Chem.* 90(22):13427–13433. https://doi.org/10.1021/acs. analchem.8b03238
- Endres, K.J. 2019. Mass spectrometry methods for macromolecules: Polymer architectures, cross-linking, and surface imaging. Ph.D. Dissertation, The University of Akron. http://rave.ohiolink.edu/etdc/view?acc_num=akron1553096604194835
- Farenc, M., Corilo, Y.E., Lalli, P.M., Riches, E., Rodgers, R.P., Afonso, C., Giusti, P. 2016. Comparison of atmospheric pressure ionization for the analysis of heavy petroleum fractions with ion mobility-mass spectrometry. *Energy Fuels* 30(11):8896–8903. https://doi.org/10.1021/acs.energyfuels.6b 01191
- Feldermann, A., Toy, A.A., Davis, T.P., Stenzel, M.H., Barner-Kowollik, C. 2005. An in-depth analytical approach to the mechanism of the

- RAFT process in acrylate free radical polymerizations via coupled size exclusion chromatography–electrospray ionization mass spectrometry (SEC–ESI-MS). *Polymer 46*(19):8448–8457. https://doi.org/10.1016/J.POLYMER.2005.01.101
- Fenn, J.B., Mann, M., Meng, C.K., Wong, S.F., Whitehouse, C.M. 1989. Electrospray ionization for mass spectrometry of large biomolecules. *Science* 246(4926):64–71. https://doi.org/10. 1126/science.2675315
- Foley, C.D., Zhang, B., Alb, A.M., Trimpin, S., Grayson, S.M. 2015. Use of ion mobility spectrometry–mass spectrometry to elucidate architectural dispersity within star polymers. *ACS Macro Lett.* 4(7):778–782. https://doi.org/10.1021/acsmacrolett. 5b00299
- Forbes, T.P., Sisco, E. 2018. Recent advances in ambient mass spectrometry of trace explosives. *Analyst* 143:1948–1969. https://doi.org/10.1039/C7AN02066J
- Fortman, D.J., Brutman, J.P., De Hoe, G.X., Snyder, R.L., Dichtel, W.R., Hillmyer, M.A. 2018. Approaches to sustainable and continually recyclable cross-linked polymers. *ACS Sustain. Chem. Eng.* 6(9): 11145–11159. https://doi.org/10.1021/acssuschemeng.8b02355
- Fouquet, T., Mertz, G., Desbenoit, N., Frache, G., Ruch, D. 2014. TOF-SIMS/MALDI-TOF combination for the molecular weight depth profiling of polymeric bilayer. *Mater. Lett.* 128: 23–26. https://doi.org/10.1016/J.MATLET.2014.04.119
- Fouquet, T., Barrère-Mangote, C., Farenc, M., Afonso, C., Giusti, P. 2015. Atmospheric solid analysis probe mass spectrometry vs electrospray tandem mass spectrometry of polydimethylsiloxanes in positive and negative ionization modes. *Rapid Commun. Mass Spectrom.* 29(10):982–986. https://doi.org/10.1002/rcm.7182
- Fouquet, T., Sato, H. 2017. Extension of the Kendrick mass defect analysis of homopolymers to low resolution and high mass range mass spectra using fractional base units. *Anal. Chem.* 89(5): 2682–2686. https://doi.org/10.1021/acs.analchem.6b05136
- Fouquet, T.N.J. 2019. The Kendrick analysis for polymer mass spectrometry. *J. Mass Spectrom*. 54(12):933–947. https://doi.org/10.1002/jms.4480
- Fouquet, T.N.J., Amalian, J.-A., Aniel, N., Carvin-Sergent, I., Issa, S., Poyer, S., Crozet, D., Giusti, P., Gigmes, D., Trimaille, T., Charles, L. 2021. Reactive desorption electrospray ionization mass spectrometry to determine intrinsic degradability of poly(lactic-co-glycolic acid) chains. *Anal. Chem.* 93(35):12041–12048. https://doi.org/10.1021/ACS. ANALCHEM.1C02280
- Fouquet, T.N.J., Pizzala, H., Rollet, M., Crozet, D., Giusti, P., Charles, L. 2020. Mass spectrometry-based analytical strategy for comprehensive molecular characterization of biodegradable poly(lactic-co-glycolic acid) copolymers. *J. Am. Soc. Mass Spectrom.* 31(7):1554–1562. https://doi.org/10.1021/jasms.0c00137
- Friia, M., Legros, V., Tortajada, J., Buchmann, W. 2012. Desorption electrospray ionization—Orbitrap mass spectrometry of synthetic polymers and copolymers. *J. Mass Spectrom.* 47(8): 1023–1033. https://doi.org/10.1002/JMS.3057
- Fussell, R.J., Chan, D., Sharman, M. 2010. An assessment of atmospheric-pressure solids-analysis probes for the detection of chemicals in food. *Trends Anal. Chem.* 29(11):1326–1335. https://doi.org/10.1016/j.trac.2010.08.004

- Gabelica, V., Livet, S., Rosu, F. 2018. Optimizing native ion mobility Q-TOF in helium and nitrogen for very fragile noncovalent structures. J. Am. Soc. Mass Spectrom. 29(11): 2189–2198. https://doi.org/10.1007/s13361-018-2029-4
- Gabelica, V., Marklund, E. 2018. Fundamentals of ion mobility spectrometry. Curr. Opin. Chem. Biol. 42:51–59. https://doi. org/10.1016/j.cbpa.2017.10.022
- Gerişlioğlu, S., Wesdemiotis, C. 2017. Chain-end and backbone analysis of poly(*N*-isopropylacrylamide)s using sequential electron transfer dissociation and collisionally activated dissociation. *Int. J. Mass Spectrom.* 413:61–68. https://doi.org/10.1016/j.ijms.2016.08.001
- Gidden, J., Wyttenbach, T., Jackson, A.T., Scrivens, J.H., Bowers, M.T. 2000. Gas-phase conformations of synthetic polymers: Poly(ethylene glycol), poly(propylene glycol), and poly(tetramethylene glycol). *J. Am. Chem. Soc. 122*(19): 4692–4699. https://doi.org/10.1021/ja993096+
- Gies, A.P. 2012. Ionization techniques for polymer mass spectrometry.
 In: Barner-Kowollik, C., Gruendling, T., Falkenhagen, J.,
 Weidner, S. (Eds.). Mass Spectrometry in Polymer Chemistry,
 Wiley-VCH Verlag GmbH & Co. KGaA, Weinheim, Germany,
 chapter 2, pp. 33–56. https://doi.org/10.1002/9783527641826.ch2
- Gies A.P., Heath, W.H., Keaton, R.J., Jimenez, J.J., Zupancic, J.J. 2013. MALDI-TOF/TOF CID study of polycarbodiimide branching reactions. *Macromolecules* 46(19):7616–7637. https://doi.org/10.1021/ma401481g
- Gies, A.P., Hercules, D.M. 2014. Collision-induced dissociation study of ester-based polyurethane fragmentation reactions. Anal. Chim. Acta 808:199–219. https://doi.org/10.1016/j.aca. 2013.09.035
- Gies, A.P., Nonidez, W.K. 2004. A technique for obtaining matrix-assisted laser desorption/ionization time-of-flight mass spectra of poorly soluble and insoluble aromatic polyamides. *Anal. Chem.* 76(7):1991–1997. https://doi.org/10.1021/Ac035299T
- Gies, A.P., Vergne, M.J., Orndorff, R.L., Hercules, D.M. 2007. MALDI-TOF/TOF CID study of polystyrene fragmentation reactions. *Macromolecules* 40(21):7493–7504. https://doi.org/ 10.1021/ma0712450
- Girod, M., Antoine, R., Lemoine, J., Dugurd, P. 2011. End-group characterization of poly(styrene sulfonate sodium salt) by activated electron photo-detachment dissociation. *Rapid Commun. Mass Spectrom.* 25(21):3259–3266. https://doi.org/ 10.1002/rcm.5228
- Girod, M., Brunet, C., Antoine, R., Lemoine, J., Dugourd, P., Charles, L. 2012. Efficient structural characterization of poly (methacrylic acid) by activated-electron photodetachment dissociation. J. Am. Soc. Mass Spectrom. 23(1):7–11. https:// doi.org/10.1007/s13361-011-0279-5
- Girod, M., Phan, T.N.T., Charles, L. 2008. Microstructural study of a nitroxide-mediated poly(ethylene oxide)/polystyrene block copolymer (PEO-b-PS) by electrospray tandem mass spectrometry. J. Am. Soc. Mass Spectrom. 19(8):1163–1175. https:// doi.org/10.1016/j.jasms.2008.04.030
- González-Manzano, S., Santos-Buelga, C., Pérez-Alonso, J.J., Rivas-Gonzalo, J.C., Escribano-Bailón, M.T. 2006. Characterization of the mean degree of polymerization of proanthocyanidins in red wines using liquid chromatography-mass spectrometry (LC-MS). J. Agric. Food Chem. 54(12):4326–4332. https://doi.org/10.1021/JF060467E

- Gruendling, T., Guilhaus, M., Barner-Kowollik, C. 2008. Quantitative LC-MS of polymers: Determining accurate molecular weight distributions by combined size exclusion chromatography and electrospray mass spectrometry with maximum entropy data processing. *Anal. Chem.* 80(18):6915–6927. https://doi.org/10.1021/AC800591J
- Haines, P.J. 2002. Principles of Thermal Analysis and Calorimetry, Royal Society of Chemistry, Cambridge, UK. https://doi.org/ 10.1039/9781847551764
- Hajslova, J., Cajka, T., Vaclavik, L. 2011. Challenging applications offered by direct analysis in real time (DART) in food-quality and safety analysis. *Trends Analyt. Chem.* 30(2):204–218. https://doi.org/10.1016/j.trac.2010.11.001
- Hale, O.J., Cooper, H.J. 2020. In situ mass spectrometry analysis of intact proteins and protein complexes from biological substrates. *Biochem. Soc. Trans.* 48(1):317–326. https://doi. org/10.1042/bst20190793
- Hankin, J.A., Barkley, R.M., Murphy, R.C. 2007. Sublimation as a method of matrix application for mass spectrometric imaging. J. Am. Soc. Mass Spectrom. 18(9):1646–1652. https://doi.org/ 10.1016/J.JASMS.2007.06.010
- Hanton, S.D., Parees, D.M. 2005. Extending the solvent-free MALDI sample preparation method. *J. Am. Soc. Mass Spectrom.* 16(1):90–93. https://doi.org/10.1016/j.jasms.2004.09.019
- Hanton, S.D., Parees, D.M., Owens, K.G. 2004. MALDI PSD of low molecular weight ethoxylated polymers. *Int. J. Mass Spectrom.* 238(3):257–264. https://doi.org/10.1016/j.ijms.2004.09.028
- Hanton, S.D., Owens, K.G. 2012. Polymer MALDI sample preparation.
 In: Barner-Kowollik, C., Gruendling, T., Falkenhagen, J.,
 Weidner, S. (Eds.). Mass Spectrometry in Polymer Chemistry,
 Wiley-VCH Verlag GmbH & Co. KGaA, Weinheim, Germany,
 chapter 5, pp. 119–147. https://doi.org/10.1002/9783527641826.ch5
- Haque, F.M, Grayson, S.M. 2020. The synthesis, properties and potential applications of cyclic polymers. *Nat. Chem.* 12(5): 433–444. https://doi.org/10.1038/s41557-020-0440-5
- Harrison, A.G., Young, A.B., Bleiholder, C., Sahai, S., Paizs, B. 2006. Scrambling of sequence information in collision-induced dissociation of peptides. *J. Am. Chem. Soc.* 128(32): 10364–10365. https://doi.org/10.1021/ja062440h
- Hassellöv, M., Hulthe, G., Lyvén, B., Stenhagen, G. 2006. Electrospray mass spectrometry as online detector for low molecular weight polymer separations with flow field-flow fractionation. J. Liq. Chromatogr. Relat. Technol. 20 16-17): 2843–2856. https://doi.org/10.1080/10826079708005596
- Hill, J.A., Endres, K.J., Mahmoudi, P., Matsen, M.W., Wesdemiotis, C., Foster, M.D. 2018. Detection of surface enrichment driven by molecular weight disparity in virtually monodisperse polymers. ACS Macro Lett. 7(4):487–492. https://doi.org/10.1021/acsmacrolett.7b00993
- Hill, J.A., Endres, K.J., Meyerhofer, J., He, Q., Wesdemiotis, C., Foster, M.D. 2018. Subtle end group functionalization of polymer chains drives surface depletion of entire polymer chains. ACS Macro Lett. 7(7):795–800. https://doi.org/10.1021/ acsmacrolett.8b00394
- Hilton, G.R., Jackson, A.T., Thalassinos, K., Scrivens, J.H. 2008. Structural analysis of synthetic polymer mixtures using ion mobility and tandem mass spectrometry. *Anal. Chem.* 80(24): 9720–9725. https://doi.org/10.1021/ac801716c

- Ho, C.S., Lam, C.W.K., Chan, M.H.M., Cheung, R.C.K., Law, J.K., Lit, L.C.W., Ng, K.F., Suen, M.W.M., Tai, H.L. 2003. Electrospray ionisation mass spectrometry: Principles and clinical applications. *Clin. Biochm. Rev.* 24(1):3–12. https:// www.ncbi.nlm.nih.gov/pmc/articles/PMC1853331/
- Hopfgartner, G., Husser, C., Zell, M. 2003. Rapid screening and characterization of drug metabolites using a new quadrupole-linear ion trap mass spectrometer. *J. Mass Spectrom.* 38(2):138–150. https://doi.org/10.1002/jms.420
- Hoskins, J.N., Trimpin, S., Grayson, S.M. 2011. Architectural differentiation of linear and cyclic polymeric isomers by ion mobility spectrometry-mass spectrometry. *Macromolecules* 44(17):6915–6918. https://doi.org/10.1021/ma2012046
- Huo, X., Shi, Z., Cheng, H. C., Sun, X., Ma, S. 2017. Fuel additive, and preparation method and usage method thereof. PCT Int. Appl., WO Patent 2017075197 A1 WO 20170504. https://patents.google.com/patent/WO2017075197A1/en
- Ieritano, C., Hopkins, W.S. 2021. Assessing collision cross-section calculations using MobCal-MPI with a variety of commonly used computational methods. *Mater. Today Commun.* 27: 102226. https://doi.org/10.1016/j.mtcomm.2021.102226
- Ikonomou, M.G., Blades, A.T., Kebarle, P. 1991. Electrospray-ion spray: A comparison of mechanisms and performance. *Anal. Chem.* 63(18):1989–1998. https://doi.org/10.1021/ac00018a017
- Izunobi, J.U., Higginbotham, C.I. 2011. Polymer molecular weight analysis by 1 H NMR *spectroscopy. J. Chem. Educ. 88*(8): 1098–1104. https://doi.org/10.1021/ed100461v
- Jackson, A.T., Yates, H.T., Scrivens, J.H., Critchley, G., Brown, J., Green, M.R., Bateman, R.H. 1996. The application of matrix-assisted laser desorption/ionization combined with collision-induced dissociation to the analysis of synthetic polymers. Rapid Commun. Mass Spectrom. 10(13): 1668–1674. https://doi.org/10.1002/(SICI)1097-0231(199610)10:13<1668::AID-RCM703>3.0.CO;2-I
- Jarrold, M.F. 2022. Applications of charge detection mass spectrometry in molecular biology and biotechnology. *Chem. Rev.* 122(8):7415–7441. https://doi.org/10.1021/acs.chemrev. 1c00377
- Jedliński, Z., Adamus, G., Kowalczuk, M., Schubert, R., Szewczuk, Z., Stefanowicz, P. 1998. Electrospray tandem mass spectrometry of poly(3-hydroxybutanoic acid) end groups analysis and fragmentation mechanism. *Rapid Commun. Mass Spectrom.* 12(7):357–360. https://doi.org/10.1002/(SICI) 1097-0231(19980415)12:7<357::AID-RCM172>3.0.CO;2-C
- Karar, N., Gupta, T.K. 2015. Study of polymers and their blends using TOF-SIMS ion imaging. *Vacuum 111*:119–123. https://doi.org/10.1016/J.VACUUM.2014.10.006
- Karas, M., Bachmann, D., Bahr, U., Hillenkamp, F. 1987. Matrix-assisted ultraviolet laser desorption of non-volatile compounds. *Int. J. Mass Spectrom. Ion Proc.* 78:53–68. https://doi.org/10.1016/0168-1176(87)87041-6
- Karas, M., Krüger, R. 2003. Ion formation in MALDI: The cluster ionization mechanism. *Chem. Rev.* 103(2):427–40. https://doi.org/10.1021/cr010376a
- Kassalainen, G.E., Williams, S.K.R. 2003. Coupling thermal field-flow fractionation with matrix-assisted laser desorption/ionization time-of-flight mass spectrometry for the analysis of synthetic polymers. *Anal. Chem. 75*(8):1887–1894. https://doi.org/10.1021/ac020594j

- Katzenmeyer, B.C., Cool, L.R., Williams, J.P., Craven, K., Brown, J.M., Wesdemiotis, C. 2015. Electron transfer dissociation of sodium cationized polyesters: Reaction time effects and combination with collisional activation and ion mobility separation. *Int. J. Mass Spectrum.* 378:303–311. https://doi. org/10.1016/j.ijms.2014.09.021
- Katzenmeyer, B.C., Hague, S.F., Wesdemiotis, C. 2016. Multidimensional mass spectrometry coupled with separation by polarity or shape for the characterization of sugar-based nonionic surfactants. *Anal. Chem. 88*(1):851–857. https://doi. org/10.1021/acs.analchem.5b03400
- Keating, A.R., Wesdemiotis, C. 2023. A rapid and simple quantitation of average polymer molecular weight and composition via ESI-MS and a Bayesian universal charge deconvolution. *Rapid Commun. Mass Spectrom.* 37(8):e9478. https://doi.org/10.1002/rcm.9478
- Keller, C., Maeda, J., Jayaraman, D., Chakraborty, S., Sussman, M.R., Harris, J.M., Ané, J.-M., Li, L. 2018. Comparison of vacuum MALDI and AP-MALDI platforms for the mass spectrometry imaging of metabolites involved in salt stress in *Medicago truncatula*. Front. Plant. Sci. 9:1238. https://doi.org/10.3389/fpls.2018.01238
- Kendrick, E. 1963. A mass scale based on CH₂ = 14.0000 for highresolution mass spectrometry of organic compounds. *Anal. Chem.* 35(13):2146–2154. https://doi.org/10.1021/ac60206a048
- Konermann, L., Ahadi, E., Rodriguez, A.D., Vahidi, S. 2013. Unraveling the mechanism of electrospray ionization. *Anal. Chem.* 85(1):2–9. https://doi.org/10.1021/ac302789c
- Kötter, F., Benninghoven, A. 1998. Secondary ion emission from polymer surfaces under Ar⁺, Xe⁺ and SF₅⁺ ion bombardment. *Appl. Surf. Sci. 133*(1-2):47–57. https://doi.org/10.1016/S0169-4332(97)00515-1
- Krueger, K., Terne, C., Werner, C., Freudenberg, U., Jankowski, V., Zidek, W., Jankowski, J. 2013. Characterization of polymer membranes by MALDI mass-spectrometric imaging techniques. *Anal. Chem.* 85(10):4998–5004. https://doi.org/10. 1021/ac4002063
- Kussmann, M., Roepstorff, P. 2000. Sample preparation techniques for peptides and proteins analyzed by MALDI-MS. In: Chapman, J.R. (Ed.). *Mass Spectrometry of Proteins and Peptides*, Humana Press, Totowa, NJ, pp. 405–424. https://doi.org/10.1385/1-59259-045-4:405
- Lacroix-Andrivet, O., Moualdi, S., Hubert-Roux, M., Loutelier Bourhis, C., Mendes Siqueira, A.L., Afonso, C. 2022. Molecular characterization of formulated lubricants and additive packages using Kendrick mass defect determined by Fourier transform ion cyclotron resonance mass spectrometry. J. Am. Soc. Mass Spectrom. 33(7):1194–1203. https://doi.org/ 10.1021/jasms.2c00050
- Laiko, V.V., Moyer, S.C., Cotter, R.J. 2000. Atmospheric pressure MALDI/ion trap mass spectrometry. *Anal. Chem.* 72(21): 5239–5243. https://doi.org/10.1021/ac000530d
- Lattimer, R.P. 1989. Field ionization and field desorption mass spectrometry: Past, present, and future. *Anal. Chem.* 61(21): 1201A–1215A. https://doi.org/10.1021/ac00196a001
- Lattimer, R.P., Polce, M.J., Wesdemiotis, C. 1998. MALDI-MS analysis of pyrolysis products from a segmented polyurethane. *J. Anal. Appl. Pyrol. 48*(1):1–15. https://doi.org/10.1016/S0165-2370(98)00092-8

- Lebeau, D., Ferry, M. 2015. Direct characterization of polyurethanes and additives by atmospheric solid analysis probe with time-of-flight mass spectrometry (ASAP-TOF-MS). *Anal. Bioanal. Chem.* 407:7175–7187. https://doi.org/10.1007/s00216-015-8881-1
- Lee, S., Choi, H., Chang, T., Staal, B. 2018. Two-dimensional liquid chromatography analysis of polystyrene/polybutadiene block copolymers. *Anal. Chem.* 90(10):6259–6266. https://doi.org/10. 1021/acs.analchem.8b00913
- Li, X., Chan, Y.-T., Newkome, G.R., Wesdemiotis, C. 2011. Gradient tandem mass spectrometry interfaced with ion mobility separation for the characterization of supramolecular architectures. *Anal. Chem.* 83(4):1284–1290. https://doi.org/10. 1021/ac1022875
- Li, X., Guo, L., Casiano-Maldonado, M., Zhang, D., Wesdemiotis, C. 2011. Top-down multidimensional mass spectrometry methods for synthetic polymer analysis. *Macromolecules* 44(12): 4555–4564. https://doi.org/10.1021/ma200542p
- Ligon, S.C., Liska, R., Stampfl, J., Gurr, M., Mulhaupt, R. 2017.
 Polymers for 3D printing and customized additive manufacturing. *Chem. Rev.* 117(15):10212–10290. https://doi.org/10.1021/acs.chemrev.7b00074
- Liu, X.M., Mariarz, E.P., Heiler, D.J., Grobe, G.L. 2003. Comparative studies of poly(dimethyl siloxanes) using automated GPC-MALDI-TOF MS and on-line GPC-ESI-TOF MS. *J Am Soc Mass Spectrom* 14(3):195–202. https://doi.org/10.1016/S1044-0305(02)00908-X
- Liu, X., Lin, K., Kasko, A.M., Wesdemiotis, C. 2015. Tandem mass spectrometry and ion mobility mass spectrometry for the analysis of molecular sequence and architecture of hyperbranched glycopolymers. *Analyst* 140:1182–1191. https://doi. org/10.1039/C4AN01599A
- Liu, Y., Lee, J., Mansfield, K.M., Ko, J.H., Sallam, S., Wesdemiotis, C., Maynard, H.D. 2017. Trehalose glycopolymer enhances both solution stability and pharmacokinetics of a therapeutic protein. *Bioconjugate Chem.* 28(3):836–845. https://doi.org/10.1021/acs.bioconjchem.6b00659
- Lou, X., van Dongen, J.L.J., Peeters, J.W., Janssen, H.M. 2022. Disentangle a complex MALDI TOF mass spectrum of polyethylene glycols into three separate spectra via selective formation of protonated ions and sodium or potassium adducts. *J. Am. Soc. Mass Spectrom.* 33(12):2333–2337. https://doi.org/10.1021/jasms.2c00250
- Lydic, T.A., Busik, J.V., Esselman, W.J., Reid, G.E. 2009. Complementary precursor ion and neutral loss scan mode tandem mass spectrometry for the analysis of glycerophosphatidylethanolamine lipids from whole rat retina. *Anal. Bioanal. Chem.* 394:267–275. https://doi.org/10.1007/s00216-009-2717-9
- Ma, Q., Zhang, Y., Zhai, J., Chen, X., Du, Z., Li, W., Bai, H. 2019. Characterization and analysis of non-ionic surfactants by supercritical fluid chromatography combined with ion mobility spectrometry-mass spectrometry. *Anal. Bioanal. Chem.* 411(13): 2759–2765. https://doi.org/10.1007/s00216-019-01777-3
- Mao, J., Zhang, B., Zhang, H., Elupula, R., Grayson, S.M., Wesdemiotis, C. 2019. Elucidating branching topology and branch lengths in star-branched polymers by tandem mass spectrometry. *J. Am. Soc. Mass Spectrom.* 30(10):1981–1991. https://doi.org/10.1007/s13361-019-02260-0

- Mao, J., Zhang, W., Cheng, S.Z.D., Wesdemiotis, C. 2019. Analysis of monodisperse, sequence-defined, and POSS-functionalized polyester copolymers by MALDI tandem mass spectrometry. *Eur. J. Mass Spectrom.* 25(1):164–174. https://doi.org/10.1177/1469066719828875
- Marshall, A.G., Rodgers, R.P. 2008. Petroleomics: Chemistry of the underworld. *Proc. Natl. Acad. Sci. USA* 105(47):18090–18095. https://doi.org/10.1073/pnas.0805069105
- Marty, M.T. 2022. UniDec Version 5.1.1. https://github.com/ michaelmarty/UniDec/releases (accessed on 18 September 2022).
- Marty, M.T., Baldwin, A.J., Marklund, E.G., Hochberg, G.K.A., Benesch, J.L.P., Robinson, C.V. 2015. Bayesian deconvolution of mass and ion mobility spectra: From binary interactions to polydisperse ensembles. *Anal. Chem. 87*(8):4370–4376. https:// doi.org/10.1021/acs.analchem.5b00140
- May, J.C., McLean, J.A. 2015. Ion mobility-mass spectrometry: Time-dispersive instrumentation, *Anal. Chem.* 87(3): 1422–1436. https://doi.org/10.1021/ac504720m
- McCullough, B.J., Patel, K., Francis, R., Cain, P., Douce, D., Whyatt, K., Bajic, S., Lumley, N., Hopley, C. 2020. Atmospheric solids analysis probe coupled to a portable mass spectrometer for rapid identification of bulk drug seizures. J. Am. Soc. Mass Spectrom. 31(2):386–393. https://doi.org/10.1021/jasms.9b00020
- McEwen, C.N., McKay, R.G., Larsen, B.S. 2005. Analysis of solids, liquids, and biological tissues using solids probe introduction at atmospheric pressure on commercial LC/MS instruments. *Anal. Chem.* 77(23):7826–7831. https://doi.org/10.1021/ac051470k
- Mei, H., Laws, T.S., Mahalik, J.P., Li, J., Mah, A.H., Terlier, T., Bonnesen, P., Uhrig, D., Kumar, R., Stein, G.E., Verduzco, R. 2019. Entropy and enthalpy mediated segregation of bottlebrush copolymers to interfaces. *Macromolecules* 52(22): 8910–8922. https://doi.org/10.1021/acs.macromol.9b01801
- Mei, H., Laws, T.S., Terlier, T., Verduzco, V., Stein, G.E. 2022. Characterization of polymeric surfaces and interfaces using time-of-flight secondary ion mass spectrometry. *J. Polym. Sci.* 60(7):1174–1198. https://doi.org/10.1002/POL.20210282
- Meier, F., Park, M.A., Mann, M. 2021. Trapped ion mobility spectrometry and parallel accumulation–serial fragmentation in proteomics. *Mol. Cell. Proteomics* 20:100138. https://doi.org/ 10.1016/j.mcpro.2021.100138
- Metwally, H., Duez, Q., Konermann, L. 2018. Chain ejection model for electrospray ionization of unfolded proteins: Evidence from atomistic simulations and ion mobility spectrometry. *Anal. Chem.* 90(16):10069–10077. https://doi.org/10.1021/acs.analchem.8b02926
- Mikhael, A., Fridgen, T.D., Delmas, M., Banoub, J. 2021 Top-down lignomics analysis of the French oak lignin by atmospheric pressure photoionization and electrospray ionization quadrupole time-of-flight tandem mass spectrometry: Identification of a novel series of lignans. *J. Mass Spectrom.* 56(1):e4676. https://doi.org/10.1002/jms.4676
- Molenaar, S.R.A., van de Put, B., Desport, J.S., Samanipour, S., Peters, R.A.H., Pirok, B.W.J. 2022. Automated feature mining for two-dimensional liquid chromatography applied to polymers enabled by mass remainder analysis. *Anal. Chem.* 94(14): 5599–5607. https://doi.org/10.1021/acs.analchem.1c05336

- Montaudo, G., Carroccio, S., Puglisi, C. 2002. Thermal oxidation of poly(bisphenol A carbonate) investigated by SEC/MALDI. Polym. Degrad. Stabil. 77(1):137–146. https://doi.org/10.1016/ S0141-3910(02)00092-7
- Montaudo, G., Samperi, F., Montaudo, M.S. 2006. Characterization of synthetic polymers by MALDI-MS. *Progr. Polym. Sci.* 31(3): 277–357. https://doi.org/10.1016/j.progpolymsci.2005.12.001
- Morgan, T.E., Ellacott, S.H., Wootton, C.A., Barrow, M.P., Bristow, A.W.T., Perrier, S., O'Connor, P.B. 2018. Coupling electron capture dissociation and the modified Kendrick mass defect for sequencing of a poly(2-ethyl-2-oxazoline) polymer. *Anal. Chem.* 90(19):11710–11715. https://doi.org/10.1021/acs.analchem.8b03591
- Morsa, D., Defize, T., Dehareng, D., Jérôme, C., De Pauw, E. 2014. Polymer topology revealed by ion mobility coupled with mass spectrometry. *Anal. Chem.* 86(19):9693–9700. https://doi.org/10.1021/ac502246g
- Nagy, T., Kuki, Á., Zsuga, M., Kéki, S. 2018. Mass-remainder analysis (MARA): A new data mining tool for copolymer characterization. *Anal. Chem.* 90(6);3892–3897. https://doi. org/10.1021/acs.analchem.7b04730
- Nefliu, M., Venter, A., Cooks, R.G. 2006. Desorption electrospray ionization and electrosonic spray ionization for solid- and solution-phase analysis of industrial polymers. *Chem. Commun.* 8:888–890. https://doi.org/10.1039/B514057A
- Neira-Velázquez, M.G., Rodríguez-Hernández, M.T., Hernández-Hernández, E., Ruiz-Martínez, A.R.Y. 2013. Polymer molecular weight measurement. In: Saldívar-Guerra, E., Vivaldo-Lima, E. (Eds.). Handbook of Polymer Synthesis, Characterization, and Processing, John Wiley & Sons, Hoboken, New Jersey, chapter 17, pp. 355–366. https://doi.org/10.1002/9781118480793.ch17
- Neumann, E.K., Djambazova, K.V., Caprioli, R.M., Spraggins, J.M. 2020. Multimodal imaging mass spectrometry: Next generation molecular mapping in biology and medicine. *J. Am. Soc. Mass Spectrom.* 31(12):2401–2415. https://doi.org/10.1021/ jasms.0c00232
- Nielen, M.W.F. 1999. Maldi time-of-flight mass spectrometry of synthetic polymers. *Mass Spectrom. Rev.* 18(5):309–344. https://doi.org/10.1002/(SICI)1098-2787(1999)18:5<309::AID-MAS2>3.0.CO;2-L
- Nielen, M.W.F., Buijtenhuijs (Ab), F.A. 1999. Polymer analysis by liquid chromatography/electrospray ionization time-of-flight mass spectrometry. *Anal. Chem.* 71(9):1809–1814. https://doi.org/10.1021/ac981141a
- Nielen, M.W.F., Malucha, S. 1997. Characterization of polydisperse synthetic polymers by size-exclusion chromatography/matrix-assisted laser desorption/ionization time-of-flight mass spectrometry. *Rapid Commun. Mass Spectrom. 11*(11):1194–1204. https://doi.org/10.1002/(SICI)1097-0231(199707)11:11<1194:: AID-RCM935>3.0.CO;2-L
- Nyadong, L., Hohenstein, E.G., Galhena, A., Lane, A.L., Kubanek, J., Sherrill, C.D., Fernández, F.M. 2009. Reactive desorption electrospray ionization mass spectrometry (DESI-MS) of natural products of a marine alga. *Anal. Bioanal. Chem.* 394(1):245–254. https://doi.org/10.1007/S00216-009-2674-3
- O'Neill, J.M., Mao, J., Haque, F.M., Barroso-Bujans, F., Grayson, S.M., Wesdemiotis, C. 2022. Separation, identification, and confirmation

- of cyclic and tadpole macromolecules via UPLC-MS/MS. *Analyst* 147(10):2089–2096. https://doi.org/10.1039/D2AN00208F
- Osorio, J., Aznar, M., Nerín, C., Elliott, C., Chevallier, O. 2022. Comparison of LC-ESI, DART, and ASAP for the analysis of oligomers migration from biopolymer food packaging materials in food (simulants). *Anal. Bioanal. Chem.* 414:1335–1345. https://doi.org/10.1007/s00216-021-03755-0
- Pasch, H. 2013. Hyphenated separation techniques for complex polymers. *Polym. Chem.* 4(9):2628–2650. https://doi.org/10. 1039/c3py21095b
- Patil, A.A., Chiang, C.-K., Wen, C.-H., Peng, W.-P. 2018. Forced dried droplet method for MALDI sample preparation. *Anal. Chim. Acta* 1031:128–133. https://doi.org/10.1016/j.aca.2018.05.056
- Pavlovich, M.J., Musselman, B., Hall, A.B. 2018. Direct analysis in real-time—Mass spectrometry (DART-MS) in forensic and security applications. *Mass Spectrom. Rev.* 37(2):171–187. https://doi.org/10.1002/mas.21509
- Payne, M.E., Kareem, O.O., Williams-Pavlantos, K., Wesdemiotis, C., Grayson, S.M. 2021. Mass spectrometry investigation into the oxidative degradation of poly(ethylene glycol). *Polym. Degrad. Stabil.* 183:109388. https://doi.org/10.1016/j.polymdegradstab. 2020.109388
- Pierson, E.E., Midey, A.J., Forrest, W.P., Shah, V., Olivos, H.J., Shrestha, B., Teller, R., Forster, S., Bensussan, A., Helmy, R. 2020. Direct drug analysis in polymeric implants using desorption electrospray ionization–mass spectrometry imaging (DESI-MSI). *Pharm. Res.* 37(6):1–11. https://doi.org/10. 1007/S11095-020-02823-X
- Pimlott, D.J.D., Konermann, L. 2021. Using covalent modifications to distinguish protein electrospray mechanisms: Charged residue model (CRM) vs. chain ejection model (CEM). *Int. J. Mass Spectrom.* 469:116678. https://doi.org/10.1016/j.ijms. 2021.116678
- Pizzo, J.S., Cruz, V.H.M., Santos, P.D.S., Silva, G.R., Souza, P.M., Manin, L.P., Santos, O.O., Visentainer, J.V. 2022. Instantaneous characterization of crude vegetable oils via triacylglycerols fingerprint by atmospheric solids analysis probe tandem mass spectrometry with multiple neutral loss scans. *Food Control* 134:108710. https://doi.org/10.1016/j.foodcont.2021. 108710
- Polce, M.J., Ocampo, M., Quirk, R.P., Wesdemiotis, C. 2008. Tandem mass spectrometry characteristics of silver-cationized polystyrenes: Backbone degradation via free radical chemistry. Anal. Chem. 80(2):347–354. https://doi.org/10.1021/ac071071k
- Polce, M.J., Wesdemiotis, C. 2010. Tandem mass spectrometry and polymer ion dissociation. In: Li, L. (Ed.). MALDI Mass Spectrometry for Synthetic Polymer Analysis, John Wiley & Sons, Inc., Hoboken, NJ, pp. 85–127. https://doi.org/10.1002/ 9780470567234.ch5
- Pretorius, N.O., Rhode, K., Simpson, J.M., Pasch, H. 2015. Characterization of complex phthalic acid/propylene glycolbased polyesters by the combination of 2D chromatography and MALDI-TOF mass spectrometry. *Anal. Bioanal. Chem.* 407(1):217–230. https://doi.org/10.1007/S00216-014-7762-3
- Prian, K., Aloui, I., Legros, V., Buchmann, W. 2019. Study of the gas-phase decomposition of multiply lithiated polycaprolactone, polytetrahydrofurane and their copolymer by two different activation methods: Collision-induced dissociation

- and electron transfer dissociation. *Anal. Chim. Acta 1048*: 85–95. https://doi.org/10.1016/j.aca.2018.10.003
- Pringle, S.D., Giles, K., Wildgoose, J.L., Williams, J.P., Slade, S.E., Thalassinos, K., Bateman, R.H., Bowers, M.T., Scrivens, J.H. 2007. An investigation of the mobility separation of some peptide and protein ions using a new hybrid quadrupole/travelling wave IMS/oa-ToF instrument. *Int. J. Mass Spectrom.* 261(1):1–12. https://doi.org/10.1016/j.ijms.2006.07.021
- Quirk, R.P., Kim, H., Polce, M.J., Wesdemiotis, C. 2005. Anionic synthesis of primary amine functionalized polystyrenes via hydrosilation of allylamines with silyl hydride functionalized polystyrenes. *Macromolecules 38*(19):7895–7906. https://doi.org/10.1021/ma0513261
- Quirk, R.P., Mathers, R.T., Wesdemiotis, C., Arnould, M.A. 2002. Investigation of ethylene oxide oligomerization during functionalization of poly(styryl)lithium using MALDI-TOF MS and NMR. *Macromolecules* 35(8):2912–2918. https://doi.org/10.1021/ma011978z
- Quirk, R.P., Ocampo, M., King, R.L., Polce, M.J., Wesdemiotis, C. 2008. Anionic synthesis of trialkoxysilyl-functionalized polymers. *Rubber Chem. Technol.* 81(1):77–95. https://doi.org/10. 5254/1.3548199
- Rabbani, S., Barber, A.M., Fletcher, J.S., Lockyer, N.P., Vickerman, J.S. 2011. TOF-SIMS with argon gas cluster ion beams: A comparison with ${\rm C_{60}}^+$. *Anal. Chem. 83*(10): 3793–3800. https://doi.org/10.1021/ac200288v
- Räder, H.J., Schrepp, W. 1999. MALDI-TOF mass spectrometry in the analysis of synthetic polymers. *PActa Polymer*. 49(6):272–293. https://doi.org/10.1002/(SICI)1521-4044(199806) 49:6<272::AID-APOL272>3.0.CO;2-1
- Rial-Otero, R., Galesio, M., Capelo, J.L., Simal-Gándara, J. 2009. A review of synthetic polymer characterization by pyrolysis– GC-MS. *Chromatographia* 70:339–348. https://doi.org/10.13 65/s10337-009-1254-1
- Rivas, D., Ginebreda, A., Pérez, S., Quero, C., Barceló, D. 2016. MALDI-TOF MS imaging evidences spatial differences in the degradation of solid polycaprolactone diol in water under aerobic and denitrifying conditions. *Sci. Total Environ*. 566-567: 27–33. https://doi.org/10.1016/J.SCITOTENV.2016.05.090
- Roling, O., DeBruycker, K., Vonhören, B., Stricker, L., Körsgen, M., Arlinghaus, H.F., Ravoo, B.J., DuPrez, F.E. 2015. Rewritable polymer brush micropatterns grafted by triazolinedione click chemistry. *Angew. Chem. Int. Ed.* 54(44):13126–13129. https:// doi.org/10.1002/anie.201506361
- Rolland, A.D., Prell, J.S. Computational insights into compaction of gas-phase protein and protein complex ions in native ion mobility-mass spectrometry. 2019. *Trends Anal. Chem. 116*: 282–291. https://doi.org/10.1016/j.trac.2019.04.023
- Roszak, I., Oswald, L., Al Ouahabi, A., Bertin, A., Laurent, E., Felix, O., Carvin-Sergent, I., Charle, L., Lutz, J.-F. 2021. Synthesis and sequencing of informational poly(amino phosphodiester)s. *Polym. Chem.* 12:5279–5282. https://doi.org/10.1039/D1PY01052B
- Roy, R., Meszynska, A., Laure, C., Charles, L., Verchin, C., Lutz, J.-F. 2015. Design and synthesis of digitally encoded polymers that can be decoded and erased. *Nat. Commun.* 6:7237. https://doi. org/10.1038/ncomms8237
- Rymuszka, D., Terpiłowski, K., Borowski, P., Holysz, L. 2016. Timedependent changes of surface properties of polyether ether

- ketone caused by air plasma treatment. *Polym. Int. 65*(7): 827–834. https://doi.org/10.1002/PI.5141
- Saglam, N., Korkusuz, F., Prasad, R. (Eds.) 2021. *Nanotechnology Applications in Health and Environmental Sciences*, Springer Nature, Cham, Switzerland, https://doi.org/10.1007/978-3-030-64410-9
- Sallam, S., Dolog, I., Paik, B.A., Jia, X., Kiick, K.L., Wesdemiotis, C. 2018. Sequence and conformational analysis of peptide-polymer bioconjugates by multidimensional mass spectrometry. *Biomacromolecules* 19(5):1498–1507. https://doi.org/10.1021/acs.biomac.7b01694
- Sato, H., Nakamura, S., Teramoto, K., Sato, T. 2014. Structural characterization of polymers by MALDI spiral-TOF mass spectrometry combined with Kendrick mass defect analysis. *J. Am. Soc. Mass Spectrom.* 25(8):1346–1355. https://doi.org/ 10.1007/s13361-014-0915-y
- Schoenmakers, P., Aarnoutse, P. 2014. Multi-dimensional separations of polymers. *Anal. Chem. 86*(13):6172–6179. https://doi.org/10.1021/ac301162b
- Scionti, V., Katzenmeyer, B.C., Solak, N., Li, X., Wesdemiotis, C. 2012. Interfacing multistage mass spectrometry with liquid chromatography or ion mobility separation for synthetic polymer analysis. *Eur. J. Mass Spectrom.* 18(2):113–137. https://doi.org/10.1255/ejms.1175
- Scionti, V., Wesdemiotis, C. 2012a. Electron transfer dissociation versus collisionally activated dissociation of cationized biodegradable polyesters. *J. Mass Spectrom.* 47(11):1442–1449. https://doi.org/10.1002/jms.3097
- Scionti, V., Wesdemiotis, C. 2012b. Tandem mass spectrometry analysis of polymer structures and architectures. In: Barner-Kowollik, C., Gruendling, T., Falkenhagen, J., Weidner, S. (Eds.). Mass Spectrometry in Polymer Chemistry, Wiley-VCH Verlag GmbH & Co. KGaA, Weinheim, Germany, chapter 3, pp. 57–84. https://doi.org/10.1002/9783527641826.ch3
- Selby, T.L., Wesdemiotis, C., Lattimer, R.P. 1994. Dissociation characteristics of $[M + X]^+$ ions (X = H, Li, Na, K) from linear and cyclic polyglycols. *J. Am. Soc. Mass Spectrom.* 5: 1081–1092. https://doi.org/10.1016/1044-0305(94)85069-0
- Seo, S.E., Hawker, C.J. 2020. The beauty of branching in polymer science. *Macromolecules* 53(9):3257–3261. https://doi.org/10.1021/acs.macromol.0c00286
- Shao, Y., Chen, J., Ren, X.-K., Zhang, X., Yin, G.-Z., Li, X., Wang, J., Wesdemiotis, C., Zhang, W.-B., Yang, S., Sun, B., Zhu, M. 2019. Synthesis, self-assembly and characterization of tandem triblock BPOSS-PDI-X shape amphiphiles. *Molecules 24*(11): 2114. https://doi.org/10.3390/molecules24112114
- Shi, C., Gerişlioğlu, S., Wesdemiotis, C. 2016. Ultrahigh performance liquid chromatography interfaced with mass spectrometry and orthogonal ion mobility separation for the microstructure characterization of amphiphilic block copolymers. Chromatographia 79:961–969. https://doi.org/10.1007/s10337-016-3077-1
- Shimada, K., Lusenkova, M.A., Sato, K., Saito, T., Matsuyama, S., Nakahara, H., Kinugasa, S. 2001. Evaluation of mass discrimination effects in the quantitative analysis of polydisperse polymers by matrix-assisted laser desorption/ionization time-of-flight mass spectrometry using uniform oligostyrenes. *Rapid Commun. Mass Spectrom.* 15(4):277–282. https:// doi.org/10.1002/rcm.224

- Shimizu, Y., Munson, B. 1979. Pyrolysis/chemical ionization mass spectrometry of polymers. *J. Polym. Sci.: Polym. Chem. 17*(7): 1991–2001. https://doi.org/10.1002/pol.1979.170170709
- Siddhant, M., Smita, G., Vaishali, J., Ashish, J. 2018. HPLC—high-performance liquid chromatography & UPLC—ultra performance liquid chromatographic system—A review on modern liquid chromatography. *Indo Am. J. Pharm. Sci. 5*(8): 7590–7602. https://doi.org/10.5281/zenodo.1401201
- Silva, L.M.A., Alves Filho, E.G., Simpson, A.J., Monteiro, M.R., Cabral, E., Ifa, D., Venâncio, T. 2017. DESI-MS imaging and NMR spectroscopy to investigate the influence of biodiesel in the structure of commercial rubbers. *Talanta* 173:22–27. https://doi.org/10.1016/J.TALANTA.2017.05.060
- Sisco, E., Staymates, M.E., Forbes, T.P. 2020. Optimization of confined direct analysis in real-time mass spectrometry (DART-MS). Analyst 145:2743-2750. https://doi.org/10.1039/ D0AN00031K
- Siuzdak, G. 2006. The Expanding Role of Mass Spectrometry in Biotechnology, 2nd ed, MCC Press, San Diego, CA. https://masspec.scripps.edu/learn/mass-spectrometry-in-biotechnology-2nd-ed-gary-siuzdak.pdf
- Skelton, R., Dubois, F., Zenobi, R. 2000. A MALDI sample preparation method suitable for insoluble polymers. *Anal. Chem.* 72(7):1707–1710. https://doi.org/10.1021/ac991181u
- Smith, M.J.P., Cameron, N.R., Mosely, J.A. 2012. Evaluating atmospheric pressure solids analysis probe (ASAP) mass spectrometry for the analysis of low molecular weight synthetic polymers. *Analyst* 137:4524–4530. https://doi.org/10.1039/C2AN35556F
- Snyder, S.R., Wei, W., Xiong, H., Wesdemiotis, C. 2019. Sequencing side-chain liquid crystalline copolymers by matrix-assisted laser desorption/ionization tandem mass spectrometry. *Polymers* 11(7):1118. https://doi.org/10.3390/ polym11071118
- Snyder, S.R., Wesdemiotis, C. 2021. Elucidation of low molecular weight polymers in vehicular engine deposits by multi-dimensional mass spectrometry. *Energy Fuels 35*(2): 1691–1700. https://doi.org/10.1021/acs.energyfuels.0c02702
- Soeriyadi, A.H., Whittaker, M.R., Boyer, C., Davis, T.P. 2013. Soft ionization mass spectroscopy: Insights into the polymerization mechanism. *J. Polym. Sci. A: Polym. Chem.* 51(7):1475–1505. https://doi.org/10.1002/pola.26536
- Solak Erdem, N., Alawani, N., Wesdemiotis, C. 2014. Characterization of polysorbate 85, a nonionic surfactant, by liquid chromatography vs. ion mobility separation coupled with tandem mass spectrometry. *Anal. Chim. Acta 808*:83–93. https://doi.org/10.1016/j.aca.2013.07.026
- Song, L., Chuah, W.C., Remsen, X.L., Bartmess, J.E. 2018. Ionization mechanism of positive-Ion nitrogen direct analysis in real-time. *J. Am. Soc. Mass Spectrom.* 29(4):640–650. https://doi.org/10.1007/s13361-017-1885-7
- Striegel, A.M. 2005. Multiple detection in size-exclusion chromatography of macromolecules. *Anal. Chem.* 77(5):104A-113A. https://doi.org/10.1021/ac053345e
- Takáts, Z., Wiseman, J.M., Cooks, R.G. 2005. Ambient mass spectrometry using desorption electrospray ionization (DESI): Instrumentation, mechanisms and applications in forensics, chemistry, and biology. *J. Mass Spectrom.* 40(10):1261–1275. https://doi.org/10.1002/JMS.922

- Takáts, Z., Wiseman, J.M., Gologan, B., Cooks, R.G. 2004. Mass spectrometry sampling under ambient conditions with desorption electrospray ionization. *Science* 306(5695): 471–473. https://doi.org/10.1126/science.1104404
- Tanaka, K., Waki, H., Ido, Y., Akita, S., Yoshida, Y., Yoshida, T., Matsuo, T. 1988. Protein and polymer analyses up to m/z 100,000 by laser ionization time-of flight mass spectrometry. *Rapid Commun. Mass Specttrom.* 2(20):151–153. https://doi. org/10.1002/rcm.1290020802
- Teraoka, I. 2004. Calibration of retention volume in size exclusion chromatography by hydrodynamic radius. *Macromolecules* 37(17):6632–6639. https://doi.org/10.1021/ma0494939
- Thakur, V.K., Thakur, M.K., Raghavan, P., Kessler, M.R. 2014.
 Progress in green polymer composites from lignin for multifunctional applications: A review. ACS Sustainable Chem. Eng. 2(5):1072–1092. https://doi.org/10.1021/sc500087z
- Thalassinos, K., Jackson, A.T., Williams, J.P., Hilton, G.R., Slade, S.E., Scrivens, J.H. 2007. Novel software for the assignment of peaks from tandem mass spectrometry spectra of synthetic polymers. *J. Am. Soc. Mass Spectrom.* 18(7): 1324–1331. https://doi.org/10.1016/j.jasms.2007.04.006
- Thomas, R.K., Penfold, J. 1996. Neutron and X-ray reflectometry of interfacial systems in colloid and polymer chemistry. *Curr. Opin. Colloid Interface Sci. 1*(1):23–33. https://doi.org/10.1016/S1359-0294(96)80040-9
- Toney, M., Baiamonte, L., Smith, W.C., Williams, S.K.R. 2021. Field-flow fractionation techniques for polymer characterization. In: Malik, M.I., Mays, J., Shah, M.R. (Eds.). *Molecular Characterization of Polymers*, Elsevier, Amsterdam, Netherlands, chapter 4, pp. 129–171. https://doi.org/10.1016/B978-0-12-819768-4.00004-X
- Torikai, N. 2011. Neutron reflectometry. In: Imae, T., Kanaya, T., Furusaka, M., Torikai, N. (Eds.). *Neutrons in Soft Matter*, John Wiley & Sons, Hoboken, NJ, chapter II.2, pp. 115–145. https://doi.org/10.1002/9780470933886.CH5
- Tose, L.V., Murgu, M., Vaz, B.G., Romão, W. 2017. Application of atmospheric solids analysis probe mass spectrometry (ASAP-MS) in petroleomics: Analysis of condensed aromatics standards, crude oil, and paraffinic fraction. *J. Am. Soc. Mass Spectrom.* 28(11):2401–2407. https://doi.org/10.1007/ s13361-017-1764-2
- Town, J.S., Jones, G.R., Hancox, E., Shegiwal, A., Haddleton, D.M. 2019. Tandem mass spectrometry for polymeric structure analysis: A comparison of two common MALDI-ToF/ToF techniques. *Macromol. Rapid Commun.* 40(13):1900088. https://doi.org/10.1002/marc.201900088
- Treat, N.D., Brady, M.A., Smith, G., Toney, M.F., Kramer, E.J., Hawker, C J., Chabinyc, M.L. 2011. Interdiffusion of PCBM and P3HT reveals miscibility in a photovoltaically active blend. *Adv. Energy Mater.* 1(1):82–89. https://doi.org/10.1002/aenm.201000023
- Trimpin, S., Keune, S., Räder, H.J., Müllen, K. 2006. Solvent-free MALDI-MS: Developmental improvements in the reliability and the potential of MALDI in the analysis of synthetic polymers and giant organic molecules. *J. Am. Soc. Mass Spectrum.* 17(5): 661–671. https://doi.org/10.1016/j.jasms.2006.01.007
- Trimpin, S., Wijerathne, K., McEwen, C.N. 2009. Rapid methods of polymer and polymer additives identification: Multi-sample solvent-free MALDI, pyrolysis at atmospheric pressure, and

- atmospheric solids analysis probe mass spectrometry. *Anal. Chim. Acta 654*(1):20–25. https://doi.org/10.1016/j.aca.2009. 06.050
- Tsuge, S., Ohtani, H. 1997. Structural characterization of polymeric materials by pyrolsis-GC/MS. *Polym. Degrad. Stabil. 58*(1-2): 109–130. https://doi.org/10.1016/S0141-3910(97)00031-1
- Uliyanchenko, E. 2017. Applications of hyphenated liquid chromatography techniques for polymer analysis. *Chromatographia* 80:731–750. https://doi.org/10.1007/s10337-016-3193-y
- Uliyanchenko, E., Cools, P.J.C.H., van der Wal, S., Schoenmakers, P.J. 2012. Comprehensive two-dimensional ultrahigh-pressure liquid chromatography for separations of polymers. *Anal. Chem.* 84(18):7802–7809. https://doi.org/10.1021/ac3011582
- Vaclavik, L., Krynitsky, A.J., Rader, J.I. 2014. Mass spectrometric analysis of pharmaceutical adulterants in products labeled as botanical dietary supplements or herbal remedies: A review. *Anal. Bioanal. Chem.* 406(27):6767–6790. https://doi.org/10. 1007/s00216-014-8159-z
- Van der Heide, P. 2014. Secondary Ion Mass Spectrometry: An Introduction to Principles and Practices. John Wiley & Sons, Inc., Hobokem, NJ. https://doi.org/10.1002/9781118916780
- Vandencasteele, N., Reniers, F. 2010. Plasma-modified polymer surfaces: Characterization using XPS. J. Electron Spectrosc. 178-179:394–408. https://doi.org/10.1016/J.ELSPEC.2009.12.003
- Vaysse, P.-M., Heeren, R.M.A., Porta, T., Balluff, B. 2017. Mass spectrometry imaging for clinical research—Latest developments, applications, and current limitations. *Analyst 142*: 2690–2712. https://doi.org/10.1039/C7AN00565B
- Vickerman, J.C., Gilmore, I.S. (Eds.). 2009. Surface Analysis: The Principal Techniques, 2nd ed., John Wiley & Sons Ltd., Chichester, United Kingdom. https://doi.org/10.1002/9780470721582
- Volmer, D.A., Jessome, L.L. 2006. Ion suppression: A major concern in mass cpectrometry. *LCGC North America 24*(5): 498–510. https://www.chromatographyonline.com/view/ion-suppression-major-concern-mass-spectrometry
- Wang, S.-F., Li, X., Agapov, R.L., Wesdemiotis, C., Foster, M.D. 2012. Probing surface concentration of cyclic/linear blend films using surface layer MALDI-TOF mass spectrometry. ACS Mcro Lett. 1(8):1024–1027. https://doi.org/10.1021/ MZ300271W
- Waters Corporation. 2017. Atmospheric Pressure Ionization Sources: Their Use and Applicability. White Paper. Milford, MA. https://www.waters.com/webassets/cms/library/docs/72 0005935en.pdf
- Wei, B., Gerislioglu, S., Atakay, M., Salih, B., Wesdemiotis, C. 2019. Characterization of supramolecular peptide-polymer bioconjugates using multistage tandem mass spectrometry. *Int. J. Mass Spectrom.* 436:130–136. https://doi.org/10.1016/j.ijms. 2018.12.005
- Wei, J., Tang, Y., Ridgeway, M.E., Park, M.A., Costello, C.E., Lin, C. 2020. Accurate identification of isomeric glycans by trapped ion mobility spectrometry-electronic excitation dissociation tandem mass spectrometry. *Anal. Chem.* 92(19):13211–13220. https://doi.org/10.1021/acs.analchem.0c02374
- Weibel, D., Wong, S., Lockyer, N., Blenkinsopp, P., Hill, R., Vickerman, J.C. 2003. A C₆₀ primary ion beam system for time

- of flight secondary ion mass spectrometry: Its development and secondary ion yield characteristics. *Anal. Chem.* 75(7): 1754–1764. https://doi.org/10.1021/ac0263380
- Weidner, S.M., Falkenhagen, J. 2009. Imaging mass spectrometry for examining localization of polymeric composition in matrix-assisted laser desorption/ionization samples. *Rapid Commun. Mass Spectrom. 23*(5): 653–660. https://doi.org/10.1002/rcm.3919
- Wesdemiotis, C. Multidimensional mass spectrometry of synthetic polymers and advanced materials. 2017. *Angew. Chem. Int. Ed.* 56(6):1452–1464. https://doi.org/10.1002/anie.201607003
- Wesdemiotis, C., Solak, N., Polce, M.J., Dabney, D.E., Chaicharoen, K., Katzenmeyer, B.C. 2011. Fragmentation pathways of polymer ions. Mass Spectrom. Rev. 30(4):523–559. https://doi.org/10.1002/ mas.20282
- Weston, D.J. 2010. Ambient ionization mass spectrometry: Current understanding of mechanistic theory; analytical performance and application areas. *Analyst 135*, 661–668. https://doi.org/10.1039/B925579F
- Williams, D.H., Bradley, C., Bojesen, G., Santikarn, S., Taylorlb, L.C.E. 1981. Fast atom bombardment mass spectrometry: A powerful technique for the study of polar molecules. J. Am. Chem. Soc. 103(19):5700–5704. https://doi. org/10.1021/ja00409a013
- Williams, K. 2019. How does multi-detector GPC/SEC work? https://www.materials-talks.com/how-does-multi-detector-gpc-sec-work/. (Accessed on 5 February 2023).
- Williams, S.K.R., Lee, D. 2006. Field-flow fractionation of proteins, polysaccharides, synthetic polymers, and supramolecular assemblies. J. Sep. Sci. 29(12):1720–1732. https://doi.org/10. 1002/jssc.200600151
- Williams-Pavlantos, K., Wesdemiotis, C. 2021. Surface layer matrix assisted laser desorption ionization mass spectrometry imaging (SL-MALDI-MSI) of pharmaceutical-loaded polymer films. Proceedings of the 2021 ASMS Conference, October 31–November 4, 2021, Philadelphia, PA and Online. https://www.asms.org/publications/abstracts-and-proceedings
- Wójtowicz, A., Wietecha-Posłuszny, R. 2019. DESI-MS analysis of human fluids and tissues for forensic applications. *Appl. Phys. A* 125(5):312. https://doi.org/10.1007/s00339-019-2564-2
- Wollyung, K.M., Wesdemiotis, C., Nagy, A., Kennedy, J.P. 2005. Synthesis and mass spectrometry characterization of centrally and terminally amine-functionalized polyisobutylenes. J. Polym. Sci. A: Polym. Chem. 43(5):946–958. https:// doi.org/10.1002/pola.20566
- Wolstenholme, W.E. Correlation of physical and polymer chain properties. 1968. *Polym. Eng. Sci.* 8(2):142–150. https://doi.org/10.1002/pen.760080210
- Xie, T.-Z., Endres, K.J., Guo, Z., Ludlow, J.M. III, Moorefield, C.N., Saunders, M.J., Wesdemiotis, C., Newkome, G.R. 2016. Controlled interconversion of superimposed-bistriangle, octahedron, and cuboctahedron cages constructed using a single, terpyridinyl-based polyligand and Zn²⁺. J. Am. Chem. Soc. 138(38):12344–12347. https://doi.org/10.1021/jacs.6b07969
- Yang, P., Gao, W., Shulman, J.E., Chen, Y. 2018. Separation and identification of polymeric dispersants in detergents by twodimensional liquid chromatography. J. Chromatogr. A 1566: 111–117. https://doi.org/10.1016/j.chroma.2018.06.063

9982787, 2024, 3, Downloaded from https://amajt.cia.decience.journals.onlinethrary.viley.com/doi/10.1002/mas.21844 by Clrys Wesdenionis - University Of Abron Bierce Library, Wiley.Online Library on [23/07/2024]. See he Ferms and Conditions (https://onlinethrary.viley.com/drems-and-conditions) on Wiley Online Library for rules of use; O.A articles are governed by the applicable Creative Common

Yang, S.H., Chen, B., Wang, J., Zhang, K. 2020. Characterization of high molecular weight multi-arm functionalized PEG-maleimide for protein conjugation by chargereduction mass spectrometry coupled to two-dimensional liquid chromatography. Anal. Chem. 92(12):8584-8590. https://doi.org/10.1021/acs.analchem.0c01567

Yao, M. 2014. Determining polymer blend surface concentration using surface layer matrix-assisted laser desorption ionizationtime of flight mass spectrometry (SL-MALDI-TOF MS). M.S. Thesis, The University of Akron. http://rave.ohiolink.edu/ etdc/view?acc_num=akron1407941345

Yol, A.M., Dabney, D.E., Wang, S.-F., Laurent, B.A., Foster, M.D., Quirk, R.P., Grayson, S.M., Wesdemiotis, C. 2013. Differentiation of linear and cyclic polymer architectures by MALDI tandem mass spectrometry (MALDI-MS²). J. Am. Soc. Mass Spectrom. 24(1):74-82. https://doi.org/10.1007/s13361-012-0497-5

Yol, A.M., Janoski, J., Quirk, R.P., Wesdemiotis, C. 2014. Sequence analysis of styrenic copolymers by tandem mass spectrometry. Anal. Chem. 86(19):9576-9582. https://doi.org/10.1021/ ac5019815

Yunus, S., Delcorte, A., Poleunis, C., Bertrand, P., Bolognesi, A., Botta, C. 2007. A route to self-organized honeycomb microstructured polystyrene films and their chemical characterization by ToF-SIMS imaging. Adv. Funct. Mater. 17(7):1079-1084. https://doi.org/10.1002/ ADFM.200600470

Žagar, E., Kržan, A., Adamus, G., Kowalczuk, M. 2006. Sequence distribution in microbial poly(3-hydroxybutyrate-co-3hydroxyvalerate) co-polyesters determined by NMR and MS. Biomacromolecules 7(7):2210–2216. https://doi.org/10.1021/ bm060201g

Zhang, L., Reilly, J.P. 2009. Peptide photodissociation with 157 nm light in a commercial tandem time-of-flight mass spectrometer. Anal. Chem. 81(18):7829-7838. https://doi.org/10.1021/ ac9012557

Zhang, R., Miyoshi, T., Sun, P. (Eds.). 2019. NMR Methods for Characterization of Synthetic and Natural Polymers, Royal Society of Chemistry, Cambridge, UK. https://doi.org/10.1039/ 9781788016483

Zheng, J., Smith Callahan, L.A., Hao, J., Guo, K., Wesdemiotis, C., Weiss, R.A., Becker, M.L. 2012. Strain-promoted cross-linking of PEG-based hydrogels via copper-free cycloaddition. ACS macro Lett. 1(8):1071–1073. https://doi.org/10.1021/mz30 03775

Zhou, W., Håkansson, K. 2011. Structural characterization of carbohydrates by Fourier transform tandem mass spectrometry. Curr. Proteomics 8(4):297-308. https://doi.org/10.2174/ 157016411798220826

Zhou, X.-L., Chen, S.-H. 1995. Theoretical foundation of X-ray and neutron reflectometry. Phys. Rep. 257(4-5):223-348. https:// doi.org/10.1016/0370-1573(94)00110-O

Zughaibi, T.A., Steiner, R.R. 2020. Differentiating nylons using direct analysis in real time coupled to an AccuTOF time-offlight mass spectrometer. J. Am. Soc. Mass Spectrom. 31(4): 982–985. https://doi.org/10.1021/jasms.0c00051

Zydel, F., Smith, J.R., Pagnotti, V.S., Lawrence, R.J., McEwen, C.N., Capacio, B.R. 2012. Rapid screening of chemical warfare nerve agent metabolites in urine by atmospheric solids analysis probe-mass spectroscopy (ASAP-MS). Drug Test. Anal. 4(3-4): 308-311. https://doi.org/10.1002/dta.1331

AUTHOR BIOGRAPHIES



Chrys Wesdemiotis completed his PhD at Technische Universität Berlin in 1979. After a postdoctoral fellowship with Fred W. McLafferty at Cornell University (1980) and military service in Greece (1981-1983), he

returned to Cornell as senior research associate (1983-1989). In 1989, he joined the University of Akron, where he currently is Distinguished Professor of Chemistry, Polymer Science, and Integrated Bioscience. Research in the Wesdemiotis group focuses on the development and applications of multidimensional mass spectrometry methods for the characterization and imaging of synthetic macromolecules and polymerbiomolecule conjugates. Particular interest is on top-down techniques that reveal the complete microstructure of synthetic polymers (sequence, topology, architecture), the use of noncovalent polyelectrolyte tags to determine protein higher order structure, and surface analysis methods that probe the top molecular layer of solid materials.



Kayla N. Williams-Pavlantos studied chemistry with a concentration in forensic science at Malone University (BA in 2017). In the fall of 2017, she interned at the Canton Crime Lab and assisted in establishing a mass spec-

trometry fragment database of illegal narcotics. She joined Prof. Chrys Wesdemiotis research group at the University of Akron in 2018 as a PhD student. The focus of her research is on the characterization of synthetic polymers with multidimensional mass spectrometry techniques (MS/ MS and IM-MS) and SL-MALDI-MS-Imaging of pharmaceutical-loaded polymer films.



Addie R. Keating studied chemistry at Xavier University and completed her BS degree with a minor in forensic science in 2018. She began working for Prof. Chrys Wesdemiotis in the summer of 2017 as an REU

intern where she helped develop site-specific,

0982787, 2024, 3, Downloaded from https://analyticalsciencejournals.onlinelibrary.wiley.com/doi/10.1002/mas.21844 by Chrys Wesdemiotis



Andrew S. McGee studied chemistry at the University of Akron (BSc in 2020) and conducted research on mechanochemical methods for synthesizing chlorophosphazenes. He joined the research group of Prof. Chrys

Wesdemiotis as a PhD student at the University of Akron in August of 2020 and received his MSc in 2022. His research focuses on the characterization of synthetic polymers with mass spectrometry (ESI and MALDI), polymer and supramolecular structures with IM-ESI-MS, and polymer detection using static HS-GC-MS.



Calum Bochenek studied Chemistry at Ohio Northern University (BSc in 2021) and conducted research on PFOA/perfluorinated compound sensing and Py-GC/MS for the analysis of commercial polymers. He joined the research group of

Prof. Chrys Wesdemiotis as a PhD student at the University of Akron in 2021. His research focuses on using energy-resolved mass spectrometry (ER-MS) to gain insight on the stability of polyelectrolyte complexes and investigating fragmentation mechanisms and structural characterization of mechanopolymers.

How to cite this article: Wesdemiotis C., Williams-Pavlantos K.N., Keating A.R., McGee A.S., Bochenek C. Mass spectrometry of polymers: A tutorial review. *Mass Spectrom Rev.* 2024;43: 427-476. https://doi.org/10.1002/mas.21844